DEVELOPMENT OF A PERFUSION BIOREACTOR STRATEGY FOR HUMAN ADIPOSE-DERIVED STEM CELL EXPANSION

by

Sarah Alicia-Ann Fleming

A thesis submitted to the Department of Chemical Engineering

In conformity with the requirements for

the degree of Master's of Applied Science

Queen's University

Kingston, Ontario, Canada

(October, 2011)

Abstract

Developing an optimized growth environment for adipose-derived stems cells (ASCs) to obtain clinically useable cell quantities from relatively small tissue biopsies would significantly impact the field of tissue engineering. To date, ASCs have been differentiated into adipose, bone, cartilage, smooth muscle, endothelial, skeletal muscle, nervous, and cardiac tissue. Therefore, ASCs have potential for use in the treatment of a wide variety of clinical conditions ranging from myocardial infarction, to musculoskeletal disorders, and the repair of soft tissue defects.

In this work, a custom-designed, 3-dimensional (3-D) scaffold-based perfusion bioreactor system was investigated in the culture of ASCs. Decellularized adipose tissue (DAT) was used to provide a 3-dimensional scaffold, as it possesses the native extracellular matrix (ECM) architecture and composition of human adipose tissue. The DAT had a permeability of 149 m^2, based on a perfusion rate of 1.5 mL/min over a 200 mg DAT sample, and the culturing medium was evenly perfused throughout the DAT, thereby permitting possible cell growth within the central regions. Initial culturing studies of human ASCs on tissue culture polystyrene (TCPS) demonstrated that hypoxic (5% O_2) conditions decreased the doubling time, and resulted in enhanced cell proliferation, as compared to normoxic (21% O_2) conditions.

The cell imaging and DNA quantification results showed that suspension seeding of the ASCs permitted cell attachment to the DAT scaffold, but did not support long-term ASC growth. In contrast, when the ASCs were seeded as multicellular aggregates, the cells attached and underwent measurable proliferation. The optimal seeding density observed was 1 x 10^6 ASCs/scaffold; or 50 aggregates (20,000 ASCs/aggregate) per scaffold. Based on the confocal imaging, the ASCs remained spherical in morphology during the entire culturing period. Moreover, results illustrated that the perfusion bioreactor provided an improved culturing environment for ASCs over traditional static culturing. Hypoxic (5% O_2) conditions showed

improved proliferation over normoxic (21% O_2) conditions, within the bioreactor system. After a 14-day hypoxic culturing period in the perfusion bioreactor, the seeded ASCs retained the ability to undergo adipogenesis, as indicated by Glycerol-3-Phsophate Dehydrogenase (GPDH) enzymatic activity measurements, demonstrating the promise of this approach for soft tissue engineering applications.

Acknowledgements

I would like to thank my supervisor Dr. Lauren Flynn for her support and guidance throughout this thesis. I am thankful for the opportunities she gave me and motivated me to reach my full potential in research and as a person outside the lab. It was a memorable experience working with her and I will take away a greater knowledge of research, an open mind, and a critical eye. I would also like to thank Drs. Brian Amsden and Stephen Waldman for the use of their laboratory equipment and for their guidance and teaching throughout my studies at Queen's University. Thanks to Drs. J. F. Watkins, M. Harrison, K. Meathrel, J. Davidson, C. Watters and Mrs. K. Martin, for their clinical collaborations facilitating tissue transition.

I can't thank enough the Flynn Lab Group, especially Mrs. Allison Turner and Ms. Hoi Ki Cheung for all their support inside and outside the lab. There were many late nights spent working alongside these people. These people are my role models and I couldn't have chosen better lab mates. Thank you to Mr. James Hayami and Mr. James Kaupp for their technological assistance and knowledge. I would also like to thank Dr. Tim Bryant and the HMRC-CREATE program for providing me opportunities to expand my knowledge and exposure to the greater picture of research.

Thanks also to my friends outside the laboratory, especially Mr. Joe Steele, Ms. Kaitlin Reilly, Ms. Caitlin Hesketh, Ms. Stephanie Kenny, Ms. Allison Thomas and Ms. Priyanka Taneja for keeping me level headed and their undying support. A big thanks goes to my boyfriend Mr. Nevin Cimolai for being there for me during my thesis writing and supporting me throughout the process.

Lastly, I would like to thank my parents Mr. Brian Fleming and Mrs. Ann Hutchinson for their everlasting support, guidance, and helping me get through all the good and bad times.

Table of Contents

List of Figures

List of Tables

List of Acronyms

a-FABP	Adipocyte fatty acid binding protein	KGF	Keratinocyte growth factor
ALP	Alkaline phosphatase	KLF	Krüppel-like factor
ASCs	Adipose-derived stem cells	LPL	Lipoprotein lipase
bFGF	basic fibroblast growth factor	MA	Multicellular aggregate
BMI	Body mass index	MMP	Matrix metalloproteinase
BMP	Bone morphogenetic proteins	MSC	Mesenchymal stem cell
BSP	Bone sialoprotein	NSC	Neural stem cell
C/EBP	CCAAT/enhancer binding protein	OCN	Osteocalcin
DAT	Decellularized adipose tissue	ON	Osteonectin
DMEM	Dulbecco's Modified Eagle's Medium	OP	Osteopontin
ECM	Extracellular matrix	PBS	Phosphate buffered saline
ESC	Embryonic stem cell	PCL	Poly(ϵ-caprolactone)
FAT	Fatty acid synthase	Pdx1	Pancreatic duoderal homeobox
FBS	Fetal bovine serum	PEG	Poly(ethylene glycol)
GLUT	Glucose transporter	PGA	Poly(glycolic acid)
GMP	Good manufacturing practice	PPAR	Peroxisome proliferation-
GPDH	Glycerol-3-phosphate dehydrogenase		activated receptor
HDF	Human dermal fibroblast	ROS	Reactive oxygen species
HGF	Hepatocyte growth factor	SDS	Sodium dodecyl sulphate
HSC	Hematopoietic stem cell	SVF	Stromal vascular fraction
HSL	Hormone-sensitive lipase	TCPS	Tissue culture poly(styrene)
IBMX	Isobutylmethylxanthine	TGF	Transforming-growth factor
IGF	Insulin growth factor	TNF	Tumor necrosis factor

Chapter 1

Introduction

1.1 Background and Rationale

A stem cell is defined to be any cell that is capable of self-renewal and has the capacity to differentiate into at least one functional cell type [1]. Stem cells are being investigated for a broad array of clinical applications including the treatment of diabetes, rheumatoid arthritis, Crohn's disease, liver cirrhosis, fistulas, cardiovascular disease, limb ischemia, lipodystophy, graft-versus-host disease, neurological dysfunctions such as Parkinson's disease and Alzheimer's, multiple sclerosis, soft tissue augmentation, skin wounds and bone tissue repair [1-3].

Stem cells have been isolated from multiple sources in the human body including blood, bone marrow, muscle, liver, pancreas, and intestine [2], as well as from embryonic tissues and the placenta. Recently, adipose tissue has been identified as a source of self-renewing, multilineage regenerative cells known as adipose-derived stem cells (ASCs) [4]. These cells have the capacity to proliferate in culture and differentiate into multiple mature populations, displaying markers associated with adipocytes, osteoblasts, chrondrocytes, neural populations, endocrine pancreatic cells, hepatocytes, endothelial cells, smooth muscle cells and cardiomyocytes, depending on the culture conditions, including inductive media formulations containing stimulatory cytokines and growth factors [5, 6]. The advantages of ASCs over other stem cell sources include the availability and accessibility of adipose tissue, the ease of stem cell extraction, high cell yields (2.6-10.2 x 10^6ASCs/ 100 grams adipose tissue [5]), and ease of culturing. Further, the use of stem cells isolated from adult tissues avoids the ethical concerns associated with embryonic stem cells [6, 7]. ASCs have also been shown to be immunoprivileged [8]. For example, the presence

of cultured allogenic human ASCs did not activate a response from host T-cells within a human rheumatoid arthritis model [3, 8].

Common ASC isolation methods involve mincing of the extracted adipose tissues followed by collagenase digestion at 37°C. The resulting sample is then filtered to remove any undigested tissue fragments or debris, and the supernatant containing the mature adipocytes is removed, as they naturally float to the top due to their high intracellular lipid content. The collagenase is deactivated in medium containing fetal bovine serum, followed by centrifugation. The resulting pellet contains the stromal vascular fraction (SVF), including the ASC population [9]. This pellet is then further separated through filtration and centrifugation to obtain an ASC-rich pellet [10]. The ASCs are selected through their adherence to tissue culture plastic during culturing. However, the resulting population is still relatively heterogeneous, as measured by the expression of characteristic cell surface markers, as well as the genetic profile [1]. ASCs are typically grown in 2-dimensional tissue culture flasks (T-flasks) or well plates. The main advantages of these culturing methods are their ease of handling and simplicity. However, the 2-dimensional culturing methods that are typically employed for isolating and expanding ASCs are limited in terms of the number of cells that can be produced before negatively impacting ASC proliferation and differentiation. The exchange of gases between the ASCs and the culturing environment, such as oxygen and carbon dioxide, is limited to the medium/gas interface, and concentration gradients are created in the medium (for pH, dissolved oxygen, nutrients, metabolities, etc.). Long-term culturing to obtain clinically-relevant cell populations can result in substantial alterations in the cellular phenotype and differentiation potential, and traditional culturing methods are often associated with a loss in the stem cell potential to both proliferate and differentiate.

To circumvent the limitations of 2-D static culture on tissue culture polystyrene (TCPS), multicellular aggregate culture methods for ASCs have been developed [11]. These techniques improve cell-cell interactions, to provide a 3-dimensional mirco-environment for the ASCs that supports cell growth [12]. Cell-cell interactions are known to be important mediators of many cellular functions including proliferation, differentiation, apoptosis, and angiogenesis [12]. The production of extracellular matrix (ECM) proteins, such as tenascin C, collagen VI and fibronectin, and secreted soluble factors, such as hepatocyte growth factor (HGF), matrix metalloproteinase-2 (MMP2) and matrix metalloproteinase-14 (MMP14), are increased in ASCs cultured as multicellular aggregates versus monolayer cultures [13]. This suggests that the use of multicellular aggregates may improve tissue regeneration, promoting a more native growth environment for the ASCs.

The ECM is involved in many important roles in the body through its interactions with neighbouring cells, degrading enzymes and soluble cues. These cell-ECM interactions influence cell shape, survival, proliferation, differentiation, migration, and trafficking [14]. The main components of the ECM include collagens, laminins, tenascin, integrins, and proteoglycans. Bioscaffolds have been successfully developed from most tissues in the body through the use of chemical, physical, and biological decellularization processes that release the cells and other antigenic components from the ECM. These decellularization processes can maintain the structural integrity and composition of the ECM, while removing the majority of cells and cellular components. Therefore, these decellularized tissues are ideal candidates as scaffolding materials for cell growth, as they accurately mimic the native cellular micro-environment found within the body.

In addition to cell-cell and cell-ECM interactions, oxygen is another important factor to consider in the development of strategies for large-scale stem cell expansion. More specifically, oxygen is required for all aerobic metabolic cycles and is a potent cell signaling molecule. As such, oxygenation is one of the most important factors in the cellular microenvironment [15]. Interestingly, hypoxic concentrations (oxygen concentrations under 5%) have been shown to up-regulate the production of anti-apoptotic and angiogenic growth factors in human ASCs, such as vascular endothelial growth factor (VEGF) and basic fibroblast growth factor (bFGF), stimulating the growth of blood vessels and promoting tissue regeneration [16, 17]. Further, ASC proliferation is increased when the cells are cultured under hypoxic conditions, and the conditioned medium from ASCs in hypoxic cultures (2% O_2) has been shown to stimulate collagen production and cell migration in cultured human dermal fibroblasts [17].

The mass-transfer limitations that restrict the *ex vivo* growth of 3-dimensional tissues are a major challenge in the development of clinically-relevant tissue engineering strategies. Within traditional 2-D culture systems, soluble nutrients can become limiting factors for the *in vitro* proliferation of ASCs. For example, necrotic centers will develop in cellular aggregates with diameters larger than 0.5 mm [18]. To overcome these limitations, bioreactors have been shown to improve the proliferation of ASCs, and can produce cellular phenotypes that are more similar to those found in the native physiological environment [19].

Moving towards the optimization of the *in vitro* cell culture methods for human ASCs, the proliferation of ASCs as multicellular aggregates seeded on decellularized adipose tissue (DAT) [11, 20] and cultured within a custom-designed perfusion bioreactor system was investigated in this project. Within this system, the effect of a hypoxic growth environment on ASC proliferation was explored. Further, to probe the potential application of these constructs in adipose tissue

engineering, the adipogenic differentiation potential of the ASCs within the system was characterized in terms of glycerol-3-phosphate dehydrogenase (GPDH) activity, a key enzyme involved in triglyceride synthesis.

It is anticipated that the use of a bioreactor will enhance the cell response by improving nutrient delivery and waste removal. Further, the oxygen concentration within the culture system was hypothesized to affect the proliferation of the ASCs, with hypoxic conditions (5% oxygen) supporting greater ASC proliferation than normoxic conditions (21% oxygen) [21]. The use of multicellular aggregate seeding techniques was probed to improve ASC proliferation on the DAT, relative to seeding single-cell suspensions, and the cell seeding density was assessed as an important factor in mediating attachment and proliferation. More specifically, the use of the cellular aggregates was expected to increase the cell-cell interactions within the DAT, in order to support ASC attachment, long-term viability, and proliferation [12].

ASCs can be induced to differentiate into adipocytes through the addition of adipogenic medium. The cultured ASCs should be confluent before the induction of adipogenesis, as cell-cell interactions and cell-matrix interactions are involved in up-regulating the differentiation process [22]. Adipogenesis results in the formation of lipid vacuoles, increased secretion of leptin, glucose transporter 4 (GLUT4) and adiponectin, and the presence of adipogenic genes including adipocyte fatty acid binding protein (a-FABP), aP2 (protein involved in lipid accumulation adipocytes), peroxisome proliferator-activated receptor γ (PPARγ) and lipoprotein lipase (LPL) [9, 22]. The use of multicellular aggregates increases cell-cell interactions, and was investigated as a potential method for improving adipogenesis of ASCs.

1.2 Clinical Significance

The development of an optimized growth environment for ASCs in clinically useable quantities would have a significant impact in the field of tissue engineering. ASCs have been shown to differentiate into adipose, bone, cartilage, smooth muscle, endothelial, skeletal muscle, nervous and cardiac tissue. Therefore, ASCs could be useful in new treatments for a large variety of clinical applications, including liver failure, diabetes, Crohn's disease, stress urinary incontinence, spinal cord injuries and other neurologic disorders, myocardial infarction, dental implants, musculoskeletal disorders, cosmetic surgery, and soft tissue defects [3, 6, 9]. The ability to culture large populations of multipotent stem cells from small tissue biopsies will be critical for future clinical successes in all of these applications.

In particular, the fields of plastic and reconstructive surgery show a large potential for ASC-based therapies, including soft tissue defects from tumor resections, trauma, congenital abnormalities and aging. Current treatments often involve the use of synthetic fillers, which can cause a foreign body reaction, the formation of fibrous scar tissue, comparatively high infection rates and the need for re-operation [10, 21]. The current gold standard treatment for large-volume soft tissue augmentation involves the transfer of vascularized flaps of skin, fat, and muscle, which is very expensive and results in the creation of substantial donor site defects. The use of ASCs for soft tissue reconstruction could allow for patient-tailored treatment. To achieve this, ASCs seeded on an appropriate scaffolding material could be induced to undergo adipogenesis and implanted into the host. In this thesis, decellularized adipose tissue (DAT) was used to provide a 3-dimensional scaffold for soft tissue regeneration, since it has the same ECM architecture and composition that is found within healthy adipose tissues [20].

1.3 Hypothesis

The hypothesis for this project is that use of a perfusion bioreactor will enhance ASC attachment and proliferation on decellularized adipose tissue (DAT) scaffolds cultured under hypoxic conditions, as compared to static cultures. The implementation of the bioreactor strategy will also enhance *in vitro* adipogenesis of the ASCs cultured on the DAT.

1.4 Research Objectives

The main objective of this research program is to obtain clinically-relevant quantities of ASCs ($10^9 – 10^{10}$) from small tissue biopsies. This research is highly valuable to tissue engineering applications, as it would facilitate the translation of autologous stem cells, which could be differentiated and implanted for a wide range of regenerative strategies.

The ability to obtain these large ASC quantities will be realized through the investigation of the proliferation of ASCs on DAT scaffolding within a perfusion bioreactor system. Through the modification of the scaffold microenvironment, medium flow rate, and systemic oxygen concentration, the growth conditions for ASC proliferation will be optimized.

The specific objectives of this thesis project were:

1. To compare the proliferation of ASCs cultured in normoxic (21%) versus hypoxic (5%) environments.
2. To optimize the initial seeding protocols and density of human ASCs on DAT scaffolds cultured within the perfusion bioreactor system, in terms of proliferation under hypoxic (5%) conditions in comparison to static culturing.
3. To confirm the adipogenic differentiation potential of ASCs cultured on DAT scaffolds within the perfusion bioreactor system.

Chapter 2

Literature Review

Stem cell research has been in the public eye recently due to its potential to treat many diseases such as diabetes, myocardial infarction, autoimmune diseases, musculoskeletal disorders, and central nervous system damage, as well as to regenerate damaged tissue and organs [9]. There are many different types of stem cells within the human body, including embryonic stem cells (ESCs), mesenchymal stem cells (MSCs), hematopoietic stem cells (HSCs), and neural stem cells (NSCs) [2]. There is controversy over the use of ESCs, since their harvest requires the use of human embryos raising ethical concerns. MSCs can be found in adult tissues derived from the embryonic mesenchyme including bone marrow, blood, muscle, liver, pancreas, and intestine [2].

Adipose derived stem cells (ASCs) are those derived from adult adipose tissue and have the ability to differentiate into cells of osteogenic, adipogenic, myogenic and chondrogenic cell lines [22]. Adipose tissue as a source of stem cells has the advantages of causing minimal harm to the donor during extraction, initiating minimal immune reactions if autologous, and being readily available [4].

2.1 Physiology of Adipose Tissue

The main function of adipose tissue is to insulate and cushion the body. There are at least 5 types of adipose tissue existing within the human body including bone marrow, mammary, mechanical, brown adipose tissue and white adipose tissue [23]. The main function of brown adipose tissue (BAT) is to provide heat to the body in neonates, while white adipose tissue (WAT) is primarily an energy source. However, WAT also functions as an endocrine organ with

the secretion of angiotensinogen, acylation-stimulating protein, adiponectin, adipsin, retinol binding protein, tumour neorosis factor- α (TNF- α), interleukin-6 (IL-6), plasminogen activator inhibitor-1 (PA- I), and it plays roles in the metabolism of sex hormones [1, 24].

Along with ASCs, mature adipocytes, fibroblasts, vascular smooth muscle cells, endothelial cells, resident macrophages, nerve cells, and lymphocytes are found within adipose tissue [6]. Mature adipocytes are non-proliferating, and are therefore not good candidates as cell sources for tissue engineering. These mature cells are composed of approximately 90% intracellular lipid, and are surrounded by a complex matrix of collagen fibers [24].

2.2 The Extracellular Matrix

Along with cells, the extracellular matrix (ECM) composes all of the tissues in the human body. The ECM is involved in mediating many important cellular functions through its interactions with neighbouring cells, degrading enzymes, and soluble cues. These cell-ECM interactions influence cell shape, survival, proliferation, differentiation, migration, and trafficking [14].The main components of the ECM include collagens, glycosaminoglycans, non-collagenous structural proteins, and proteoglycans. The basement membrane is an important type of ECM that is composed of laminin, network-forming collagen type IV, nidogen, and perlecan [25]. Adipose tissue is enriched in basement membrane, which forms the network that surrounds every mature adipocyte. The basement membrane plays important roles during embryonic development, wound healing, and angiogenesis.

Collagens are responsible for the basic structure of the ECM, providing its structural integrity. Many of the fibrillar collagens, including types I, II, III, V, and XI, impart tensile strength [25] in healthy tissues. Laminins are produced by epithelial cells, smooth muscle, skeletal muscle and cardiac muscle cells, nerve cells, endothelial cells, and bone marrow cells,

amongst others, in more than 12 different isoforms that are secreted primarily into the basement membrane. Through binding with cell-surface integrins, laminins promote interactions between cells and the basement membrane, leading to cell adhesion, migration and differentiation [25]. Mechanical continuity is achieved through the linking of integrins with the intracellular actin microfilament system of the cytoskeleton through a variety of proteins. Signaling conducted through integrin-integrin interactions influences cell survival, proliferation, the structure and functional activity of the cytoskeleton, and gene transcription [25].

Other ECM components include the cell-adhesive glycoprotein fibronectin, paracrine signaling molecules including TGF-β (hormone involved in cell growth and differentiation and the composition of the ECM), fibroblast growth factor (FGF), and other growth factors that mediate cell behavior and function [14].

2.3 Stem Cell-based Therapies in Tissue Engineering

Tissue engineering aims to replace or repair failing organs through the combination of stem cells, biomaterials and growth factors [23]. The ideal stem cell source for use in tissue engineering needs to be easily harvested in a minimally invasive procedure, found in large quantities, capable of differentiating in a controlled and reproducible manner, safe and effective in autologous or allogeneic applications, and can be produced according to "Good Manufacturing Practice" (GMP) guidelines [23].

Stem cells are currently being investigated in clinical applications for the treatment of diabetes, rheumatoid arthritis, Crohn's disease, liver cirrhosis and regeneration, fistulas, cardiovascular disease, limb ischemia, lipodystophy, graft-versus-host disease, neurological dysfunctions such as Parkinson's disease and Alzheimer's, multiple sclerosis, soft tissue augmentation, skin wounds and bone tissue repair [1-3]. To date, there have been human trials

using stem cells to treat heart disease, chronic wounds, neurological and nervous disorders, soft tissue reconstruction and orthopedic applications [1]. For example, hematopoietic stem cells (HSCs) are currently being applied in bone marrow transplants for cancer patients to improve the hematopoietic system weakened from radiation or chemotherapy [2]. Similarly, neural stem cells (NSCs) have the potential to repair spinal cord or brain injuries, such as a stroke, and neurodegenerative diseases, such as Parkinson's disease or Alzheimer's [2].

In the field of soft-tissue engineering, current treatments often require the use of synthetic fillers or foreign implants into the body, which often cause a foreign body reaction, the formation of fibrous scar tissue, high infection rates, and the need for re-operation [10, 21]. One proposed strategy is to obtain a sample of the patient's own adipose tissue through liposuction or fat biopsy to use in isolating ASCs and endothelial cells. Once expanded *ex vivo*, these cells can be seeded onto a biodegradable polymer scaffold, which degrades as the ASCs proliferate and differentiate into mature adipose tissue, and a supporting microvascular system is formed by the co-cultured endothelial cells [26].

For the treatment of diabetes, ASCs have been shown to be able to differentiate into insulin-producing cells using a glucose-regulated method that involves controlled gene expression. When injected into diabetic rats, these modified ASCs reduced glucose levels and were able to maintain a normoglycemic state [6]. Clinical trials on therapies using ASCs include graft-versus-host disease, autoimmune-induced rheumatoid arthritis (RA), Crohn's disease, and chronic ulcers [3]. The results to date have shown no significant adverse effects and highlight the ability of the ASCs to suppress T-cell and inflammatory responses, while stimulating antigen-specific regulatory T-cells to enhance wound healing [3]. It is believed that ASCs improve injured or diseased tissue through the secretion of cytokines and growth factors, recruiting

endogenous stem cells to the regenerating tissues and promoting their differentiation along the required lineage [23].

In order to achieve tissue growth and the manufacture of bioartificial tissues similar to those found in their native environment, the optimization of scaffolds and bioreactors is needed for controlled 3-dimensional cell growth and *ex vivo* tissue formation [27].

2.4 Stem Cell Sources

Stem cells can be classified as either embryonic stem cells (ESCs) or adult stem cells. ESCs are pluripotent, meaning they have the ability to differentiate into any cell lineage except those involved in the formation of extra-embryonic membranes or the placenta, and are isolated from the inner cell mass of developing blastocysts [28]. Adult stem cells are found in multiple tissues including bone marrow, adipose tissue, blood, muscle, brain, skin, testis, liver, pancreas and intestine [1, 2, 29]. Advantages of using adult stem cells are that they are not associated with the same ethical issues present for the use of ESCs and they have the potential to be used in autologous therapies, avoiding immunological issues [29].

2.4.1 Mesenchymal Stem Cells

Mesenchymal stem cells (MSCs) are found throughout the body and are typically isolated from the stromal cell fraction of tissues derived from the mesenchymal lineage through the selection of the adherent cell fraction on tissue culture plastic [2, 4]. MSCs are multipotent and have the potential to differentiate into multiple cell types including adipocytes, chondrocytes, myoblasts, osteoblasts, tenocytes and nerve-like cells [7, 24]. The *ex vivo* expansion of MSCs is required to obtain sufficient numbers for clinical applications. MSCs have a fibroblast-like morphology when cultured *in vitro* [24].

2.4.1.1 Bone Marrow-Derived Mesenchymal Stem Cells

Bone marrow-derived MSCs are isolated from the stromal component of bone marrow. The major limitations of the use of bone marrow-derived MSCs in tissue engineering are that their extraction procedure is painful, causes cell morbidity and produces low yields [7]. It has been shown that as the MSC donor ages, the yield significantly decreases [29].

2.4.1.2 Adipose-Derived Stem Cells

ASCs are also multipotent, having the ability to differentiate and display markers associated with mature adipocytes, osteoblasts, chondrocytes, neurons, endocrine pancreatic cells, hepatocytes, endothelial cells, and cardiomyocytes [6]. ASCs have been shown to induce angiogenesis through the expression of multiple hematopoietic and angiogenic cytokines, including vascular endothelial growth factor (VEGF) [16].

The proliferation rate and differentiation capacity of ASCs have been shown to be donor dependent and are affected by the age of the donor, type of adipose tissue extracted (white versus brown adipose tissue), site of extraction (subcutaneous versus visceral adipose tissue), extraction procedure, isolation methods, culturing conditions, media formulations and plating density [30]. When cultured *ex vivo* for extended periods, ASCs experience changes to their proliferation and differentiation capacities [24].

ASCs are an attractive stem cell source due to their much greater abundance in the body than bone marrow-derived MSCs, with ASCs representing 1% of adipose cells and bone marrow-derived MSCs representing only 0.001-0.02% of bone marrow cells [6]. ASCs can be obtained through relatively simple and painless procedures, such as liposuction or fat biopsy, with reduced morbidity. In addition to the general abundance of adipose tissue, ASCs are easier to culture and also proliferate faster than bone marrow-derived MSCs [6, 7, 26]. The average doubling time of

tissue cultured ASCs is between 4 to 5 days [31]. Further, ASCs have been shown to be immunoprivileged, and they do not express major histocompatibility complex (MHC) class II antigens [16].

2.4.2 ASC Immunophenotype

In order to classify ASCs, the expression of several markers is required. Genes for cell adhesion, matrix proteins, growth factors and receptors, and proteases are commonly used in the identification. Table 2.1 illustrates the expression profile of human ASCs.

Table 2.1: Human ASC expression profile [4, 5, 9, 32]

	Human ASC Expression Markers
High Expression	***Adhesion Molecules*** HLA- ABC, CD9 (tetraspan protein), CD10 (neutral endopeptidase or common acute lymphocytic leukemia antigen; CALLA), CD13 (aminopeptidase), CD29 (integrin β1), CD34 (cell-cell adhesion molecule and surface glycoprotein), CD44 (cell surface glycoprotein for hyaluronate receptor; also binds to laminin, collagen and fibronectin), CD49e (integrin α5/VLA- 5), CD51 (integrin αV), CD54 (intercellular adhesion molecule 1; ICAM-1), CD55 (decay accelerating Factor), CD59 (complement protectin), CD71 (transferring receptor), CD73 (ecto-5'-nucleotidase), CD90 (Thy-1; related with multipotent progenitor activity), CD 146 (MUC-18; expressed in human endothelium), CD166 (activated lymphocyte cell adhesion molecule; ALCAM)

	Growth Factor-Related FGFs 2, 6, and 7, FGF receptor 3, neuropilin-1,TGF-β receptors 2 and 3; SPARC (osteonectin), osteopontin, fibronectin-1, VEGF-D, TNF-α, CD105 (endoglin; regulatory component of the TGF-β receptor complex through the mediation of cellular responses to TGF-β1) ***Matrix-Related*** (MMP2) gelatinase A, smooth muscle actin, vimentin
Variable Expression	CD49b (integrin α2/VLA-2), CD49d (integrin α4/VLA-4), CD61 (integrin β3), CD138 (syndecan-1), and CD140a (PDGFR-β)
No Expression	HLA-DR, CD4, CD8a, CD11a (integrin αL), CD11b (integrin αM), CD11c (integrin αX), CD14 (lipopolysaccharide receptor; LPS), CD18 (integrin β2), CD41a (gpIIb), CD45 (leukocyte common antigen; LCA), CD49f (integrin α6/VLA-6), CD62L (L-selectin), CD62P (P-selectin), CD106 (vascular cell adhesion molecule; VCAM-1; α4-β1 ligand), CD117 (c-kit), CD133, CD243 (MDR-1), and ABCG2

ASCs produce collagen I and III, support angiogenesis through the secretion of VEGF, TGF-β, and hepatocyte growth factor (HGF); support hematopoietic events through the secretion of granulocyte colony-stimulating factor (G-CSF), macrophage colony-stimulating factor (M-CSF), granulocyte macrophage colony-stimulating factor (GM-CSF) and interleukin-7; and mediate inflammation through the secretion of interleukin-6, interleukin-8, interleukin-11, and TNF-α [1].

The expression profile of ASCs is very consistent and is over 90% similar to that of bone marrow-derived MSCs, with a few differences [23]. MSCs have been shown to express CD106, which is not always expressed in ASCs, while ASCs express CD49d, which is not always found in MSCs [1, 22]. *In vitro* culturing leads to changes in ASC immunophenotype. The expression of CD34, MHC class I and II molecules, CD80, CD86, CD45, CD11a, CD14, CD117, HLA-DR, CDKN1B, INS, ITGA5, NOG, UTF1, WNT6 and WNT8A often decrease with culturing, while the expression of CD9, CD13, CD29, CD44, CD63, CD73, CD90, CD105, CD166, ACTG2, ACVR1, BMPR2, CTNNB1, CCNE1, CDH1, COL6A2, HSPA9, IL6, ITGA8, ITGB1, ITGB5, MDM2, PTEN, PUM2, SNAI2, TGFBR1 and VEGF-A tend to increase [1]. This results in a more homogeneous cell population with extended culturing [3].

An important property of ASCs is their lack of HLA-DR expression, which is involved in their immunoprivileged status. ASCs also suppress the proliferation of activated allogenic lymphocytes and the production of inflammatory cytokines through CD4 T-helper cells; induce the production of the anti-inflammatory cytokine IL-10 via monocytes and T cells; and induce the production of antigen-specific regulatory T cells [3].

2.4.3 Cell Extraction Techniques

With the rise in obesity, there are large quantities of adipose tissue that can be obtained through minimally-invasive surgeries. Adipose tissue is generally obtained from either resection, tumescent liposuction or ultrasound-assisted liposuction. Oesayrajsingh-Varma *et al.* (2006) found the yield of stromal vascular cells was approximately 0.5-0.7 x 10^6 cells/g adipose tissue, with ~ 82% viability after the extraction procedure [5]. Ultrasound-assisted liposuction decreases the frequency of proliferating ASCs, and ASCs extracted with these methods typically have longer doubling times [5]. In the study, approximately 6% of the stromal vascular fraction from

resected adipose tissue was plastic adherent and proliferated, as compared to only 0.4 % from ultra-sound assisted liposuction [5].

Common ASC isolation methods involve mincing the extracted adipose tissue followed by collagenase digestion at 37°C. The resulting sample is then filtered to remove any undigested tissue, and the supernatant containing the mature adipocytes is removed. The mature adipocytes naturally float to the top due to their high lipid content. The collagenase is neutralized by the addition of medium containing fetal bovine serum followed by centrifugation. The resulting pellet contains the stromal vascular fraction [9]. This pellet is then further separated through pipetting and repeated centrifugation to obtain an ASC-rich pellet [10]. The ASCs are selected through their adherence to tissue culture plastic (TCPS) during culturing [1].

Zhu *et al.* (2009) showed that the age of the donor did not affect the adipogenic potential of the ASCs, however the osteogenic potential decreased with increasing donor age. In this study, the proliferation rate was slightly slower among ASCs obtained from older donors, but this was relationship not significant [7]. Mojallal *et al.* (2011) found that the age and body mass index (BMI) do not statistically significantly affect the yield and proliferation rate of ASCs. While there was a slight decrease in proliferation rate with increasing BMI, this was not significant [33].

2.4.4 ASC Expansion in Culture

The main goal of *ex vivo* expansion of ASCs is to produce high enough numbers of stem cells for use in clinical applications [27]. ASCs are typically grown in 2-dimensional tissue culture flasks (T-flasks) or well plates. The main advantages of these culturing methods are their standardization, ease of handling and simplicity. However, the exchange of gases, such as oxygen and carbon dioxide, is limited to the medium/gas interface, and the creation of concentration gradients in the medium (for pH, dissolved oxygen, nutrients, metabolities, etc.) is a major

disadvantage. On-line monitoring and control of culturing parameters is very difficult using traditional static culturing methods [34]. In order to obtain clinically relevant yields of ASCs, large numbers of T-flasks are needed, which requires significant incubator space, increased manual labour spent feeding and passaging cells, high costs, and increased risk of contamination [34]. This process also requires 3 – 5 weeks of culturing, which is significant for tissue engineering applications. Therefore culturing methods that reduce the cell culturing time and costs are of great importance [35]. *In vitro* expansion of the adherent cells from the stromal vascular fraction of adipose tissue results in a homogeneous population of ASCs, which depending on the culture conditions, can maintain their multilineage differentiation potential to some extent [3].

Fetal bovine serum (FBS) is typically added to the culture media at concentrations around 10%. FBS provides the ASCs with nutrients, attachment factors and growth factors, but unfortunately serum formulations are mostly uncharacterized. Lot-to-lot variability in the serum composition makes it difficult to produce consistent results. To obtain large-scale use in clinical applications, any animal products must be removed from the cell culture processes to eliminate any xenogeneic-related safety issues, such as the transfer of xenogeneic antibodies, bacterial or viral infections, prions or generating an immune response [1, 3]. As such, recent research efforts have focused on the use of human serum or serum alternatives for culturing ASCs [36, 37].

2.4.4.1 Impact of Oxygen Tension on ASC Expansion

Oxygen is required for ASC survival as it is involved in all aerobic metabolic cycles, and it is often the limiting factor on the maximum number of cells that can be grown in culture or the final size of a tissue-engineered construct. The oxygen solubility in the average culture medium at atmospheric oxygen conditions is 0.2 mmol O_2/L [15]. This is much lower than the solubility of

other important nutrients, such as glucose (20 mM), and stresses the importance of replacing the medium, or in the case of bioreactors, constant circulation.

However, high oxygen concentrations can also negatively affect the growth of ASCs. The production of reactive oxygen species (ROS) is increased when pure oxygen is used instead of air or when the gas pressure is increased [15]. The presence of ROS is known to cause damage to cell membranes DNA and proteins, therefore changing the normal cell function. Further, both hypoxic and hyperoxic environments have been linked to apoptosis (programmed cell death) [38].

Oxygen is also an essential signal stimulus. ASCs play an important role in normal wound healing through the production of soluble factors including VEGF and bFGF. Lee *et al.* (2009) have shown that the production of these two proteins, as well as the ASC proliferation rate, is significantly increased under hypoxic conditions. Hypoxia also augments the production of collagen and accelerates cell migration, to enhance wound healing [17].

Hypoxic culturing is typically performed with an oxygen concentration of 5% or less. Hypoxic culturing for human ESCs has been shown to decrease the amount of spontaneous cell differentiation, with no effect on their growth [38]. In work by Potier *et al.* (2007), bone marrow-derived MSCs exposed to hypoxic conditions for 48 h showed no signs of increased cell apoptosis. However, when the MSCs were grown for 72 or 120 hours under hypoxic conditions, they experienced a 3% and 55% increase in cell death rates respectively [39].

In another study using human bone marrow-derived MSCs, Dos Santos *et al.* (2010) studied the effects of hypoxia on cell proliferation kinetics and metabolism. At every time point during the 12 day experiment, the MSCs cultured under hypoxic conditions had higher cell numbers, higher specific consumption of nutrients (glucose and glutamine), lower production of inhibitory metabolites (lactate and ammonia) and greater colony forming unit (CFU-F) expansion

[35]. Cell kinetics showed that the hypoxic MSCs experienced a shorter lag phase, and therefore entered the cell cycle earlier during culture. However, the immunpohenotype and differentiation potential of the MSCs was not affected by the oxygen concentration in the culturing environment [35].

2.5 Multilineage Differentiation of ASCs

The potential to differentiate into multiple cell lineages including adipose, bone, cartilage, smooth muscle, endothelial, skeletal muscle, nervous and cardiac tissue requires the addition of lineage-specific induction factors. There is large donor variability in the differentiation capacity of ASCs. This can be affected by the gender, anatomic harvest location, age, and BMI [1].

2.5.1 Adipogenic Differentiation

ASCs can be induced to differentiate into adipocytes through the addition of adipogenic medium. This medium typically contains insulin or insulin-like growth factor-1 (IGF-1), isobutylmethylxanthine (IBMX; phosphodiesterase inhibitor), hydrocortisone or dexamethasone (glucocorticoid receptor agonist), indomethacin or a thiazolidinedione (peroxisome proliferator activated receptor-γ ligand), pantothenate, biotin, transferrin and/or triiodothyronine [3, 9]. The cultured ASCs must also reach confluence before the induction of adipogenesis, as cell-cell interactions and cell-matrix interactions are involved in the process. Once the ASCs commit to the preadipocyte lineage, their proliferation is stopped [22].

Adipogenesis results in the formation of lipid vacuoles, increased secretion of leptin, glucose transporter 4 (GLUT4) and adiponectin, and the presence of adipogenic genes including adipocyte fatty acid binding protein (a-FABP), aP2 (protein involved in lipid accumulation adipocytes), peroxisome proliferator-activated receptor-γ (PPARγ) and lipoprotein lipase (LPL)

[9, 22]. Adipogenesis is also accompanied with the increased expression of lipid-metabolizing enzymes, including glycerol-3-phosphate dehydrogenase (GPDH), fatty acid synthetase (FAT), fatty acid transporter, and hormone-sensitive lipase (HSL) [40].

Adipogenic differentiation is a two-step process. In the first step (determination), the ASC commits to the adipogenic lineage, followed by terminal differentiation, where the committed cell becomes a mature adipocyte. In determination, the ASC becomes a pre-adipocyte, and while it has the same morphology, it has a reduced capacity to differentiate into other lineages. Terminal differentiation is characterized by the formation of intracellular lipid droplets, and increased secretion of adipocyte-specific proteins [41]. Adipogenesis is a very complex process and our understanding of it is still growing. Expression of various transcription factors in a defined sequence mediates the process. PPARγ is considered the master regulator of adipogenesis, and its presence is required for the initiation of adipogenesis [40, 41].

Other regulators of adipogenesis include the TGF-β superfamily members, bone morphogenetic proteins (BMPs), myostatin, insulin and insulin growth factor-1 (IGF1). While adipose tissue and mature adipocytes express TGF-β, its presence inhibits the differentiation of pre-adipocytes [41].

2.5.2 Osteogenic Differentiation

Osteogenesis requires the formation of a low density cell culture, since the 3-dimensional environment and cell spreading are critical to the process [9]. Osetogenic medium typically includes ascorbate, β-glycerophosphate, dexamethasone and vitamin D3 [9].

Osteogenesis results in increased expression of alkaline phosphatase (ALP), bone morphogenic proteins (BMP), bone sialoprotein (BSP), CBFA-1/RUNX2, osteocalcin (OCN), osteonectin (ON), osteopontin (OP), and collagen type I, amongst other genes and proteins. Bone

matrix production is an important step of the process in which calcium phosphate mineral is deposited within the ECM, along with collagen, OP and BSP [9, 22]. The ASCs also undergo a change in morphology from spindle-shaped to cuboidal [7]. Common techniques used to confirm osteogenesis include measuring ALP activity and von Kossa staining for ECM calcification [31].

2.5.3 Chondrogenic Differentiation

In order to induce the differentiation of ASCs into chondrocytes, ASCs are cultured in pellet culture, which resembles the pre-cartilage condensation during embryonic development and increases cell-cell interactions. Chondrogenic medium containing transforming growth factor-β1 (TGF-β1), ascorbate-2-phosphate, L-proline and dexamethasone is typically added.

Chondrogenesis results in the formation of nodules and increased expression and secretion of cartilage ECM proteins including collagen type II and VI, aggrecan, keratin and chondroitin-4-sulfate. There is also an increased amount of sulfated glycosaminoglycan in the cartilage matrix. Common methods to confirm chondrogenesis include Toluidine Blue staining for charged proteoglycans in the ECM and immunohistochemistry for collagen type II [3, 22, 31].

2.5.4 Alternative Lineages

In the presence of specific induction media, ASCs also have the ability to differentiate into many other cell types including myocyte (including smooth muscle, skeletal myocyte and cardio myocyte), neural lineage, endothelial and hepatocyte-like cells. More specifically, hepatocyte-like cells that express albumin and α-fetoprotein can be induced through the addition of growth factors including HGF, FGF1 and FGF4 [3, 6]. ASCs have also shown the ability to differentiate into early neural cells. Upon induction, the ASCs retract, forming compact cell bodies with elongated cytoplasmic processes similar to that of axons, with a bipolar or branching arrangement. The differentiating cells express proteins associated with neural cell populations

including nestin, intermediate filament M, and glial fibrillary acidic protein (GFAP; protein associated with oligodendrocyte differentiation) However, the expression of mature neuronal subtypes was absent, meaning that the cells present were only early neuronal cells with limited function [3, 22, 31].

ASCs also have the potential to differentiate along the myogenic lineage. ASCs form multi-nucleated cells capable of expressing myosin heavy chain; transcription factors including myf6, myf5, myod1 and myogenin; and structural proteins such as desmin, an intermediate filament protein. When cultured with TGF-β and sphingosylphosphorylcholine, ASCs differentiate into smooth muscle cells, expressing α-smooth muscle actin and calponin. Differentiation into skeletal myocytes is associated with the expression myoD, myogenin, and myosin light chain kinase. Cardiomyocytes have been produced through the addition of 5-azacytadine. These cells showed spontaneous beating and expressed the cardiomyocyte specific proteins, troponin I, myosin heavy chain, sarcomeric α-actinin, desmin, and connexin 43 [6, 22].

2.6 Effects of Long-term 2-D Static Culture

As discussed, ASCs are typically cultured on 2-dimensional TCPS. However, the attachment of ASCs to tissue culture plastics and their passaging significantly affects the cellular phenotype. The stromal vascular fraction of adipose tissue that is isolated and initially plated on the TCPS is very heterogeneous and contains cells from the hematopoietic and endothelial lineages, as wells as ASCs. After extended culturing, the percentage of hematopoietic and endothelial cells decreases, while that of the ASCs increases [4].

ASC growth *in vitro* generally exhibits a 48 hour lag phase, followed by a 7 day log phase, and finally, a plateau. Zhu *et al.* (2009) found an average doubling time of 53 hours for passage 1 ASCs isolated from liposuction procedures [7]. While culturing periods up to 6-8

weeks can have minimal impact on the differentiation potential of ASCs, long-term culturing of 4-5 months can lead to substantial changes in the cell populations, or in some cases, even spontaneous differentiation. Further, one study demonstrated that minor chromosomal abnormalities were detected in early passage cells using traditional culturing methods, which could have the potential to negatively affect the patient once implanted [3].

2.7 Multicellular Aggregate Culture Methods

Cellular gene expression is regulated in part by the exchange of paracrine protein signals between neighboring cells [27]. It is believed that culturing ASCs in the form of multicellular aggregates (MAs) can improve cell-cell signaling and cell-matrix signaling. The ASCs within the MAs maintain the capacity to adhere to tissue culture plastic, as well as to proliferate and differentiate along multiple lineages. MA methods are also capable of reducing the donor-to-donor variability that exists when ASCs are cultured in monolayer [13]. MAs provide the ASCs with a 3-dimensional growth microenvironment more similar to that found *in vivo*. This is believed to enhance proliferation, differentiation, and angiogenesis [12].

One method for the creation of MAs is the hanging drop method [11]. In this approach, the MAs are achieved by suspending approximately 20,000 – 25,000 ASCs in a droplet of medium on the top of a tissue culture dish, which is subsequently inverted. After 12 – 24 hours, the individual ASCs will have naturally aggregated due to the gravitational forces and these MAs can be removed for further culturing.

Amos *et al.* (2010) showed that when ASCs were formed into aggregates, the expression of extracellular matrix proteins such as tenasin C, collagen VI, and fibronectin, as well as the production of soluble factors such as HGF, VEGF, bFGF, fibrinogen, keratinocyte growth factor (KGF), matrix metalloproteinase-2 (MMP2), and MMP-14 were increased. These aggregates

were then compared to ASCs cultured in suspension for the treatment of diabetic wounds. The group found that the rate of wound closure was significantly higher when the wounds were treated with the MAs. The mechanisms for the improved functions of ASCs in MAs may be related to the increased release of paracrine signals or through the delivery, production and remodeling of the ECM [13].

In another study by Bartosh *et al.* (2010), it was found that during the formation of MAs using bone marrow-derived MSCs, a loose network was initially formed which compacted with increasing time. The size of the MSCs after 96 hours was one-fourth of that of plastic adhered MSCs, but the cells were spherical in shape. The size of the MA was dependent on the number of MSCs present in the medium droplet. They compared MAs with varying initial amounts of MSCs. While all MAs had higher expression and secretion of the anti-inflammatory molecule TNF-α stimulated gene/protein 6 (TSG-6) compared to adherent MSCs, MAs containing 25,000 MSCs had the highest expression and secretion. Almost 90% of the 25,000 MSCs in the MAs were viable at 3 days. In contrast, when the MAs were produced using 100,000 or 250,000 cells, the amount of apoptotic cells increased, resulting in the creation of a necrotic core [42]. The MSCs in the MAs also showed increased expression of other anti-inflammatory/anti-apoptotic proteins, and greater suppression of inflammatory responses in a mouse model.

2.8 Potential Limitation to Clinical Translation

The potential applications for ASCs include the repair or replacement of many damaged tissues within the human body. Research to date has involved the use of small animal models, however there have been only a small number of clinical trials involving humans.

Once implanted, any cell-based tissue-engineered construct must create its own blood supply to remain viable to promote cell growth and proliferation. The current size limit for viable

tissue implants is only a few 100 μm, as this is the diffusional limit of oxygen and nutrients. In order to produce larger tissues, the growth of new blood vessels within the construct is required. Therefore the vascularity of the ASC constructs will need to be improved, including the ability to induce the migration of endothelial progenitors cells from the host tissues [9, 16, 27].

The majority of tissue engineering applications are desired to be custom-made to meet the individual needs of each patient. Also, large numbers of ASCs are needed, therefore requiring *in vitro* expansion. Since the proliferation, differentiation capacity, phenotype and genotype are known to change with respect to culture time, culture conditions for the ASCs still need to be optimized [3]. In addition, there can be a large variation in the number of ASCs obtained from the donor, as well as their proliferation rate and differentiation capacity. For example, there is a significant negative correlation between BMI and adipogenic potential [43]. Donor health may also affect the growth of the ASCs. These effects need to be more fully understood so that we can develop predictable strategies for tissue regeneration with ASCs [1, 44].

Tissue constructs are generally evaluated by the cellular properties such as cell viability, cell expression and secretion of proteins. However, since tissue is comprised of cells and extracellular matrix, tissue-specific evaluation methods and criteria must be developed [27]. In order to identify ASCs, a panel of protein expression markers is generally used. No consensus has been reached on which markers to use, and the methods currently used are not consistent within the literature today. A better understanding of how the growth environment, including 3-dimenisonal environments, influences ASC proliferation and differentiation is required to maximize their therapeutic potential [1].

The production of ASCs for clinical applications must also meet current good manufacturing practices (GMPs) including *in vitro* quality assurance and control. The use of

bioreactors to culture the ASCs are required to: (i) reduce the risk of bacterial, fungal or viral contamination; (ii) provide continuous on-line monitoring of the culture environment, including oxygen, lactate and glucose levels; (iii) enhance proliferation and viability; and (iv) reduce costs and scale up production [9]. There is also the concern that the implantation of ASCs may result in the formation of malignant cells. Further research is needed to fully understand the long-term impact of ASCs inside the human body [10].

2.9 Bioreactor Strategies for Cell Expansion

Current limitations to the clinical use of ASCs include the ability to produce large amounts of ASCs, high manufacturing costs, mass transfer limitations, donor-to-donor variability, and microbiological contamination. Culturing ASCs in tissue culture plastic flasks is very time and labour intensive, and only a limited expansion of ASCs can be achieved. For use in therapeutic applications, 1×10^9 to 1×10^{10} stem cells may be required [34]. The complex cell-cell, cell-matrix and growth factor interactions make the proliferation and differentiation of ASCs a very technical challenge [34].

Bioreactors allow the monitoring and control of environmental and operating conditions such as pH, temperature, pressure, oxygen concentration, nutrient supply and waste removal. This is critical to meet the current GMPs, as reproducible results can be achieved. ASCs cultured in bioreactors express phenotypes more similar to those found in the native environment, as compared to those grown in static culture conditions [19]. Improved nutrient delivery and waste removal within the bioreactor could allow the formation of larger constructs [18]. Further, ASCs produce ammonia and lactate through metabolism processes, and the accumulation of these products leads to cell death in static culturing. Continual removal of these cytotoxic products in bioreactors could improve cell growth [27].

Bioreactors generally fall under two classifications: (i) batch or (ii) perfusion systems. Primary concerns with the use of bioreactors for mammalian cell culture include the amount of shear stress applied to the cells, the amount of oxygen reaching the cells, and the formation of cell aggregates. While the agitation of the medium is required to maintain the cell suspension, agitation creates turbulence, resulting in shear stress that can damage the cell or disrupt cell aggregates [27]. The amount of shear stress experienced by the cells is also dependent on the impeller diameter, geometry and positions in stirred reactors, as well as the presence of probes or other internal vessels. Shear stress has been shown to induce the differentiation of stem cells into specific cell types, including endothelial and osteogenic cells, showing the importance of determining the optimal shear stress values for each cell type [15]. Carrier *et al.* (2002) found that the use of perfusion significantly improved the spatial uniformity of cardiomyocyte cell distribution [45]. Scherberich *et al.* (2010) also showed improved formation of vasculogenic and osteogenic grafts with ASC when a perfusion bioreactor was used for culturing, as compared to static culturing [44].

ASCs can be cultured as single cells, in aggregates, or on microcarriers in the bioreactor systems. After culturing in a bioreactor, MSCs have been shown to maintain their stem cell phenotype [46]. Thus, the use of bioreactors has shown great promise for stem cell applications. Optimal design and operating conditions need to be determined for the specific tissue or application, including matching the exchange of metabolic waste and nutrients in the bioreactor to that experienced *in vivo* [34, 46].

2.9.1 Reactor Types

There is a large variety of bioreactors available for use in tissue engineering applications. The main types of reactors include spinner flasks, stirred flask bioreactors, rotating wall vessel

bioreactors (RWV), wave bioreactors, perfusion bioreactors, parallel plate bioreactors, hollow-fiber bioreactors, and fixed and fluidized bed bioreactors.

Spinner flasks were one of the first types of bioreactors, and are comprised of a reactor vessel containing an impeller to mix the contents. The scaffolds are attached to these impellers and enough medium is added to the vessel to ensure the scaffolds are covered. The use of spinner flasks to culture seeded polymer matrices resulted in improved cellularity and a more uniform cell distribution compared to static culturing. The tissues formed within the spinner flasks contained significantly higher cell densities and ECM proteins compared to static cultured tissues, reaching levels similar to those found in native tissues [47].

Stirred flask bioreactors feature a magnetic stirrer with a stir bar that rotates along the bottom of the vessel. This stirring increases the mass transport and homogeneity of the medium within the culture vessel and reduces the concentration boundary layer at the construct surface. However, this mixing also generates friction that can be harmful to cell viability. The reactor vessel is generally between 100 to 1000 mL, and general mixing speeds range from 50 to 80 rpm for cell culturing [15]. Luni *et al.* (2011) found reduced cell adhesion at the end of culturing in a stirred flask bioreactor compared to static culturing and believed this was due to the shear forces on the cells [48].

Rotating wall vessel bioreactors were designed to simulate microgravity effects. The scaffold is placed in the middle space between two concentric cylinders and oxygen is provided through gas exchange through the stationary inner cylinder. The outer cylinder rotates at a rate to maintain the scaffold in free fall by off-setting the gravitational force to the centrifugal force. The main advantage of this bioreactor is its low shear stress produced [49].

The main feature of perfusion bioreactors is the constant exchange of medium through the system, improving mass transfer of nutrients and wastes, as well as applying shear stress to the cells. Since the medium perfuses through the pores of the scaffolding, perfusion bioreactors are able to improve cell proliferation, differentiation and ECM deposition. Several types of bioreactors are included in this classification, including parallel plate, hollow-fiber, fixed bed and fluidized bed bioreactors. Parallel plate bioreactors feature tissue culture plastic surfaces in a bottom compartment, and an upper gas compartment that is separated by a membrane. While these reactors are automated and simple, partial sample collection is difficult. Hollow-fiber bioreactors feature a bundle of semi-permeable hollow fibers surrounded by a closed cylindrical vessel containing medium and cells. The main advantage to this type of system is a very large surface area for cell culturing. However, monitoring and scale-up are difficult since a relatively large number of fibers would be required. Fixed and fluidized bed bioreactors feature a column with either packed (fixed bed) or floating (fluidized fed) microcarriers. The medium flows through the bed, providing a 3-dimensional scaffold for cell attachment. Spatial concentration gradients in the fixed bed and shear stresses in the fluidized reactors can affect the cell growth and differentiation [34].

2.9.2 Perfusion Bioreactors

Perfusion bioreactors use a pump to continuously perfuse the medium through the interior porous network of a seeded scaffold. The medium is usually contained in a medium reservoir, which is attached to the scaffolds in separate chambers through tubing. In order to be classified as perfusion, the medium must flow through the scaffold.

Perfusion bioreactors have many advantages over other culturing systems including static culturing and spinner flasks. These features include improved mass transport of nutrients, wastes

and gases to and from the cells, more homogeneous growth conditions, altered cellular responses through hydrodynamic shear stress, and enhanced cell densities and numbers relative to static culturing [45, 49, 50]. The amount of shear stress applied to the cells can be controlled by the flow rate through the system, as well as the porous structure of the scaffold, scaffold microarchitecture, external and internal mixing of the medium and the bioreactor set-up [49].

The response of the cells to the shear stress is dependent on cell type, exposure time, and substrate and flow dynamics [18]. One potential response is cell rounding [45]. Cells cultured within the bioreactors as aggregates experience greater shear stresses than single cells because of their larger diameter [15]. Davies *et al.* (1986) illustrated the effect of flow dynamics on cell morphology. When exposed to laminar shear stresses, cells aligned in the direction of flow, while exposure to turbulent shear stresses led to random orientation. The researchers found that endothelial cell turnover *in vitro* is significantly more sensitive to turbulent flow shear stress than laminar flow shear stress [51].

While native tissues are vascularized, engineered tissues are not, and are therefore limited in size to approximately 100 μm thick [45]. Constant perfusion of medium provided by perfusion bioreactors can improve mass transport. Carrier *et al.* (2002) found that cells in perfused constructs experienced more homogenous microenvironmental conditions, including higher pH, higher oxygen partial pressure, and lower carbon dioxide partial pressure compared to static flasks. Perfusion also eliminates concentration gradients within constructs that are typically found when cultured in static flasks [45].

One of the major limitations in being able to monitor and control the bioreactor environment is the ability to find low cost and reliable biosensors. In-line sensors are needed to study and understand the effect of different physiological parameters on the growth of tissue

constructs and the biochemistry of the cells. Currently, probes can be placed into the medium chambers and linked to a computer system for constant monitoring of pH, temperature, and oxygen. However, this does not give a complete picture of the micro-environment within the tissue construct. Nuclear magnetic resonance (NMR) spectroscopy and magnetic resonance imaging (MRI) have shown promise for these applications, as their use is non-invasive and these techniques can allow monitoring of cell metabolism, cell density, flow rates and cell distribution within bioreactors [15].

Grayson *et al.* (2011) found that increasing the medium flow velocity significantly affected cell morphology, cell-cell interactions, matrix production and composition and the expression of osteogenic genes in cultured human MSCs. In this study, they investigated the effects of a range of superficial flow velocities on the formation of a bone construct, and found that flow velocities ranging from 400 to 800 μm/s yielded the best overall osteogenic responses. One drawback with perfusion culturing is that secreted proteins may not be retained in the ECM, due to removal with the perfused medium [50]. However, Grayson *et al.* (2011) found that when the human MSCs were cultured in bone constructs within the perfusion bioreactor, the cell numbers doubled in the first week and final cell densities after five weeks of culturing were $2.8 \pm 0.3 \times 10^7$ cells/cm^3, representing a significant improvement over the bone constructs yielded through static culturing, which had centers devoid of cells [50]. Similarly, in a study by Fröhlich *et al.* (2010), they found that perfusion led to the formation of a more uniform cell distribution within a bone construct compared to static culturing. The majority of the cellular proliferation occurred during the first 2 weeks of the 5 week culture period. The disribution of three bone-related proteins (collagen, BSP and OP) was also improved with perfusion [52].

Davisson *et al.* (2002) found a time and dose dependent effect of perfusion on the production of ECM and cell content in cartilage constructs. More specifically, they found that higher levels of perfusion during the first 3 days of culturing decreased cell content, while this higher perfusion increased cell content when cultured for 9 days. All levels of perfusion applied during the first 3 days of culturing decreased the deposition, release, formation and retention of cartilage-specific ECM, while ECM synthesis increased with 9 days of perfusion. This suggests that at early time points matrix deposition is less efficient under perfusion, but at later time points, perfusion can stimulate matrix synthesis [53].

While perfusion bioreactor systems typically hold culture volumes around 250 mL, reports have shown the effective use of culture volumes up to 1 L. However, there are still many problems with automation and scale-up concerns to be addressed. One possible solution could be the use of running multiple smaller bioreactors in parallel [54]. Constant monitoring and control of the physicochemical culture parameters, including pH, temperature and oxygen will also be required. Computational modeling of these parameters can be done online and could be used to predict the development time of the tissue [18]. The ideal system would allow for the seeding, growth, shipping and storage of the tissue construct within one container, therefore maintain sterility, reducing costs and labour [15].

2.10 Scaffolding Selection for Perfusion Bioreactor Systems

Scaffolds are used to provide a 3-dimensional environment for cell attachment, proliferation and differentiation. Once transplanted into the body, the ideal scaffold would degrade at the same rate of soft tissue regeneration [55]. Each potential biomaterial has different mechanical properties, degradation characteristics, immunogenicity, cellular response, and costs,

which have to be considered for each application. Naturally-derived scaffolds tend to have improved biodegradability and biocompatibility relative to synthetic polymers.

The scaffold must provide the appropriate structural and mechanical environment for cell proliferation and differentiation and be biocompatible for the desired application. The ideal scaffolding should mimic the microenvironment found within native tissue; promote cell-cell and cell-matrix interactions; promote cell adhesion and migration; promote cell proliferation and growth; be biodegradable; contain interconnected pores; and have an adequate surface area and porosity to support cell growth and transport characteristics [27]. The use of a bioresorbable scaffold is ideal since it provides a temporary structure for the cells to adhere to and produce a replacement ECM [56]. With the recognized importance of cell-ECM interactions on cellular behaviour, it is important to match the properties of the scaffold material to the tissue of interest. Ideally, once implanted into the host, the seeded scaffolding should induce self-repair and remodeling of the tissue, support the generation of blood vessels for the transport of nutrients and wastes, while avoiding any immune response [57, 58].

Cell adhesion to the scaffold has a significant effect on the differentiation capacity of the seeded ASCs. Cell adhesion is needed for anchorage-dependent cells and the scaffolds must also allow support cell migration. In the case of ASCs, the scaffold material and the surface topography has been shown to affect cell attachment, lipid production and gene expression [24]. A variety of naturally derived scaffolds have been used, include alginate, fibrin and collagen. Alginate is readily available and has a low toxicity, but is fragile when handled; fibrin has been shown to promote haemostasis, wound healing, tissue connection and prevent infections, but is very expensive; collagen is one of the most abundant proteins in human tissue, promotes cellular ingrowth and new matrix synthesis, and is biodegradable [59].

2.11 Synthetic Polymers as Cell-Adhesive Substrates

Synthetic polymers are often used in tissue engineering as scaffolding materials due to the ability to modify the chemical and structural properties, ease in the control of production, and that they can be designed to be biodegradable. These synthetics work as ECM substitutes by providing a temporary matrix for cell attachment, which is gradually replaced as the cells produce ECM proteins [47]. Synthetics provide an alternative to naturally derived scaffold materials, which can be costly and widely variable in composition and structure. Commonly used synthetic polymers include polyglycolic acid (PGA), polyethylene glycol (PEG), poly(tetrafluoroethylene) (PTFE), hyaluronic acid (HA), polyethylene glycol diacrylate (PEDGA), poly(lactic-co-glycolic acid) (PLGA), poly(ϵ-caprolactone) (PCL), silicon, bioactive glass and hydroxyapatite [60]. When seeded with cells and implanted *in vivo*, the degradation rates of the scaffolds increase. The polymer degrades into smaller fragments and the new space is filled with ECM proteins that are secreted by the cells, resulting in new tissue formation. The degradation products must be non-cytotoxic and should not induce an immune response [61].

For bone regeneration, composite scaffolds of PCL and collagen type I containing mineralizing peptide amphiphiles (PA) and growth factor delivering nanoporous silicon enclosure (NSE) microparticles were seeded with bone marrow-derived MSCs [57]. PCL was chosen since it has improved cell adhesion and proliferation over many other synthetic polymers and forms a more favourable degradation environment, without acidic by-product formation [57]. The constructs presented no signs of an immune response and were able to support the formation of new bone [57]. However, the use of collagen as a substrate improved cell attachment and proliferation over PCL alone, as well as greater mineralization [57]. This finding suggests that the

ideal scaffolds for tissue engineering applications may be those components native to the *in vivo* growth environment that can successfully mimic the native cell niche [57].

2.12 Decellularized Matrices as Scaffolds for Cell Expansion

Decellularized tissues have been investigated as scaffolding materials because the components of the ECM are natural ligands that benefit cell attachment, endothelialisation, and tissue regeneration [62]. The decellularization process removes the cells and cellular debris from the tissues, resulting in reduced antigenicity, to minimize immune responses and calcification, while supporting a time-dependent migration of host cells into the matrix [63]. Current decellularized tissues in use include human acellular dermal matrix (ADM), Alloderm® (decellularized human skin) and Matrigel (basement membrane prepared from Engelbreth-Holm-Swarm (EHS) mouse sarcoma) [26]. These scaffolds are able to induce host-cell infiltration and revascularization, which are critical to the long-term survival of the new tissues [29].

There are many different protocols on how to decellularize tissue. These methods include anionic detergents (sodium dodecyl sulphate or SDS), enzymatic agents (trypsin), non-ionic detergents (tert-octylphenylpolyoxyethylene or Triton X-100), physical treatments (such as agitation or sonication, mechanical massage or pressure, or freezing and thawing, and mechanical stripping), tissue fixation, nuclease digestion (DNase, RNase) and extensive PBS washing [64]. When tissue undergoes decellularization, the mechanical and structural properties of the ECM may be affected, which may impact the long-term durability of the implant [62].

A study by Liao *et al.* (2008), compared the mechanical and structural effects of SDS, trypsin, and Triton X-100 on the porcine aortic valve leaflet (AVL). In all three methods, no cell nuclei were present. With respect to the structure of the AVL, all decellularization methods did not significantly affect the overall leaflet fiber architecture, but did cause significant microscopic

disruption [62]. The gross collagen fiber structure was not affected in tissue structures created using any of the methods. The final result of the decellularization methods was a dense collagen and ECM network with treatment by SDS and a loose collagen and ECM network with increased pore size after trypsin or Triton X-100 treatments [62].

Sun *et al*. (2011) found that when using decellularized artery allograft for treatment of a facial nerve branch lesion, the decellularized scaffolds showed no immunogenicity. When the construct was seeded with ASCs, the lesion showed functional improvement and axonal growth, therefore achieving improved regeneration for the reconstruction of peripheral facial nerve defects [65].

Decellularization appears to be a possible solution to finding an appropriate scaffolding material for allografts. While the efficiency of a specific decellularization method depends on the tissue being processed, the most effective methods include a sequential process involving physical, chemical, and enzymatic treatments. The decellularized tissues should be devoid of donor cells to minimize any host immune response, while retaining the native ECM structure and composition. The final composition of the decellularized tissue, as well as the host response to the implant, depend on the type of tissue that is decellularized, the species of origin, the decellularization method used and the methods of terminal sterilization [64].

2.12.1 Decellularized Adipose Tissue

Recent research into the decellularization of human adipose tissue has shown that after a 5 day protocol involving the combination of physical, chemical, and biological treatments stages, the resulting material closely mimics the natural environment found within human fat [20]. The initial material can be obtained from human adipose tissue that is discarded during surgery, and is easily accessible and available. The resulting decellularized adipose tissue (DAT) is a loose,

white 3-dimensional scaffolding, representing approximately 30 to 45 % of the volume of the starting material, that is free of cells and cellular materials [20]. The basement membrane components laminin (LN) and collagen type IV (CIV), and the architecture of the ECM was preserved. There are different collagen regions within the matrix structure, including thick bundles of fibrous collagen interconnected with network-type collagens and branching, interwoven collagen [20]. This decellularized tissue has been shown to support the attachment of ASCs [20]. Gene and protein expression studies of the ASCs seeded on the DAT showed significantly higher expression levels of the master regulators of adipogenic differentiation (PPARγ and CEBPα), as well as glycerol-3-phosphate dehydrogenase (GPDH) activity, indicating that the microenvironment provided by the DAT is inductive for adipogenesis [20].

2.13 *Ex Vivo* Recellularization of Bioscaffolds

Recellularization can involve either the seeding of the scaffolding before implantation, or the migration and proliferation of cells once inside the host [63]. Seeding a scaffold before implantation has many advantages over the use of acellular scaffolds and can improve long-term success post-implantation. Izumi *et al.* (2003) investigated the use of acellular AlloDerm versus AlloDerm seeded with human autogeneous oral keratinocytes for wound healing. The seeded scaffolds showed greater revascularization, greater reduction in the dermal inflammatory response and a more rapid and mature epithelial coverage [66].

While the most common seeding method is static seeding of cells into scaffolds, this can lead to low seeding efficiencies and non-uniform cell distributions. To obtain higher efficiencies, the use of bioreactors to seed the scaffolds has been investigated. In one study, the use of stirred-flask bioreactors to seed ASCs led to a non-uniform distribution of the cells, with the cells located mainly on the surface of the scaffolds, with low viable seeding efficiencies [15]. In contrast,

perfusion bioreactors have the potential to perfuse the medium and cells throughout the entire scaffold, resulting in high seeding efficiency, and a more uniform cell distribution [15].

2.13.1 Bioreactor Seeding Methods

Clinical applications of tissue engineering constructs require the production of scaffolds with high cell densities. In order to improve the seeding efficiency on the scaffolds, the use of bioreactors has been compared to the traditional static seeding methods. It has been shown that the cell seeding method has a significant impact on the seeding efficiency, cell distribution, long-term survival and the quality of the resulting tissue [18]. Dynamic seeding can increase the interactions between the cells and the scaffold, therefore increasing the number of adherent cells. Flow of the cells through the scaffold can also lead to a more uniform cell distribution. This higher seeding efficiency has the potential to decrease cell expansion requirements, and therefore culturing time [18].

The specific method of dynamic seeding also has a significant impact on the seeding efficiency. Kim *et al.* (1998) showed that there was a greater seeding efficiency of smooth muscle cells (SMCs) onto PGA polymer scaffolds using agitation in an orbital shaker, when compared to both static culturing in a tissue culture dish and stirred culturing in a spinner flask. Both dynamic seeding methods resulted in a greater seeding efficiency and more uniform cell distribution relative to static culturing, and the resulting tissue had improved cellularity and increased elastin deposition [47].

The use of perfusion bioreactors for seeding scaffolds has shown great promise. One approach is to alternate the direction of the flow periodically to ensure greater cell-matrix interactions, minimize cell washout, maintain unrestricted flow through the scaffold pores and improve cell attachment. Radisic *et al.* (2003) compared the effectiveness of seeding murine

myoblast cells onto collagen sponges using either orbitally mixed Petri dishes or perfused cartridges with alternating medium flow. Cell distribution and viable cell seeding efficiency was significantly improved in the perfusion constructs. In the orbital dishes, the cells were limited to the surface layer of the matrix. There was a slight decrease in the cell numbers between 1.5 and 4.5 hours under perfusion, which was thought to be a result of the detachment and washing away of dead cells. This washing results in an improved construct, as damaged cells are known to send apoptotic signals to surrounding cells and can release intracellular compounds that are potentially harmful. Perfusion was also shown to maintain long-term cell viability, when compared to orbital dishes [67]. After seeding, the resulting constructs can be left in the perfusion bioreactor for further culturing. This allows the GMP standards to be met, as it reduces the potential for contamination and safety risks commonly encountered when transferring tissue constructs. This method has been used for the formation of vascular grafts, cartilage, and cardiac tissues [18].

2.14 Characterization of the Cellular Microenvironment

The cellular microenvironment has a significant impact on the viability and success of the cells and the tissue construct. The development of the tissue construct is a dynamic process in which the cellular microenvironment influences tissue-specific gene expression that controls the growth of the cells and the secretion of ECM proteins [14].

Implementation of bioreactors allows monitoring and control of many important parameters and physicochemical variables, including pH, oxygen concentration and temperature, as well as biochemical variables, including nutrient and waste levels, and growth factors. For clinical applications, the entire growth and differentiation process must be controllable and standardized. On-line monitoring can be paired with automated control systems. Using kinetic

data such as growth rates or cell death, metabolite uptake and production rates, or cellular events can be optimized for the operation conditions for each specific application [34].

The cellular functions of the stem cells are largely controlled by the signals present in the microenvironment. Nutrient and metabolite concentrations can affect cell proliferation, differentiation and apoptosis. The presence of growth factors can also influence the behavior of stem cells through survival, proliferation and differentiation cues [34]. For adipogenic differentiation, the rate of differentiation is influenced by the surrounding microenvironment. Oxygen concentration, and more specifically hypoxic culturing environments, can significantly impact ASC adipogenic differentiation. One method for the online monitoring of oxygen solubility in the medium is through the use of a fluorescent probe that detects the quenching of the fluorescence due to oxygen relative to a reference [21, 48].

To access the impact of the cellular microenvironment on the growth of the attached cells, proliferation assays can be completed to determine the number of cells present in the tissue construct, although most approaches are only capable of producing rough approximations [68]. There are many different methods to measure cellular proliferation, and examples include measuring metabolic activity with tetrazolium salts, CellTiter96AQueous MTS assay or alamarBlue; fluorescent DNA quantification using Hoechst 33258 or PicoGreen; uptake of radioactively-labelled DNA precursors [3H]Thymidine, and directly counting the number of cells using a hemocytmeter. For the metabolic assays, alamarBlue involves a reduction-oxidation (redox) indicator which is noncytoxic and nondestructive, while CellTiter96 involves a cytotoxic colorimetric reagent. With respect to DNA quantification, PicoGreen is a fluorescent dye that selectively binds to double-stranded DNA (dsDNA), while Hoechst dyes and ethidium bromide are more prone to interference from single-stranded DNA (ssDNA) and RNA. With the

[3H]Thymidine assay, this radioactive DNA precursor is integrated into the cellular DNA during DNA synthesis [68].

The proliferation of cells cultured in 3-dimensional environments is significantly different than for those grown in 2-dimensional culturing environments [68]. In general, the tissue constructs contain higher cell densities. The metabolic activity of the cells at these high densities does not correlate linearly with increasing cell numbers. Also, when running the metabolic assays with 3-dimensional constructs, the supernatant is generally used, as it is difficult to sample the liquid from within the tissue construct. This creates errors due to the presence of metabolite concentration gradients between the interior and exterior of the tissue construct. Therefore the accuracy of metabolic assay correlates with the ability of the metabolite to diffuse into or out of the construct [68].

Labeling the cells with [3H]Thymidine is generally sensitive, reliable and is capable of diffusing throughout the construct to reach all of the cells. However, the radioactive isotope has a relatively long half-life of 12.3 years and radioactivity has been detected in RNA, lipid, protein fractions of tissue as well as in DNA repair in nonproliferating cells [68].

Use of a hemocytometer to directly count the number of cells present is inexpensive, avoids the problems associated with signal quenching and metabolite diffusion and is able to provide specific cell numbers. However, this method is labour intensive and is highly variable between individuals, making it very error prone. Further, this method is less accurate at high cell densities due to problems obtaining a homogeneous single cell suspension [68].

While there are a range of dyes available to quantify dsDNA, the PicoGreen DNA assay (Invitrogen) is the most accurate method for measuring cell proliferation in high cell density 3-dimensonal environments, and is therefore commonly used to measure cellular proliferation [68].

This method requires the establishment of a linearly correlated DNA standard range and the sample dilution must fall within this range. A drawback of PicoGreen is that it is cytotoxic, but processing methods can be used to obtain a homogeneous suspension of the cell-scaffold construct while preserving the dsDNA structure. However, since the amount of DNA within a cell is dependent on the stage of the cell cycle, PicoGreen can only serve as an approximation of the number of cells present [68]. When the PicoGreen reagent rapidly binds to dsDNA, it becomes intensely fluorescent, with a detection limit of as low as 25 pg/mL dsDNA [69].

Chapter 3

Materials and Methods

3.1 Materials

All chemicals were used as received and purchased from Sigma-Aldrich Canada Ltd. (Oakville, ON, Canada) unless otherwise stated.

3.2 Adipose Tissue Decellularization

Subcutaneous adipose tissue samples were obtained from patients undergoing breast or abdominal reduction surgeries at the Kingston General Hospital (KGH) or Hotel Dieu Hospital (HDH) in Kingston, Ontario, and delivered to the lab within 2 h of extraction. The samples were transported to the lab in sterile cation-free phosphate buffered saline (PBS) supplemented with 20 mg/mL bovine serum albumin (BSA). To fabricate decellularized adipose tissue (DAT) scaffolds, the tissue was subjected to a 5-day detergent-free decellularization protocol (Table 3.1), previously established in the Flynn lab [20]. The adipose tissue was freeze-thawed three times in a hypotonic freezing buffer solution containing 10 mM Tris base and 5 mM ethylenediaminetetraacetic acid (EDTA), to promote cellular disruption. This was followed by multiple polar solvent extractions in 99.9% isopropanol to extract the lipid content, and enzymatic digestions to remove cells, residual lipids, and nucleic acids. The first enzymatic digestion solution contained 0.25% trypsin and 0.1% EDTA, while the second enzymatic digestion solution contained 15,000 U DNase Type II, 12.5 mg RNase Type III A and 2,000 U Lipase Type VI-S. At the end of processing, the sample was rinsed in a buffer solution containing 8 g/L sodium chloride, 200 mg/L potassium chloride, 1g/L sodium hydrogen phosphate and 200 mg/L potassium dihydrogen phosphate. All solutions (100 mL working volume) were

supplemented with 1% antibiotic-antimycotic solution (ABAM) and 1% phenylmethanesulphonylfluoride (PMSF), a protease inhibitor. Unless otherwise stated, all treatments were conducted at 37°C under constant agitation on an Excella^{TM} 24 Benchtop Incubator (New Brunswick Scientific, Edison, NJ, USA) at 150 RPM.

Table 3.1: Decellularization Protocol [20]

Day	Processing Stages
1	• Freeze-thaw 3 times in Freezing Buffer Solution • Incubate overnight in Enzymatic Digestion Solution #1 (Trypsin-EDTA)
2	• Isopropanol Extraction
3	• Isopropanol Extraction
4	• Wash 3 times in Rinsing Buffer Solution (30 minutes each) • Incubate for 6 hours in Enzymatic Digestion Solution #1 (Trypsin-EDTA) • Wash 3 times in Rinsing Buffer Solution (30 minutes each) • Incubate overnight in Enzymatic Digestion Solution #2 (DNase, RNase, Lipase)
5	• Wash 3 times in Rinsing Buffer Solution (30 minutes each) • Isopropanol Extraction • Wash 3 times in Rinsing Buffer Solution (30 minutes each)

The DAT scaffolds were cut into 200 mg pieces (wet weight), decontaminated with 3 rinses in 70% ethanol, and rehydrated by rinsing 3 times in sterile PBS. The samples were then stored aseptically in sterile PBS supplemented with 100 U/mL penicillin and 0.1 mg/mL streptomycin at 4 °C before use.

3.3 Perfusion Bioreactor System

A custom-designed perfusion bioreactor was designed in collaboration with Tissue Growth Technologies (TGT) Inc., based on modifications to their OsteoGen bioreactor system for

scaffold-based perfusion cultures (Figure 3.1). The complete bioreactor incorporated 2 parallel systems (Figure 3.1), each with 12 individual scaffold chambers (Figure 3.1) and 4 medium reservoirs (3 scaffold chambers/reservoir), which have the capacity to hold 100 mL. 5 mm inserts were placed in each scaffold chamber to secure the scaffold in place and ensure the medium perfused through the scaffolding. Medium perfusion was controlled by a MasterFlex peristaltic pump (MasterFlex, Model 07519-25) and pump drive (MasterFlex, Model 77301-21) with a benchtop controller (MasterFlex, Model 77301-22). Platinum-cured silicone gas-permeable tubing (Masterflex, Cole Parmer, RK-95802-02) was used to attach the medium reservoirs to the scaffold chambers. Within each system, the medium perfusion rate through each scaffold could be varied from 0.06 to 4.01 mL/min. The system is fully autoclavable and can be sterilized at 121°C. Each system was housed within a tri-gas incubator (Thermo Scientific, Forma Series II Water Jacket CO_2 Incubator, Model 3130), which allowed the oxygen concentration to be varied from 0 – 21 %. The system allowed for the real-time monitoring of the medium pH (0 to 14 pH), temperature (0 to 150°C) and O_2 concentration. A dual-input intelligent analyzer (Rosemount Analytical, Model 1056) was mounted inside the incubator, which was attached to a pH sensor (Broadley James Corporation, FermProbe® Electrode, Model F-635) within each medium chamber. The software program used for monitoring the system was by Tissue Growth Technologies' GrowthWorks^{TM} systems, which allows for the simultaneous monitoring of up to 8 transducers

To prepare for each run, the medium reservoirs, scaffold chambers and tubing were sterilized by steam autoclaving (121°C, 35 minutes). Each scaffold chamber was loaded with a 200 mg DAT scaffold under aseptic conditions in a biological safety cabinet, and each medium reservoir was filled with 80 mL of complete growth medium (DMEM:Ham's F12 medium, 10%

fetal bovine serum (FBS), 1% pen-strep), which was replaced every 2-3 days. Each unit was placed inside the incubator, which was set to control the temperature (37°C) and O_2 concentration.

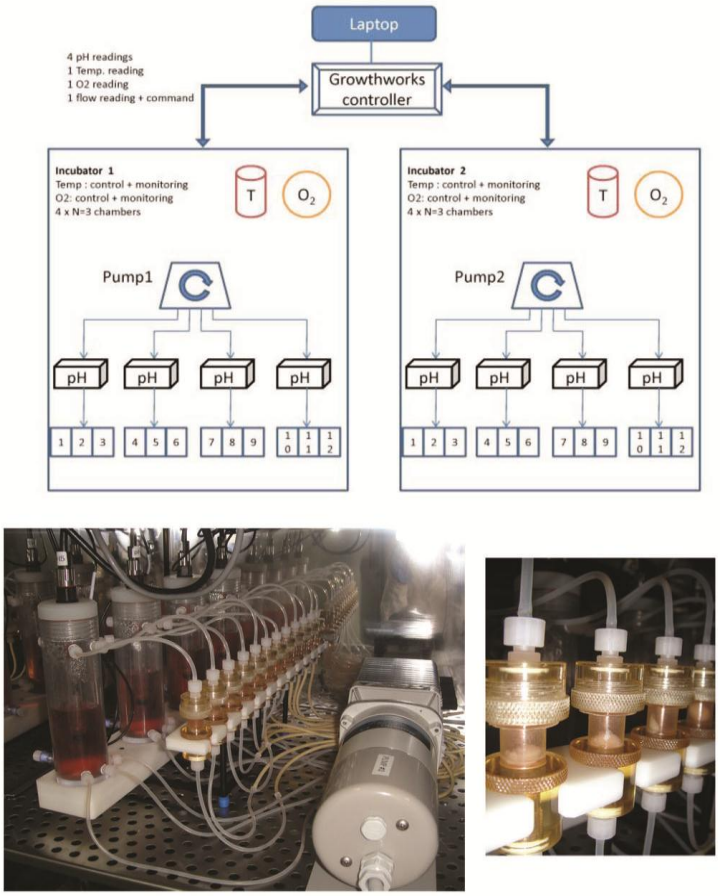

Figure 3.1: Schematic illustration of the custom-designed perfusion bioreactor system from Tissue Growth Technologies (TGT) Inc. The picture on the bottom left illustrates the overall system, while the photo on the bottom right provides a close-up of the scaffold chambers containing 200 mg pieces of DAT.

3.4 Scaffold Permeability Measurements

In order to determine the permeability of the DAT scaffolds within the perfusion bioreactor system, a research grade blood pressure transducer (Harvard Apparatus, 724496) was used to measure the pressure drop across the scaffold chambers loaded with 200 mg DAT samples in the bioreactor system. A 200 mg piece of DAT was inserted into each chamber in the system. Distilled water was placed in the medium reservoirs, representative of the typical viscosity of the aqueous culture medium used for most cell culture experimentation. The water was perfused through the system at a flow rate of 1.5 mL/min and the pressure was measured before and after the DAT-loaded chamber to calculate the pressure drop across the DAT scaffolds. This flow rate was selected based on previous work by Fröhlich et al. (2010) using decellularized bone scaffolds seeded with ASCs within a similar perfusion bioreactor culture. The DAT scaffold permeability was then approximated using Darcy's law, according to the following equation:

Equation 3.1

$$Q = \frac{-kA}{\mu}\frac{(P_b - P_a)}{L}$$

Where Q is the total discharge (25 000 m^3/s), k is the permeability of the medium (m^2), A is the cross sectional area to flow ($1.26x10^{-5}$ m^2), P_b-P_a is the pressure drop ($kg/m*s^2$), μ is the viscosity (0.001 kg/s*m) and L is the length across which the pressure drop occurs (0.01 m).

To confirm that the perfused medium within the bioreactor system was infiltrating the central regions of the DAT, to ensure adequate nutrient delivery to the central scaffold regions, an indicator dye study was also conducted. More specifically, blue food colouring was added to the distilled water in the medium reservoirs, and the dye solution was perfused through the DAT

scaffold samples in the bioreactor chambers at a flow rate of 1.5 mL/min. After 2 hours, the DAT was removed from the chambers and sectioned to investigate the dye permeation patterns.

3.5 Adipose-derived Stem Cell Isolation and Culture

Subcutaneous adipose tissue was obtained from patients undergoing breast or abdominal reduction surgery at KGH and HDH in Kingston, Ontario, for the extraction of human adipose-derived stem cells (ASCs), using previously established methods [70]. Briefly, the sample was minced in a sterile tissue culture dish, and any excess blood vessels or cauterized tissue segments were removed. The minced tissue was placed in a 50 mL Falcon tube containing 25 mL of enzymatic digestion solution comprised of 1.43 mL of 35% BSA solution, 3 mM glucose, 2 mg/mL collagenase type II (Sigma C-6885) and 25 mM HEPES, in 23.6 mL Kreb's Ringers bicarbonate (KRB) buffer. To facilitate tissue digestion, the mixture was agitated for 45 min at 37°C at 100 rpm on an orbital shaker Excella^{TM} 24 Benchtop Incubator (New Brunswick Scientific, Edison, NJ, USA). Following digestion, to remove any undigested tissue segments, the sample was filtered through a 250 µm pore stainless steel filter. The filtrate was allowed to gravity sediment for 5 min, resulting in cell separation into two layers. The top layer, composed of floating mature adipocytes, was aspirated and discarded. The lower layer contained the stromal vascular fraction of the adipose tissue, including the ASC population. To inactivate the collagenase, and equal volume of DMEM:Ham's F12 growth medium supplemented with 10% FBS, 1% pen-strep was added to the lower layer. After centrifugation at 1200 xg for 5 min, the supernatant was discarded and the cell pellet was re-suspended in 20 mL of erythrocyte lysing buffer, comprised of 0.154 M ammonium chloride, 10 mM potassium bicarbonate, and 0.1 mM EDTA, and agitated gently for 10 min at room temperature. The samples were then centrifuged at 1200 xg for 5 min, the supernatant was discarded, and the cell pellet was re-suspended in 20 mL

of DMEM:Ham's F12 complete medium (supplemented with 10% FBS, 1% pen-strep). The cell suspension was filtered through a 100 μm nylon mesh. Following centrifugation at 1200 xg for 5 min, the supernatant was aspirated and the pellet was re-suspended in DMEM:Ham's F12 complete medium. After 2 additional medium washes, the cells were plated in a T-75 flask at approximately 30,000 cells/cm^2 in 15 mL of DMEM:Ham's F12 complete medium. After 24 hours, the cells were washed with sterile PBS to remove non-adherent cells or debris, and the complete medium was replaced. Medium replacement was performed every 2-3 days thereafter.

The cells were passaged at 80% confluence by aspirating the medium, and rinsing the T-75 flask with 10 mL of sterile phosphate buffered saline (PBS) in order to remove excess proteins that interfere with trypsin. The PBS was then aspirated and 5 mL of trypsin (0.25% trypsin, 0.1% EDTA Gibco/Invitrogen 25200-072) was added to the T-75 flasks, which were incubated horizontally for 5 minutes at 37°C. The T-75 flask was then gently tapped to ensure detachment of cells and then pipetted to a 15 mL Falcon tube. To inactivate the trypsin, 5 mL of DMEM:Ham's F12 complete medium was added into the Falcon tube and the tube was centrifuged at 1200 xg for 5 minutes and the supernatant was aspirated. The cells were then split 1 to "n" (where n is either 2, 3, or 4) by resuspending the cell pellet in "n" mL of DMEM:Ham's F12 complete medium. 1 mL of the cell suspension was then added to each T-75 flask along with 14 mL of DMEM:Ham's F12 complete medium.

3.6 The Effect of Oxygen Tension on Human ASC Proliferation in 2-D Culture

The effect of the oxygen concentration in the growth environment on the proliferation of the ASCs was determined by counting the number of cells present each day for 8 days and using this to calculate the doubling time. The oxygen concentration of the hypoxic environment was 5%, while the normoxic oxygen concentration was 21%. Tissue culture polystyrene (TCPS) 6-

well plates were seeded with 20,000 ASCs per well initially, with three wells per time point. Passage 2 ASCs were used in each run. To each well, 3 mL of DMEM:Ham's F12 complete medium was added. Medium was replaced every 2-3 days.

At each time point, the 3 wells for both oxygen conditions were rinsed with sterile PBS and 2 mL of trypsin (0.25% trypsin, 0.1% EDTA Gibco/Invitrogen 25200-072) was added to the wells and incubated horizontally for 5 minutes at 37°C. The 6-well plate was then gently tapped to ensure detachment of the cells and then pipetted to a 15 mL Falcon tube. To inactivate the trypsin, 2 mL of DMEM:Ham's F12 complete medium was added to the Falcon tube. Each well was counted three times using Trypan Blue solution (Sigma, T8154) for viability staining and a hemocytometer. 10 µL aliquots of each sample were placed in a 96-well plate well and mixed thoroughly with 10 µL of Trypan Blue. A 10 µL sample was taken from this mixture and placed on the hemocytometer. The number of viable cells within the 4-square grids was counted and averaged, and using Equation 3.2 the total number of ASCs was determined.

Equation 3.2

$$total\ cells = average\ number\ of\ viable\ cells\ per\ square\ x\ DF\ x\ cell\ suspension\ volume\ x\ HF$$

Where the DF is the dilution factor (2), the cell suspension volume was 4 mL and the HF is the hemocytometer factor (10^4).

The total number of cells for each well was calculated and then the 3 wells for each oxygen concentration were averaged and plotted versus time. The slope of the exponential growth region was taken from each donor sample and this was used to calculate the doubling time for that donor.

3.7 Preparation of the DAT Scaffolds and ASCs for Confocal Imaging Studies

In order to obtain a complete picture of the proliferation of ASCs within the DAT, the ASCs were stained with CellTracker™ Green and the DAT was labeled with an amine-reactive Alexa Fluor® 350 carboxylic acid succinimdyl ester. Pictures were taken using a confocal microscope (Olympus Fluoview FV1000).

3.7.1 CellTracker™ Green Labeling of the ASCs

The ASCs that were used in the confocal analysis studies of cell distribution in the DAT scaffolds were labeled with a fluorescent probe, CellTracker™ Green CMFDA (5-chloromethylfluorescein diacetate) (Invitrogen, Burligton ON; Product Code C2925). The dye was diluted in sterile dimethyl sulfoxide (DMSO) to a stock concentration of 10 mM. Immediately prior to cell labeling, this stock solution was then diluted in serum-free DMEM:Ham's F12 medium, to achieve a final concentration of 10 µM, and warmed to 37°C, with protection against light exposure. Trypsin-released ASCs were then suspended in the working solution at a concentration of 10^7 cells/mL, and incubated at 37°C for 45 min. Following staining, the cells were collected by centrifugation at 1200 xg for 5 min, and the supernatant was aspirated. The cell pellet was then re-suspended in 10 mL of DMEM:Ham's F12 complete medium and incubated for 30 min in suspension. After this final incubation step, the sample was then centrifuged at 1200 xg for 5 min, and the supernatant was aspirated. The cell pellet was re-suspended in the required amount of DMEM:Ham's F12 complete medium to obtain the desired cell concentration for the seeding experiments. All experimental work was performed under minimal light conditions.

3.7.2 Fluorescent Labeling of the DAT Scaffolds

The DAT scaffolds that were used in the confocal analyses were labelled with an amine reactive Alexa Fluor® 350 carboxylic acid, succinimidyl ester (Molecular Probes, Burlington, Canada; Product Code A10168). The dye (5 mg) was dissolved in DMSO to achieve a stock solution concentration of 10 mg/mL. This stock solution was then diluted in 0.15 M $NaHCO_3$ to obtain a working concentration of 0.3 mg/mL. The DAT was agitated in the dye solution at a concentration of 0.25 mg/200 mg DAT in 0.15 M $NaHCO_3$ buffer for 1 h at room temperature. To stop the labeling reaction, the DAT was then incubated in 1.5 M hydroxylamine solution for 1 h. Finally, the DAT was rinsed three times for 30 min in sterile PBS, and stored at 4^oC in sterile PBS supplemented with 100 U/mL penicillin and 0.1 mg/mL streptomycin, protected from light exposure. All work was conducted under minimal light conditions.

3.8 Bioreactor Trial #1: Investigation of the Impact of Cell Seeding Density

Three different cell seeding densities were investigated in order to optimize the proliferation of the ASCs on the DAT. More specifically, the ASCs were seeded in single-cell suspension in DMEM:Ham's F12 growth medium. To release the ASCs from the tissue culture polystyrene (TCPS) plates, the DMEM:Ham's F12 growth medium was aspirated and the TCPS was rinsed with 10 mL of sterile PBS to remove excess protein that can interfere with trypsin. The PBS was then aspirated and the ASCs were incubated with 5 mL of trypsin (0.25% trypsin/0.1% EDTA, Invitrogen, 25200-072) for 5 minutes. The released ASCs were then transferred to a 15 mL plastic tube and 5 mL of DMEM:Ham's F12 growth medium was added to inactivate the trypsin. The mixture was then centrifuged at 1200 xg for 5 minutes and the supernatant was aspirated. The remaining cell pellet was then diluted using a desired amount of DMEM:Ham's F12 growth medium to obtain the required seeding density.

3.8.1 Suspension Seeding

For suspension culturing, the 200 mg sterilized DAT pieces were seeded with the desired amount of ASCs in 200 µL of DMEM:Ham's F12 growth medium (supplemented with 10% FBS, 1% Penicillin-Streptomycin (pen-strep)) within cell culture inserts (Millicell®, PICM01250) with 0.4 µm membranes placed in 6-well plates. An additional 5 mL of complete medium was added to each well outside the insert. The scaffolds were cultured for 24 hours in DMEM:Ham's F12 growth medium at 37°C with 5% CO_2, at which point the cell culture inserts were removed before use in tissue culturing experiments.

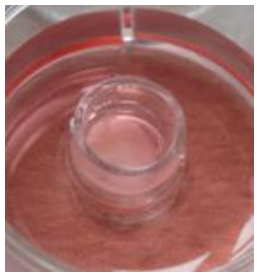

Figure 3.2: Suspension seeding with 200 mg piece of DAT within cell culture insert and ASCs suspended in 200 µL of DMEM:Ham's F12 growth medium

Three initial ASC seeding densities were compared in order to determine the optimal seeding density for ASC proliferation: 1million, 2.5 million and 5 million ASCs per 200 mg DAT.

3.8.2 Confocal Imaging Study

To investigate the effect of the initial ASC seeding density on the ASC proliferation, 200 mg pieces of Alexa Fluor® 350 carboxylic acid, succinimidyl ester (Molecular Probes, Burlington, Canada)-stained DAT were seeded with either 1milion, 2.5 million or 5 million ASCs in suspension stained with CellTracker™ Green (Invitrogen, C2925). A total of 4 samples for

each ASC density were prepared, with 2 for 7 day proliferation and 2 for 14 day proliferation. Following a 24 hour static seeding period as described above, the samples were placed into the scaffold chambers in the perfusion bioreactor (Tissue Growth Technologies, OsteoGen) and cultured for either 7 or 14 days under normoxic (21%) conditions. A confocal microscope (Olympus Fluoview FV1000) was used to obtain pictures of the samples at 100 times magnification. Images of the surface and surface pores were obtained

3.8.3 PicoGreen Analysis of Cell Proliferation

To quantify the results obtained in the confocal seeding density study, 200 mg pieces of DAT were seeded with 1 million ASCs and maintained under static conditions for 24 hours, as described above. The samples were then divided into 4 groups: (i) normoxic static, (ii) normoxic perfusion, (iii) hypoxic static and (iv) hypoxic perfusion. Three time points of 72 hours, 7 and 14 days were investigated. Three samples were prepared for each group for each time point. At each time point, the Quant-iTTM Picogreen® dsDNA assay was used to measure the dsDNA content in each of the samples, with triplicate samples (n=3) for each culturing condition.

For the fluorescent nucleic acid staining each DAT sample was rinsed 3 times for 30 minutes in PBS and then incubated in digest solution containing 1.43 mL of 35% BSA solution, 3 mM glucose, 2 mg/mL collagenase type II (Sigma C-6885) and 25 mM HEPES, in 23.6 mL Kreb's Ringers bicarbonate (KRB) buffer for 2 hours at 37°C. Following digestion the samples were centrifuged at 1200 xg for 5 minutes and the supernatant was aspirated. The pellet was resuspended in 1 mL of prepared 1X TE working solution (prepared by diluting concentrated Tris-EDTA (TE) buffer 20-fold with sterile, distilled, DNase-free water). Each sample was sonicated 3 times for 10 seconds using an ultrasonic probe to lyse the cells, and then centrifuged at 1200 xg for 5 minutes. Triplicate 100 µL samples of the supernatant containing the dsDNA

was placed in a 96-well plate. A DNA standard curve was prepared by diluting a solution of λDNA (provided with the kit) in TE 50-fold with DNase-free water to generate a 2µg/mL stock solution. A DNA standard curve was then created, ranging in concentration from 0 to 1000 ng/mL, and 100 µL of each standard was placed in duplicate wells in the 96-well plate.

A PicoGreen working solution was prepared by diluting 200-fold dye reagent (provided with the kit) with the TE working solution. 100 µL of the PicoGreen working solution was added to each sample and standard. The 96-well plate was incubated for 5 minutes and the fluorescence of each sample was measured using a SynergyTM HT multi-detection microplate reader (Excitation 480 nm, emission 520 nm) with KC4TM (Bio-Tek Instruments, Inc., Winooski, VT, USA) software. The fluorescence value of the blank standard was subtracted from all the values. The standard curve was generated using the values modified standard values. Since the decellularized adipose tissue (DAT) used in the experiments produced some background fluorescence due to non-specific interactions, the fluorescence of unseeded DAT controls was subtracted from that of the samples of DAT seeded with ASCs in every trial. The slope of the DNA standard curve was used to convert the fluorescence of the samples into DNA concentrations, were then converted to DNA per sample using the sample volume.

3.9 Bioreactor Trial #2: Investigation of Cell Aggregate Seeding Methods

3.9.1 Fabrication of ASC Aggregates

Multicellular aggregates of 20,000 ASCs per aggregate were made using methods developed in collaboration with the lab group of Dr. Adam Katz (University of Virginia). In brief, ASCs were suspended in DMEM:Ham's F12 growth medium (supplemented with 10% FBS, 1% pen-strep) at a concentration of 800,000 ASCs per mL. 25 µL drops of this suspension were placed in rows on the lid of a 10 cm culture dish. 10 mL of sterile water was added to the bottom

of the culture dish and the lid was flipped onto the base. The culture dish was incubated at 37˚C with 5% CO_2 for 25 hours, at which point the aggregates were seeded onto the DAT pieces at 50 aggregates per 200 mg DAT scaffold within 6-well plate cell culture inserts (Falcon, 353090). The scaffolds were cultured for 24 hours in DMEM:Ham's F12 growth medium (supplemented with 10% FBS, 1% pen-strep) at 37°C with 5% CO_2, at which point the cell culture inserts were removed before use in tissue culturing experiments.

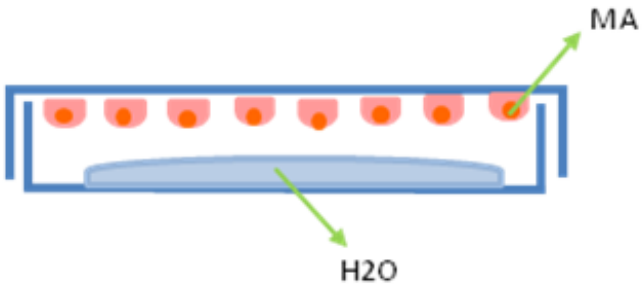

Figure 3.3: Aggregate formation using hanging drop, (Katz, 2011)

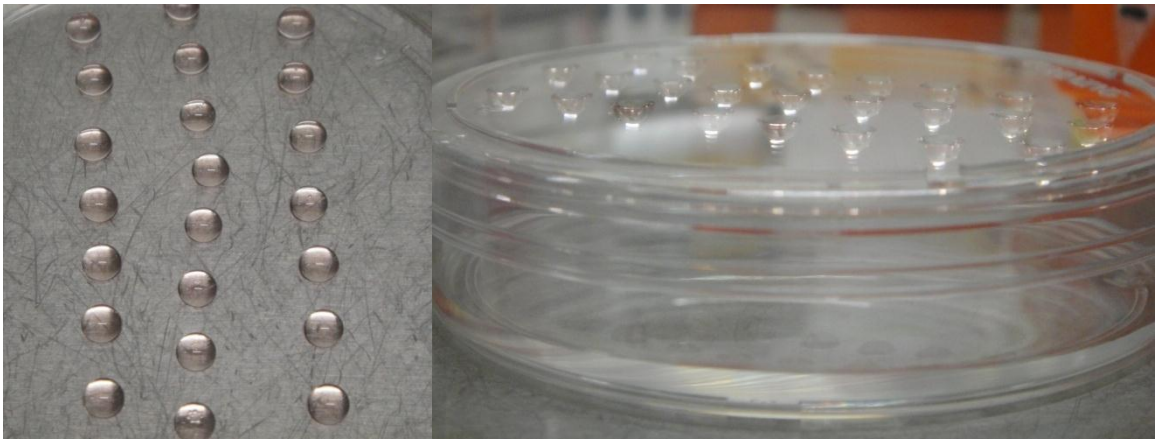

Figure 3.4: The first step in the aggregate formation process. 25 µL drops of DMEM:Ham's F12 complete medium with 20,000 ASCs are pipetted onto the top of a tissue culture dish. The top is then inverted and the drops are incubated for 12 hours.

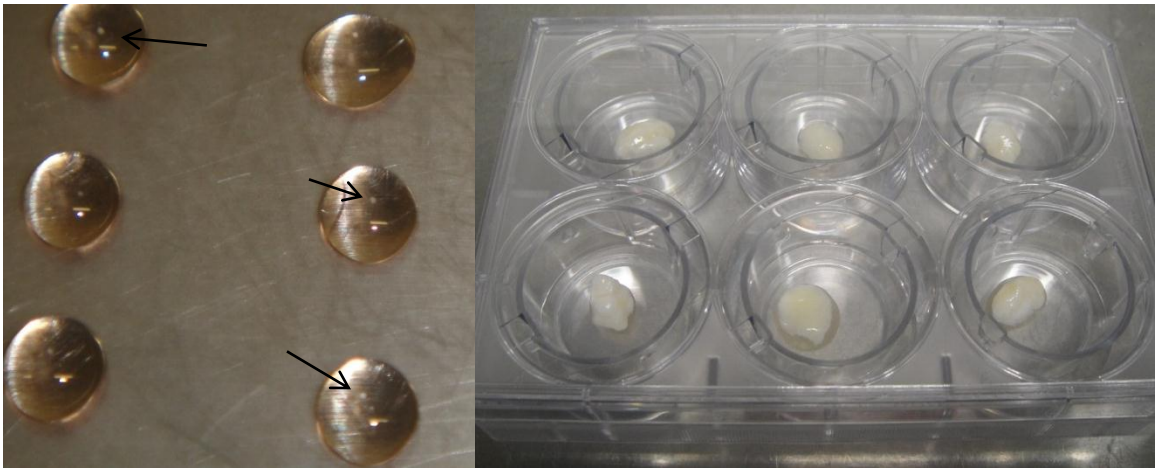

Figure 3.5: The second step of the aggregate formation process. After 12 hours of incubation, the top of the tissue culture dish was inverted again and visible cellular aggregates were present in each droplet. The aggregates were then seeded on 200 mg pieces of DAT inside a cell culture insert. The aggregates are indicated by the arrows in the above picture.

3.9.2 Confocal Analyses

To confirm ASC attachment to the DAT when seeded in the form of aggregates, an initial confocal study was completed. The ASCs were labelled with CellTracker™ Green (Invitrogen, C2925), and then used to create the aggregates. Two initial ASC seeding densities were investigated, of 25 or 50 multicellular aggregates; and therefore 500,000 or 1 million ASCs per 200 mg DAT respectively. After a 12 hour aggregate formation period, the 200 mg DAT scaffolds were placed within membrane cell culture inserts (Falcon® Model 353090, Becton Dickinson, NJ, USA), and seeded with the aggregates for an initial 24 hour attachment period. The cell culture inserts were then removed and the samples were cultured statically in 6-well TCPS plates under hypoxic (5% O_2) conditions. 2 samples were prepared for each ASC seeding density. After 72 hours, the confocal microscope (Olympus Fluoview FV1000) was used to obtain pictures of the samples. 100 times magnification was used in all experiments.

This experiment was then expanded and repeated to include three initial aggregate numbers using confocal analysis. More specifically, 200 mg DAT scaffolds were seeded with 12, 25 or 50 multicellular aggregates, which are equivalent to 250,000, 500,000 and 1 million ASCs respectively. The ASCs were pre-labeled with CellTracker^{TM} Green (Invitrogen, C2925) and grown statically under hypoxic (5% O_2) conditions for 7 days. 2 samples for each amount of aggregates were prepared.

3.9.3 Quant-iTTM Picogreen® dsDNA Analyses

The qualitative confocal results were quantitatively confirmed using the Quant-iTTM Picogreen® dsDNA assay. 200 mg DAT were seeded with 12, 25 and 50 multicellular aggregates which are equivalent to 250,000, 500,000 and 1 million ASCs respectively. Samples were grown statically under hypoxic (5% O_2) conditions. The dsDNA per sample (ng) at 72 hours and 7 days was measured, with 3 samples for each culturing condition. The triplicate samples were averaged.

3.10 Bioreactor Trial #3: Investigating the Effect of Oxygen Concentration and Perfusion on ASC proliferation

3.10.1 Quant-iTTM Picogreen® dsDNA Analyses

The aggregate seeding method experiment was expanded to include the bioreactor and four different growth conditions: (i) normoxic static, (ii) normoxic perfusion, (iii) hypoxic static and (iv) hypoxic perfusion. Based on the preliminary results, 1 million ASCs were seeded on the DAT in aggregates (50 aggregates/200 mg DAT), incubated under static conditions in a culture insert for 24 hours for cellular attachment, and then moved to either the bioreactor scaffold chambers or 6 well plates for culturing. The dsDNA per sample (ng) at 72 hours, 7 and 14 days was measured. Samples were run in triplicate and averaged.

3.10.2 Confocal Analyses

In order to further investigate the effect of perfusion and oxygen concentration on the proliferation of the ASCs, qualitative analyses were completed using the confocal microscope (Olympus Fluoview FV1000). To gain a complete picture of the ASC growth on the DAT, the DAT was 1abeled with an amine reactive Alexa Fluor® 350 carboxylic acid, succinimidyl ester (Molecular Probes, Burlington, Canada) and the ASCs were 1abeled with CellTracker™ Green (Invitrogen, C2925). The ASCs were formed into multicellular aggregates containing 20,000 ASCs per aggregate, as described. The DAT was seeded with 50 aggregates, resulting in a concentration of 1 million ASCs per 200 mg DAT. After 24 hours, the samples were split into 4 groups: normoxic static, normoxic perfusion, hypoxic static and hypoxic perfusion. The static samples were cultured in 6-well plates, while the perfusion samples were cultured in the perfusion bioreactor. Normoxic samples were cultured at 21 % O_2, while the hypoxic samples were cultured at 5% O_2. At each time point, 3 samples from each condition were analyzed under the confocal microscope using 100 x magnification.

3.11 Bioreactor Trial #4: Adipogenesis of ASC Cultured in the Bioreactor System

To confirm that the ASCs cultured on the DAT for 14 days in the bioreactor could be stimulated to undergo adipogenic differentiation, 1 million ASCs were seeded in aggregate form onto the DAT and were cultured in the three conditions that previously showed the best cell growth normoxic (21% O_2) perfusion, hypoxic static (5% O_2) and hypoxic (5% O_2) perfusion) in complete medium. After 14 days, the samples were placed in 6-well plates and adipogenic medium was added to the induced samples, as described below. Non-induced samples from each condition were used as controls, as well as cells grown on TCPS (induced and non-induced). Three samples were prepared for each of the induced and non-induced adipogenic differentiation

for each of the conditions. The samples were cultured statically in 6-well plates for 7 days, with medium replacement every 2 – 3 days. Glycerol-3-phosphate dehydrogenase (GPDH) activity was measured at 7 days after the induction of differentiation to confirm adipogenesis.

3.11.1 Adipogenic Induction

Adipogenesis was induced through the addition of adipogenic medium. Adipogenic medium was comprised of serum-free DMEM:Ham's F-12 supplemented with 15 mM NaHCO3,15 mM HEPES, 33 mM biotin,17 mM pantothenate,10 mg/mL transferrin,100 nM cortisol, 66 nM insulin,1 nM triiodothyronine (T3), 100 U/mL penicillin and 0.1 mg/mL streptomycin. For the first 72 h of differentiation, 0.25mM isobutylmethylxanthine (IBMX) and 1 mg/mL of troglitazone were added to the differentiation medium.

3.11.2 Glycerol-3-Phosphate Dehydrogenase (GPDH) Enzyme Activity

The cellular GPDH enzyme activity levels (GPDH Assay Kit, KT-010; Kamiya Biomedical Corporation) were measured at 7 days after the induction of adipogenic differentiation in the DAT samples after a 14 day proliferation period in the bioreactor under hypoxic (5% O_2) or static 6-well plates under hypoxic (5% O_2) and normoxic (21% O_2) conditions. Differentiated and undifferentiated ASCs on TCPS were included as positive and negative controls, respectively. The substrate provided in the kit contains NADH, which is a co-enzyme for GPDH, and dihydroxyacetpne phosphate (DHAP). The level of NADH decreases as the DHAP is converted into glycerol-3-phosphate by the GPDH, which can be measured spectrophotometrically. GPDH is a kinetic assay where the absorbance (340 nm) of the samples was measured with a microplate reader for 10 minutes and the linear portion of the curve was used to calculate the change in absorbance (ΔOD/min). The Bio-Rad protein assay with an albumin standard was used to determine the total cytosolic protein content within each sample to

normalize the data. The GPDH results were expressed in terms of mUnits/mg total intracellular protein (mU/mg), where 1 unit is the GPDH activity required to oxidize 1 µmole of NADH in 1 minute.

Briefly, each DAT sample was minced in 1 mL of the of the provided enzyme extraction reagent followed by three 5-second bursts of sonication to disrupt the ASCs. For the TCPS samples, 2 mL of the enzyme-extracting reagent was added to each well of the 6-well plate and the cells were disrupted with three 5-second sonications. To obtain the cytosolic protein fraction from the samples, each sample was centrifuged at 16,000 xg for 15 minutes at 4°C.

To normalize the measured GPDH activity levels, the total cytosolic protein content of the supernatant was measured using the Bio-Rad Protein Assay (Bio-Rad Laboratories Inc., Hercules, CA). A bovine albumin standard curve was prepared through serial dilutions with enzyme extracting reagent to obtain standard concentrations of 0 µg/mL, 10 µg/mL, 20 µg/mL, 40 µg/ml, 60 µg/mL and 80 µg/mL. 160 µL of the sample supernatant was mixed with 40 µL of Bio-Rad Coomassie® Brilliant Blue G-250 dye solution within a 96-well TCPS microplate well. The microplate was incubated at room temperature for 5 minutes and the absorbance was measured at 595 nm using a Synergy TM HT multi-detection microplate reader and KC4™ (Bio-Tek Instruments Inc., Winooski, VT, USA) data analysis software. The standards were measured in duplicate while each sample was measured in triplicate. The protein concentrations of the samples were calculated using the slope of the albumin standard curve.

The GPDH Activity Measurement kit from Kamiya Biomedical Corporation (Seattle, WA, USA) was used to calculate the GPDH activity of the samples. First, the GPDH substrate reagent was prepared by dissolving an aliquot provided in the kit with 4.2 mL of deionized water. Samples were run in duplicate, with 50 µL of the sample supernatant placed within a 96-well

TCPS well. Since the assay is a kinetic assay, only one column of the 96-well TCPS was measured at a time. 100 µL of the GPDH substrate reagent was added to each sample using a multi-channel pipette and thoroughly mixed. The absorbance of the samples was immediately measured at 340 nm every 15 seconds for a total of 10 minutes using a Synergy™ HT multi-detection microplate reader and KC4TM (Bio-Tek Instruments Inc., Winooski, VT, USA) data analysis software. The absorbance data was plotted as a function of time, and the change in absorbance (ΔOD/minute) was determined from the linear portion of the kinetic curve for each sample. The slopes of the duplicates for each sample were averaged and the GPDH activity levels were then normalized to the total cytosolic protein content in each sample using Equation 3.3:

Equation 3.3

$$GPDH\ Activity\ \left[\frac{mU}{mg}\right] = \frac{\Delta OD_{avg} * 0.4823 * 0.5 * 1000}{(\frac{Pr_{avg}}{1000})}$$

Where 1 Unit of GPDH activity is defined as the activity required to consume 1 µmole of NADH/minute. Data are expressed in units of mU of GPDH activity/mg of total cytosolic protein.

3.11.3 Statistical Analysis

Data are expressed as means ± standard deviations (SDs). All statistical analyses were performed with OriginPro 8.0 software (OriginLab Corp., Northampton, MA, USA) by one-way ANOVA with a Tukey's post-hoc comparison of the means. Differences were considered statistically significant at $p < 0.05$.

Chapter 4

Results

4.1 Permeability

To ensure that the DMEM:Ham's F12 growth medium adequately perfused through the middle of the decellularized adipose tissue (DAT) scaffolds, to help support the growth of cells within the interior of the scaffolds, blue food colouring was added to the water and the scaffold permeation was carefully observed, as shown in Figure 4.1. 200 mg (wet weight) DAT scaffolds were used in all experiments, sized to fit in the bioreactor chambers. Initially, the DAT was completely white and each scaffold was approximately 1 cm in diameter. The DAT was placed into one of the bioreactor chambers and distilled water was perfused through it at a flow rate of 1.5 mL/min. The food colouring was then added to the bioreactor medium reservoir and allowed to infiltrate the DAT. After 2 hours, the DAT was removed from the chamber sectioned to investigate the permeation patterns. The middle of the DAT was dyed blue, indicating complete perfusion of with the aqueous medium Figure 4.1.

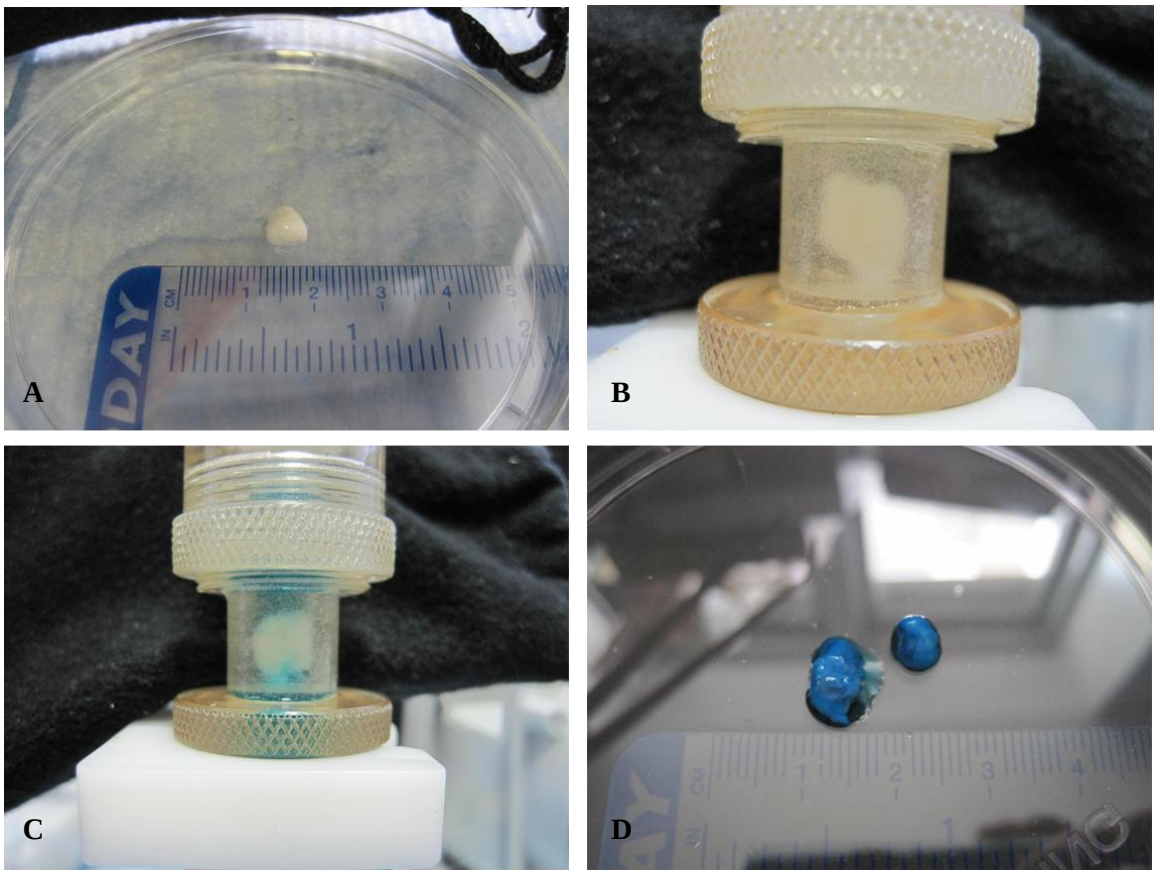

Figure 4.1: 200 mg DAT piece (A) remains in the middle of the bioreactor chamber as water is perfused through (B). Blue food colouring was added to the water (C) and the DAT was cut in half after 2 hours (D)

To further probe the suitability of the DAT as a substrate for cell growth in the bioreactor system, the permeability of the DAT was determined using a research grade blood pressure transducer (Harvard Apparatus, 724496) and Darcy's law, according to Equation 3.1 in section 3.4. The permeability was calculated using a range of flow rates and DAT size, based on the hydrated scaffold mass. Deionized water was selected as the medium, as it has a similar viscosity to the DMEM:Ham's F12 growth medium used for culturing adipose-derived stem cells (ASCs). The results are shown in Table 4.1. The device sensitivity was not small enough to measure a

pressure drop for the 200 mg, 500 mg and 750 mg DAT at 0.5 mL/min. The permeability decreased with increasing scaffold size and flow rate.

Table 4.1: Permeability of Decellularized Adipose Tissue

Flow rate mL/min	Permeability, k (m^2)			
	200 mg	**500 mg**	**750 mg**	**1000 mg**
0.5	>149*	>149*	>149*	149
1.5	149	75	75	75
2.5	75	50	50	50
3.5	50	37	37	37

***below level of sensitivity for the pressure transducer.**

4.2 Growth Environment

The effect of the oxygen concentration in the growth environment on the proliferation of the ASCs was determined by counting the number of cells present each day for 8 days, and using this growth curve to calculate the doubling time. The oxygen concentration of the hypoxic environment was 5%, while the normoxic was 21%. Tissue culture polystyrene (TSPC) 6-well plates were seeded with 20,000 ASCs per well, with three wells per day. Each well was counted three times using Trypan Blue solution (Sigma, T8154) using a hemocytometer. Figure 4.2 shows representative growth curves with cells from a single donor. Additional plots for 2 other donor sources are included in Figure 6.1 and Figure 6.2 in Appendix A. The slope of the exponential growth region was taken and used to calculate the doubling time. The corresponding doubling times for all three donors are shown in Table 4.2. For all three donors, a larger population of cells was obtained after 8 days of culture in the hypoxic environment.

Table 4.2: Effect of oxygen concentration on the growth rate of ASCs on TCPS. Data are shown as mean ± standard error

	Donor 1	Donor 2	Donor 3
Age	55	26	33
BMI	35.4	29.5	37.7
Doubling Time (Hypoxic)	1.7 days ± 0.7 days	1.5 days ± 1.6 days	1.5 days ± 0.5 days
Doubling Time (Normoxic)	3.1 days ± 2.6 days	1.8 days ± 1.4 days	1.6 days ± 1.2 days

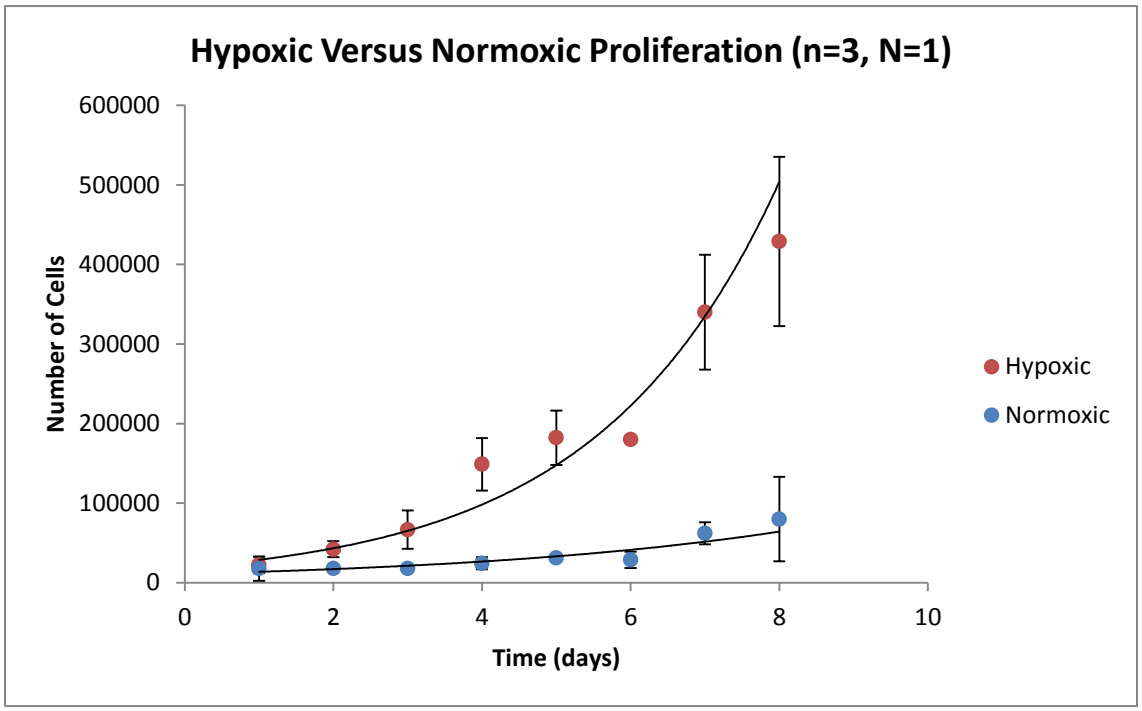

Figure 4.2: Sample growth curve illustrating Donor 1 cell counts. Donor was a 55 year old female, 84 kg, 154 cm and BMI of 35.4. Data points are given as means ± standard deviations.

4.3 Seeding Optimization

In order to investigate the optimum seeding method and density of the ASCs on the decellularized adipose tissue (DAT), qualitative analyses were completed using the confocal microscope (Olympus Fluoview FV1000). To gain a complete picture of the ASC growth on the DAT, the DAT was labeled with an amine-reactive Alexa Fluor® 350 carboxylic acid, succinimidyl ester (Molecular Probes, Burlington, Canada) and the ASCs were labeled with a fluorescent probe, CellTracker™ Green (Invitrogen, C2925). Figure 4.3 shows the ASC distribution at 7 and 14 days when the ASCs were seeded on the DAT in a single-cell suspension and then cultured in the perfusion bioreactor (Tissue Growth Technologies). Three different initial ASC seeding densities of 1, 2.5 and 5 million ASCs were investigated on 200 mg pieces of DAT.

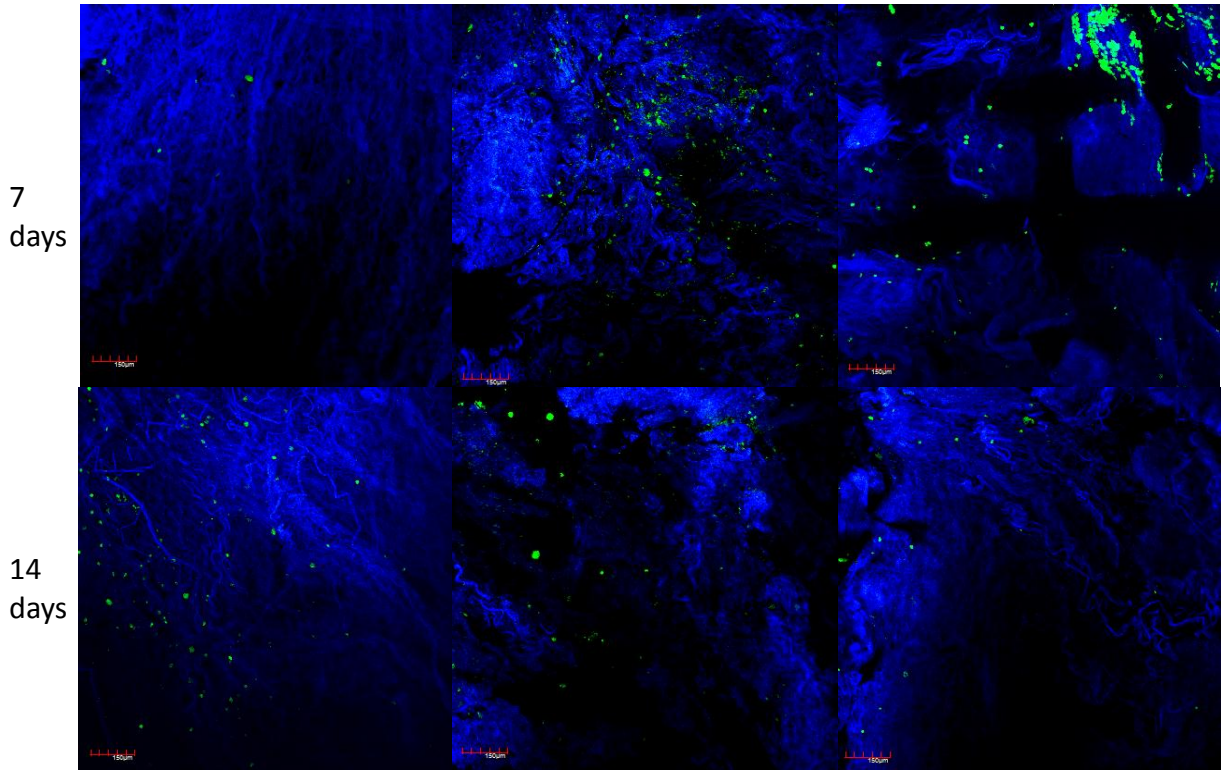

Figure 4.3: DAT (blue; stained with amine-reactive Alexa Fluor dye) seeded with ASCs (green) in single-cell suspension (1 x10^6 ASCs, 2.5 x 10^6 ASCs, or 5 x 10^6 ASCs), which were pre-stained with Cell Tracker Green. The DAT scaffolds were cultured in the perfusion bioreactor for 7 or 14 days. Donor was a 46 year old female, 70.3 kg, 155 cm and BMI of 29.3. Magnification 100x. Scale bar represents 150 microns.

The confocal pictures showed some evidence of proliferation in the DAT samples seeded with either 1 or 2.5 million ASCs. Clusters of the ASCs were found in localized regions of the DAT, rather than an even distribution of single cells. The ASCs also showed a spherical morphology, which is more similar to the cellular organization observed in the native environment, as compared to cell growth on TCPS [1, 9]. These results suggested that the seeding

of 1 million ASCs on the 200 mg pieces of DAT was the most promising density in order to support proliferation.

In order to quantify the proliferation of the ASCs, the Quant-iTTM Picogreen® dsDNA assay was used to measure the amount of double stranded DNA, which would be directly correlated to the number of ASCs present. Table 4.3 summarizes the results of the PicoGreen analysis for the first trial with 1 million ASCs per scaffold and Figure 4.4 shows the average dsDNA per sample (ng) at 72 hours, 7 days and 1 month when 1 million ASCs were seeded on the DAT in a single-cell suspension and cultured under four different conditions: normoxic static, normoxic perfusion, hypoxic static or hypoxic perfusion.

Table 4.3: dsDNA content of 200 mg DAT seeded with 1 million ASCs in suspension. Samples were grown under normoxic static, normoxic perfusion, hypoxic static or hypoxic perfusion conditions. Data are expressed as means ± SD. Donor was a 47 year old female, 85.3 kg, 168 cm and BMI of 30.2 (n=3)

Time	Normoxic (21% O_2)		Hypoxic (5% O_2)	
	Static	Perfusion	Static	Perfusion
72 hours	291 ± 70 ng dsDNA	135 ± 86 ng dsDNA	510 ± 86 ng dsDNA	467 ± 120 ng dsDNA
7 days	210 ± 72 ng dsDNA	186 ± 70 ng dsDNA	402 ± 186 ng dsDNA	599 ± 20 ng dsDNA
1 month	221 ± 84 ng dsDNA	61 ± 39 ng dsDNA	395 ± 25 ng dsDNA	486 ± 101 ng dsDNA

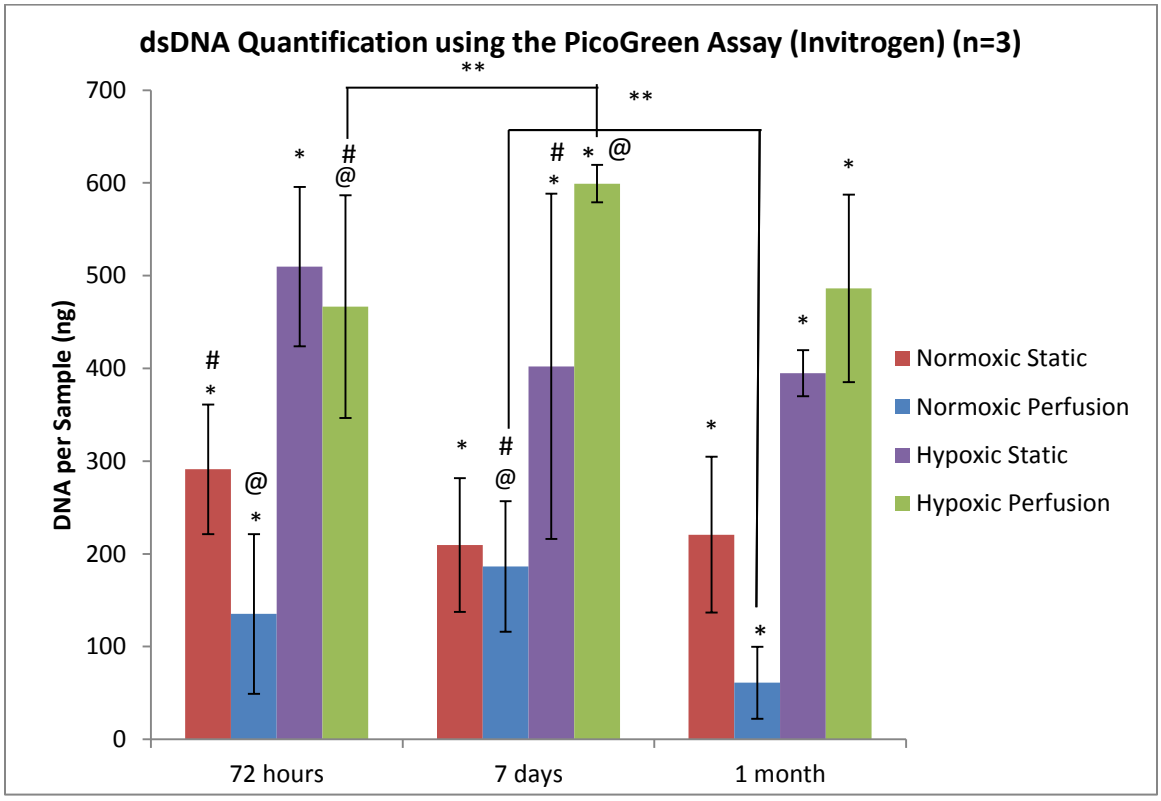

Figure 4.4: dsDNA content of 200 mg DAT seeded with 1 million ASCs in suspension. Samples were grown under normoxic static, normoxic perfusion, hypoxic static or hypoxic perfusion conditions. Data are expressed as mean ± SD. Statistical significance was determined by one-way ANOVA with a post-hoc Tukey's comparison of the means ($p<0.05$); *, @, # = statistically different from other groups at time point, ** = statistically different between time points. Donor was a 47 year old female, 85.3 kg, 168 cm and BMI of 30.2.

In general, the hypoxic (5% O_2) growth conditions induced greater proliferation as compared to the normoxic (21% O_2) growth conditions. However, there was large variability between the samples from identical growth conditions, indicating that the system required further optimization. Samples cultured under both normoxic static or hypoxic static conditions did not show statistically significant differences in dsDNA content over time, suggesting that the cells were not proliferating under these conditions. Normoxic culture conditions for both static or

perfusion samples resulted in statistically lower dsDNA than samples cultured under hypoxic static or perfusion respectively. From the results, it was concluded that the suspension seeding method for the ASCs on the DAT was insufficient to produce substantial cell proliferation and infiltration.

As an alternative seeding strategy, the use of multicellular aggregates of ASCs, prepared by methods developed in collaboration with the lab group of Dr. Adam Katz (University of Virginia), was investigated as an ASC seeding method on the 200 mg pieces of DAT. Figure 4.5 compares the proliferation of ASCs incubated statically under hypoxic conditions at 72 hours. The ASCs were labeled with a fluorescent probe, CellTracker™ Green (Invitrogen, C2925), to facilitate visualization. The DAT was seeded with either 25 or 50 multicellular aggregates of 20,000 ASCs; representing 500,000 or 1,000,000 ASCs respectively.

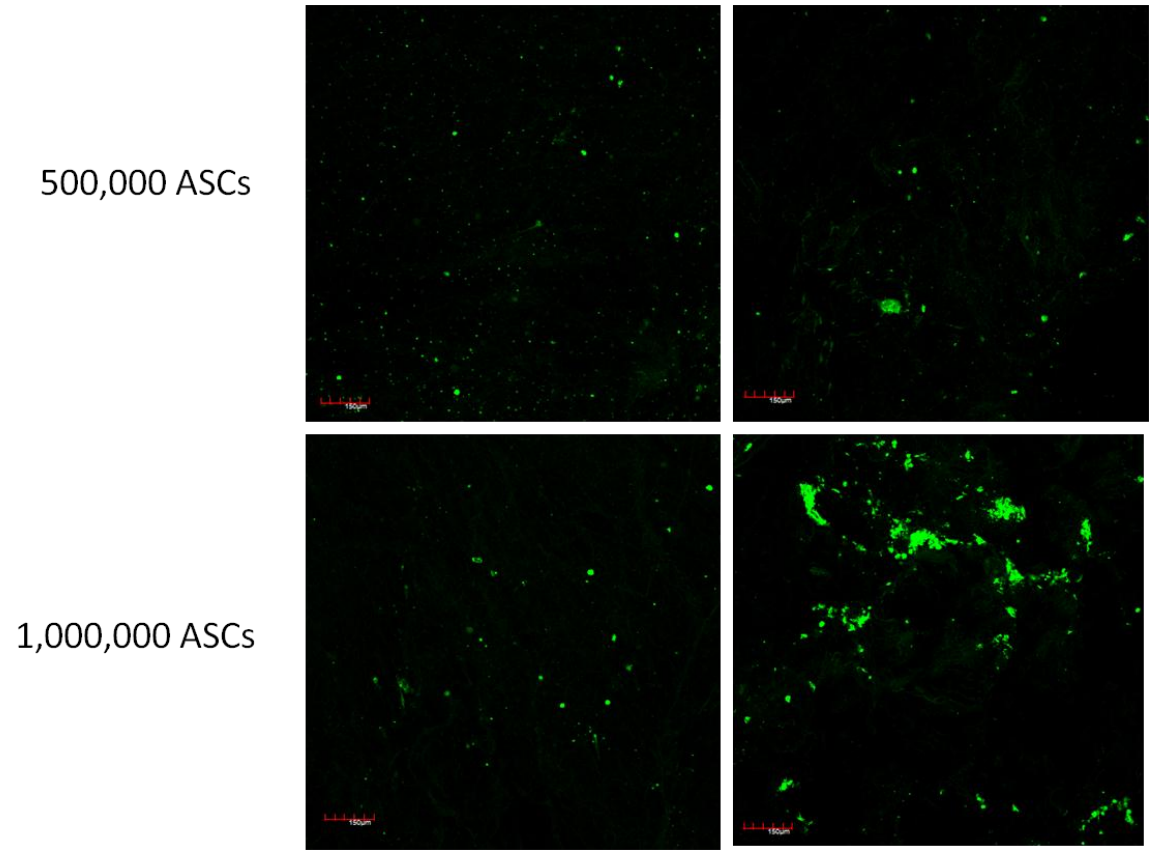

Figure 4.5: 200 mg DAT seeded with ASCs (green) in multicellular aggregates (20,000 ASCs/aggregate) and pre-stained with Cell Tracker Green. Samples were grown statically under hypoxic (5% O_2) conditions, and imaged by confocal at 72 h post-seeding. Donor was a 49 year old female, 72 kg, 154 cm and BMI of 30.4. Magnification 100x. Scale bar represents 150 microns.

ASCs were identified in significant numbers in the confocal pictures, showing evidence of successful attachment and proliferation of the multicellular aggregates. At 72 hours, the samples with 50 aggregates (1 million ACS), showed areas of high cell attachment through the surface of the scaffold while the samples with 25 aggregates (500,000 ASCs) lacked these areas of high ASC attachment. Based on this promising initial data, the experiment was expanded to

investigate three initial aggregate numbers using confocal microscopy. More specifically, 12, 25 and 50 multicellular aggregates (20,000 ASCs/aggregate), equivalent to 250,000, 500,000 and 1 million ASCs respectively, were seeded on the 200 mg DAT scaffolds. The ASCs were pre-labeled with CellTracker™ Green and cultured statically under hypoxic (5% O_2) conditions. Figure 4.6 shows the results of the cell distribution study at 7 days.

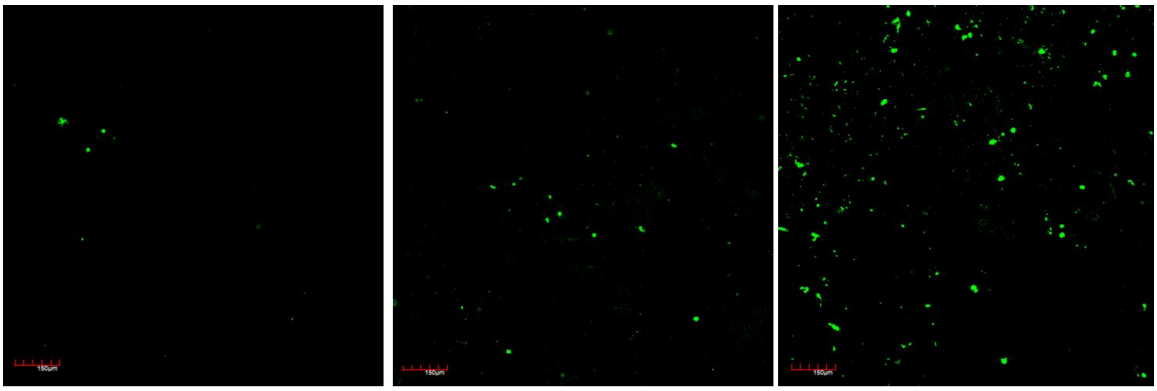

Figure 4.6: 200 mg DAT seeded with ASCs in aggregates of 20,000 cells, pre-stained with Cell Tracker Green. Samples were grown statically under hypoxic (5% O_2) conditions, with imaging at 7 days. Donor was a 62 year old female, 64 kg, 148 cm and BMI of 29.2. Magnification 100x. Scale bar represents 150 microns.

Significant cell attachment and proliferation was observed when the 200 mg DAT was seeded with 50 aggregates, corresponding to 1 million ASCs. However, at the lower densities, very few cells could be visualized in the scaffolds at 7 days.

The qualitative confocal results were quantified using Quant-iTTM Picogreen® dsDNA assay. Table 4.4 summarizes the PicoGreen calculation results and Figure 4.7 shows the dsDNA per sample (ng) at 72 hours and 7 days when each 200 mg DAT scaffold was seeded with 12, 25

or 50 multicellular aggregates, which would be equivalent to 250,000, 500,000 and 1 million ASCs respectively. The samples were grown statically under hypoxic (5% O_2) conditions.

Table 4.4: dsDNA content for 200 mg DAT seeded with multicellular aggregates comparing seeding densities of 12 (250,000 ASCs total); 25 (500,000 ASCs) and 50 (1,000,000 ASCs) multicellular aggregates per DAT scaffold. The samples were grown statically under hypoxic conditions. Data are expressed as mean ± SD. Donor was a 62 year old female, 64 kg, 148 cm and BMI of 29.2. (n=3)

Time	250,000 ASCs	500,000 ASCs	1,000,000 ASCs
72 hours	*Below threshold	78 ± 96 ng dsDNA	258 ± 39 ng dsDNA
7 days	259 ± 55 ng dsDNA	239 ± 127 ng dsDNA	883 ± 553 ng dsDNA

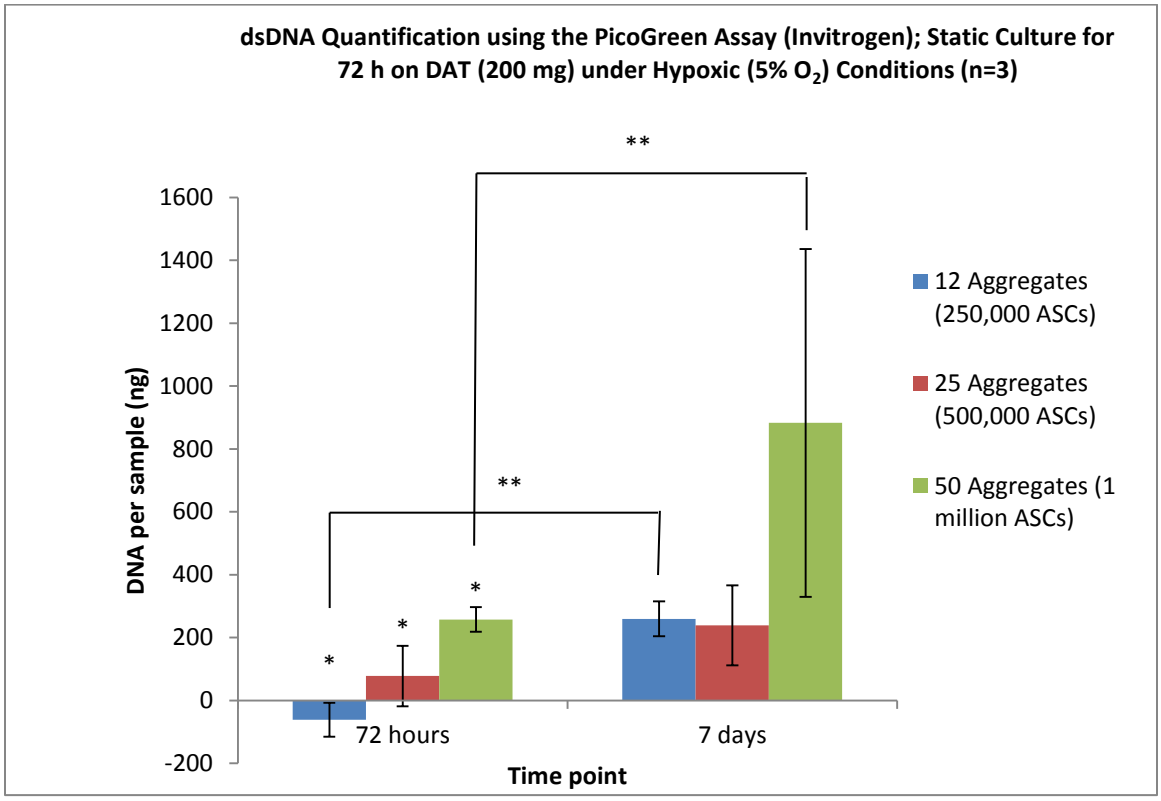

Figure 4.7: dsDNA content for 200 mg DAT seeded with multicellular aggregates comparing seeding densities of 12 (250,000 ASCs); 25 (500,000 ASCs) and 50 (1,000,000 ASCs) aggregates. Samples were grown statically under hypoxic conditions. Data are expressed as means ± SD. Statistical significance was determined by one-way ANOVA with post-hoc Tukey's comparison of the means ($p<0.05$); * = statistically different from other groups at the same time point, ** = statistically different between time points. Donor was a 62 year old female, 64 kg, 148 cm and BMI of 29.2.

At the 72 hour time point, all initial seeding showed statistically different amounts of dsDNA. The results at 7 days showed that only the samples initially seeded with 50 aggregates (1 million ASCs) had resulted in a statistically significant increase in dsDNA, indicative of cell proliferation on the DAT scaffolds. These results suggested that a minimum of 50 aggregates, corresponding to 1 million ASCs, was required for significant cell attachment and proliferation.

The seeding experiments were expanded to include four different growth conditions: normoxic static, normoxic perfusion, hypoxic static and hypoxic perfusion to explore the use of the perfusion bioreactor. Table 4.5 summarizes the results of the PicoGreen calculations and Figure 4.8 shows the dsDNA per sample (ng) at 72 hours, 7 and 14 days, when 1 million ASCs were seeded on the DAT in the form of 50 multicellular aggregates.

Table 4.5: dsDNA content for 200 mg DAT seeded with 50 multicellular aggregates of 20,000 human ASCs (seeding density of 1,000,000 ASCs). Samples were grown under normoxic static, normoxic perfusion, hypoxic static or hypoxic perfusion conditions. Data are expressed as mean ± SD. Donor was a 40 year old female, 87.8 kg, 175 cm and BMI of 28.7, (n=3).

Time	Normoxic (21% O_2)		Hypoxic (5% O_2)	
	Static	Perfusion	Static	Perfusion
72 hours	164 ± 88 ng dsDNA	75 ± 35 ng dsDNA	389 ±31 ng dsDNA	338 ± 198 ng dsDNA
7 days	379 ± 198 ng dsDNA	233 ± 701 ng dsDNA	306 ± 23 ng dsDNA	461 ± 86 ng dsDNA
14 days	427 ± 40 ng dsDNA	815 ± 177 ng dsDNA	705 ± 172 ng dsDNA	791 ± 46 ng dsDNA

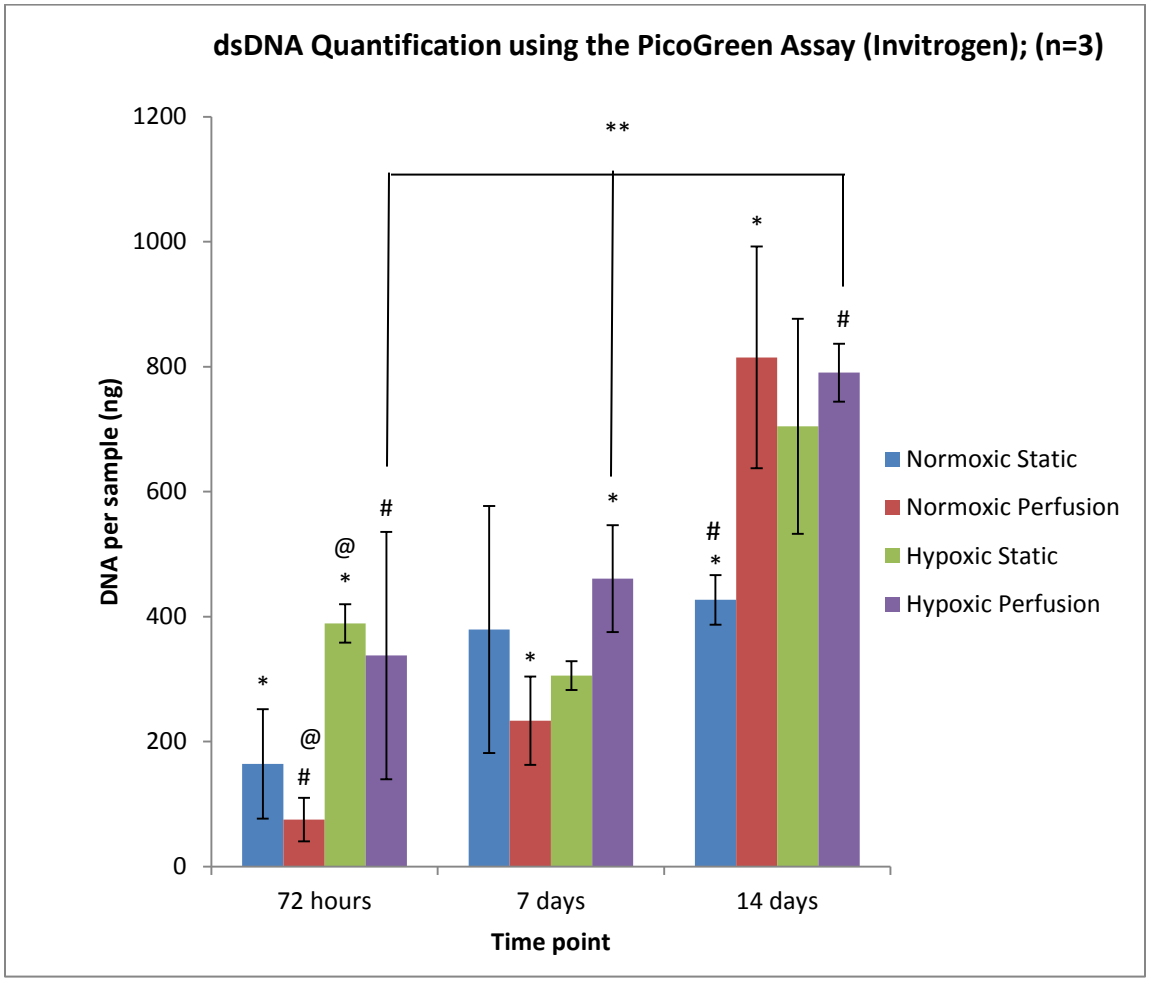

Figure 4.8: dsDNA content for 200 mg DAT seeded with 50 multicellular aggregates (20,000 ASCs/aggregate), corresponding to a seeding density of 1,000,000 ASCs. Samples were grown under normoxic static, normoxic perfusion, hypoxic static or hypoxic perfusion conditions. Data are expressed as mean ± SD. Statistical significance was determined by one-way ANOVA with post-hoc Tukey's comparison of the means ($p<0.05$); *, @, # = statistically different from other groups at the same time point, ** = statistically different between time points. Donor was a 40 year old female, 87.8 kg, 175 cm and BMI of 28.7.

Interestingly, the size of the samples cultured within the perfusion bioreactor was observed to decrease to half its original size over time, potentially indicative of cellular expansion and contraction, while the samples cultured statically did not display any detectable changes in

size over the course of the study. The dsDNA content in the hypoxic perfusion samples was statistically higher than the normoxic perfusion samples at both 72 hours and 7 days, but not at 14 days. Hypoxic static was statistically higher than the normoxic static at 72 hours, but not at the later time points. Samples cultured under normoxic static conditions did not show significant increases in dsDNA over 14 days, while those grown under normoxic perfusion showed a significant increase in dsDNA at all time points, indicating that the bioreactor provided a more permissive environment for cell expansion. The amount of dsDNA collected at 14 days from the samples cultured under hypoxic static and hypoxic perfusion conditions was significantly higher than at the earlier time points, consistent with overall cell proliferation on the DAT.

4.4 Confocal Analyses

In order to further explore the effect of medium perfusion and oxygen concentration on the proliferation of the ASCs on the DAT scaffolds, complementary qualitative studies were completed using the confocal microscope (Olympus Fluoview FV1000). To gain a more complete picture of the ASC growth on the DAT, the DAT was pre-labeled with an amine-reactive Alexa Fluor® 350 carboxylic acid, succinimidyl ester (Molecular Probes, Burlington, Canada) and the ASCs were pre-labeled with a fluorescent probe, CellTracker™ Green (Invitrogen, C2925).

The ASCs were cultured in suspension, using methods developed by Dr. Adam Katz, to form multicellular aggregates containing 20,000 ASCs per aggregate, as described in the previous chapter. Based on the previous results, each DAT scaffoldwas seeded with 50 aggregates, resulting in a concentration of 1 million ASCs per 200 mg DAT. After 24 hours, the samples were split into 4 groups: normoxic static, normoxic perfusion, hypoxic static and hypoxic perfusion. The static samples were cultured in 6-well plates, while the perfusion samples were cultured in the perfusion bioreactor. Then normoxic samples were cultured at 21 % O_2, while the

hypoxic samples were cultured at 5% O_2. The confocal imaging results are shown in Figure 4.9, Figure 4.10 and Figure 4.11, including the fluorescence for the staining of the DAT scaffolding matrix structure and the PicoGreen staining for the ASCs attached to the scaffolding. This complete picture gives a more comprehensive illustration of the growth of the ASCs. Figure 6.3, Figure 6.4 and Figure 6.5, located in Appendix B show the confocal results for the ASCs alone (without Alexa Fluor) at 72 hours, 7 days and 14 days respectively. Consistent with the previous observations, the samples from the perfusion bioreactor decreased in size relative to the static samples at 7 and 14 days.

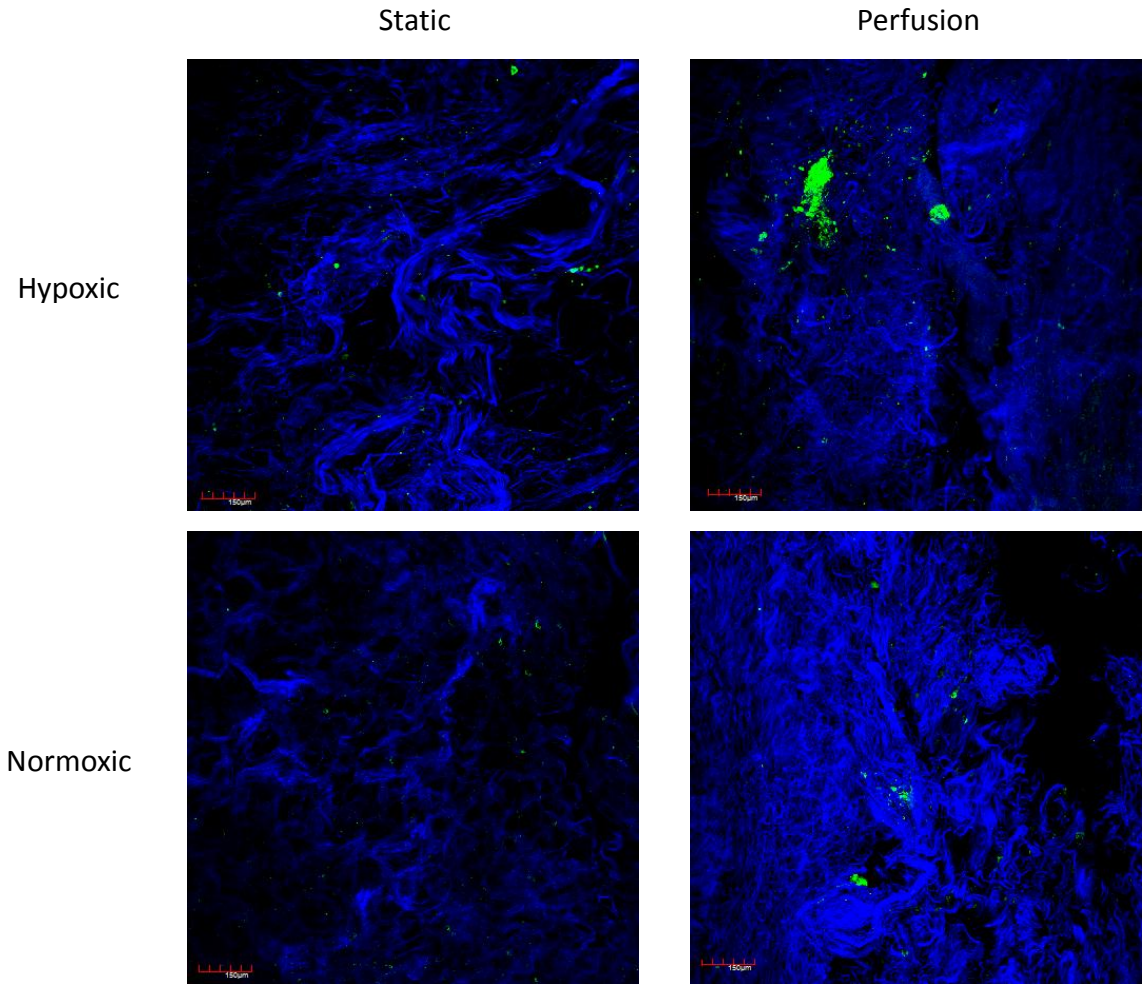

Figure 4.9: 200 mg DAT (stained with Alexa Fluor) seeded with ASCs in aggregates of 20,000 (stained with Cell Tracker Green) at 72 hours (50 aggregates/200 mg DAT). Samples were grown either statically or under perfusion in the bioreactor, and in either normoxic (21% O_2) or hypoxic (5% O_2) conditions. Donor was a 41 year old female, 98 kg, 173 cm and BMI of 32.8. Magnification 100x. Scale bars represent 150 microns.

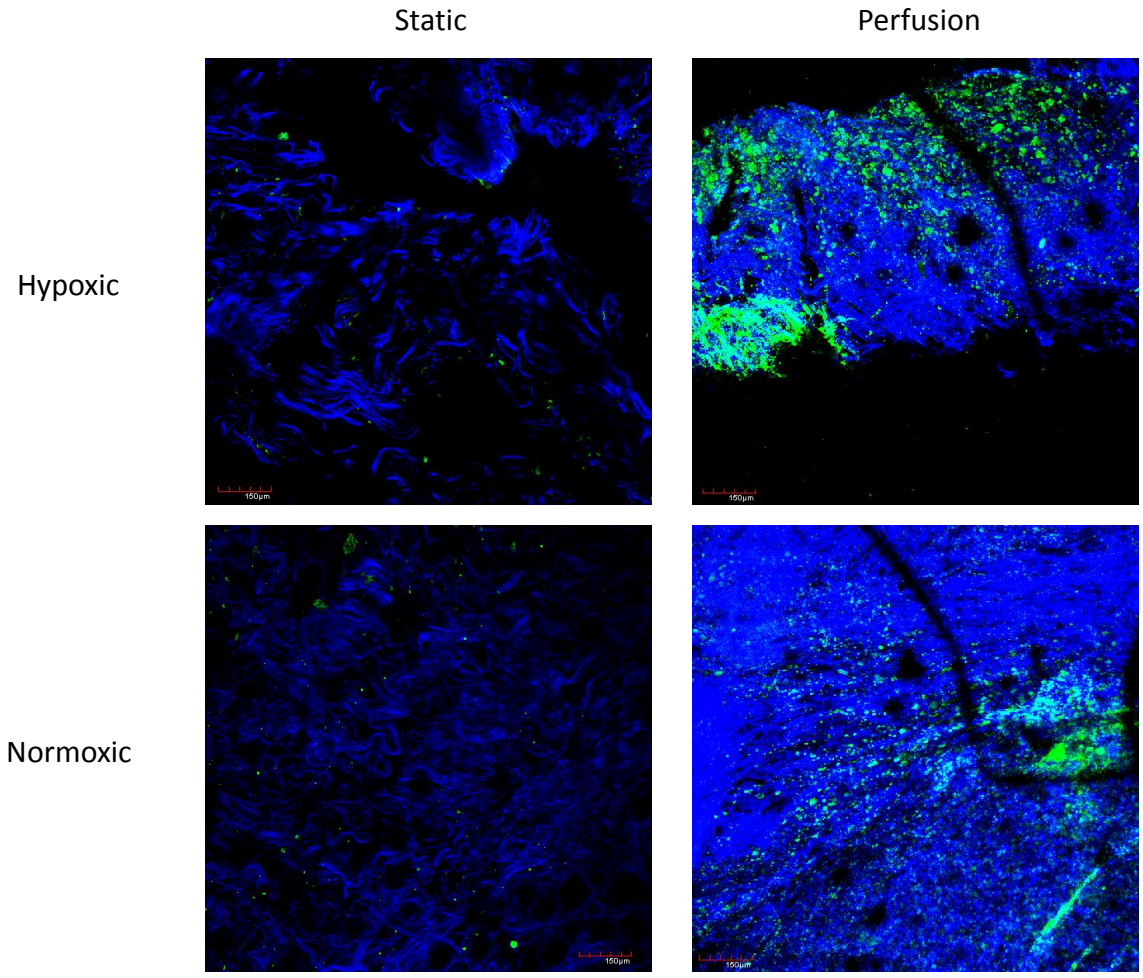

Figure 4.10: 200 mg DAT (stained with Alexa Fluor) seeded with ASCs in aggregates of 20,000 (stained with Cell Tracker Green) at 7 days (50 aggregates/200 mg DAT). Samples were grown either statically or under perfusion and in either normoxic (21% O_2) or hypoxic (5% O_2) conditions. Donor was a 41 year old female, 98 kg, 173 cm and BMI of 32.8. Magnification 100x. Scale bars represent 150 microns.

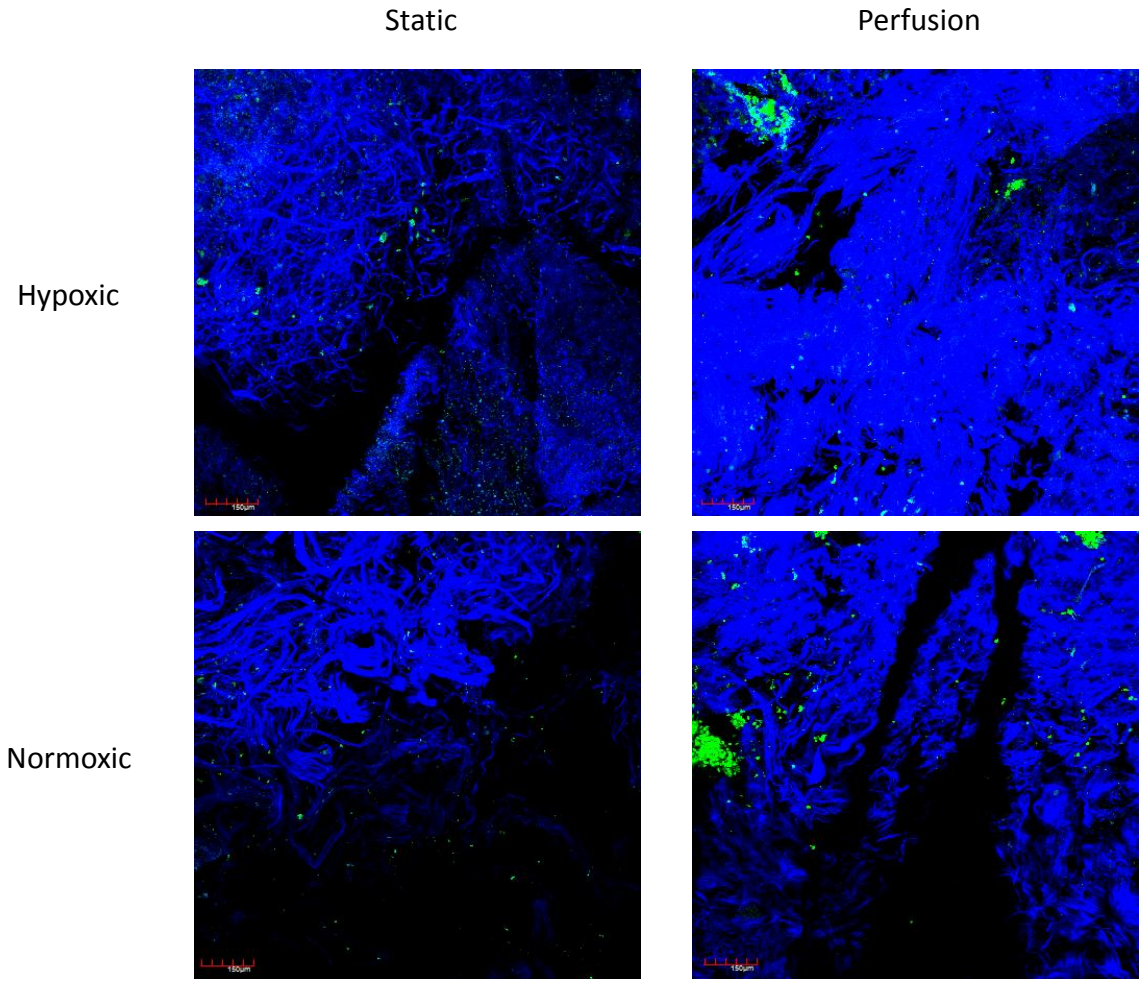

Figure 4.11: 200 mg DAT (stained with Alexa Fluor) seeded with ASCs in aggregates of 20,000 (stained with Cell Tracker Green) at 14 days (50 aggregates/200 mg DAT). Samples were grown either statically or under perfusion and in either normoxic (21% O_2) or hypoxic (5% O_2) conditions. Donor was a 41 year old female, 98 kg, 173 cm and BMI of 32.8. Magnification 100x. Scale bars represent 150 microns.

The confocal analyses was able to produce images of the DAT surface and ASC. Based on the confocal pictures, the ASCs cultured within the DAT scaffolding tended to grow in clusters within the pores of the matrix. Perfusion of the medium using the bioreactor resulted in increased ASC populations, under both oxygen tensions and at all time points, relative to the

static culturing conditions. The hypoxic conditions demonstrated slightly increased ASC numbers at each time point, as compared to the normoxic culturing; however this is difficult to quantify with the confocal analysis. There is a general trend toward increased ASC numbers with increasing culturing time in the bioreactor, consistent with the dsDNA content proliferation data.

4.5 Adipogenic Differentiation

To confirm that the bioreactor-expanded ASCs on the DAT after 14 days in culture could be stimulated to undergo adipogenic differentiation, the ASCs were seeded in aggregate form onto the DAT and were cultured under the three most promising conditions in the proliferation study (normoxic (21% O_2) perfusion, hypoxic static (5% O_2) and hypoxic (5% O_2) perfusion) in complete medium, for 14 days. These culturing conditions were selected based on the DNA quantification results that showed that these culturing conditions resulted in increases in dsDNA within the DAT. After 14 days, the samples were placed in 6-well TCPS plates and transferred into adipogenic differentiation medium. Non-induced samples cultured in proliferation medium were used as controls. The samples were cultured statically to mimic the *in vivo* environment, simulating the hypoxic conditions that would exist after the scaffolds were implanted in subcutaneous defect sites. GPDH activity was calculated at 7 days after the induction of differentiation to confirm adipogenesis. Table 4.6 summarizes the GPDH calculations and Figure 4.12 illustrates the GPDH results for the 200 mg DAT initially seeded with 1 million ASCs in aggregate form. The enzyme activity data is expressed in units of mU of GPDH activity/mg of total cytosolic protein.

Table 4.6: GPDH activity for 200 mg DAT seeded with 50 multicellular aggregates (seeding density of 1,000,000 ASCs. Samples were grown under normoxic perfusion, hypoxic static or hypoxic perfusion conditions. ASCs seeded on TCPS plates were included as a control. Data are expressed as mean ± SD. Donor was a 21 year old female, 62.1 kg, 165 cm and BMI of 22.8 (n=2)

	Induced	**Non-induced**
TCPS Control	3.65 ± 0.99 mU/mg	0.20 ± 0.28 mU/mg
Hypoxic Static	5.09 ± 0.77 mU/mg	0.56 ± 0.49 mU/mg
Hypoxic Perfusion	7.31 mU/mg	1.02 ± 0.36 mU/mg
Normoxic Perfusion	2.26 ± 1.51 mU/mg	0.99 ± 0.30 mU/mg

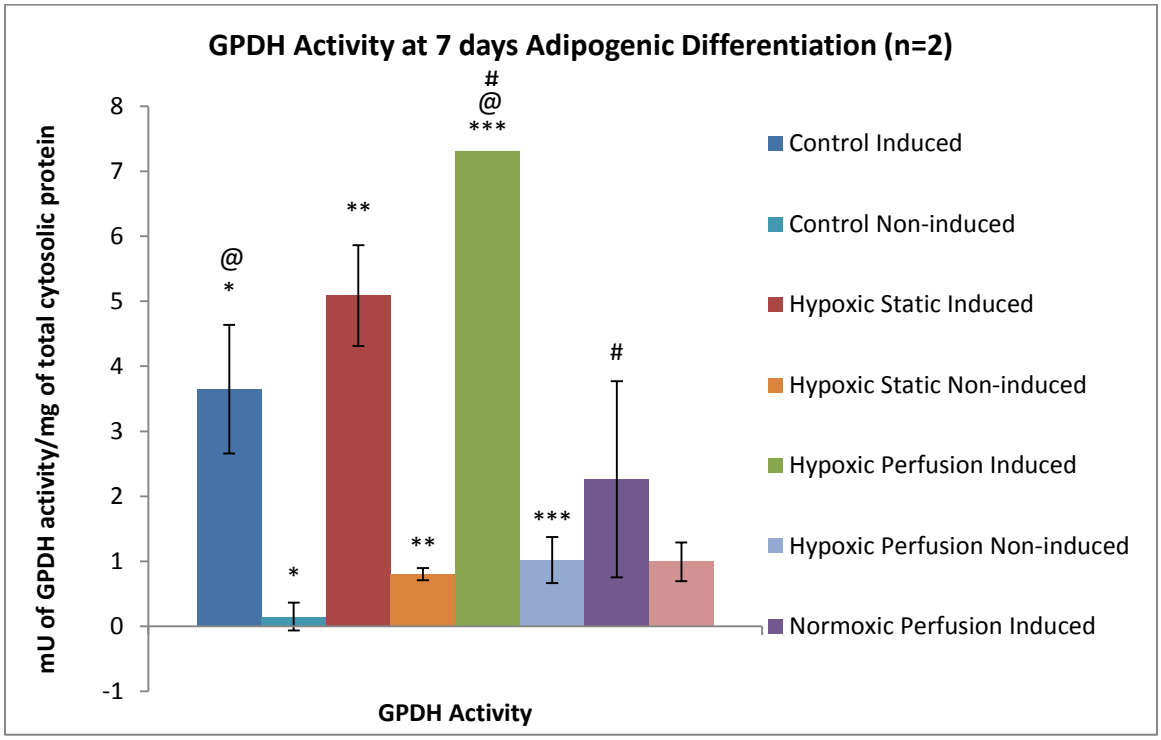

Figure 4.12: GPDH activity for 200 mg DAT seeded with 50 multicellular aggregates (seeding density of 1,000,000 ASCs). Samples were cultured for 14 days in proliferation medium under normoxic perfusion, hypoxic static or hypoxic perfusion conditions, and then transferred into adipogenic differentiation medium for 7 days under static conditions. ASCs seeded on TCPS plates were included as a control. Data are expressed as the mean ± SD. Statistical significance was determined by one-way ANOVA with post-hoc Tukey's comparison of the means ($p<0.05$); *, **, *, @, # = statistically different from other groups at the same time point. Donor was a 21 year old female, 62.1 kg, 165 cm and BMI of 22.8.**

Under all culture conditions except the normoxic perfusion, the induced samples were significantly increased. This illustrates that the ASCs seeded on the DAT and cultured in either normoxic or hypoxic conditions within the bioreactor for 14 days maintained their potential to undergo adipogenic differentiation. The hypoxic perfusion induced samples were significantly greater than the TCPS control induced samples suggesting the creation of a more permissive

microenvironment for adipogenesis, while the normoxic perfusion and hypoxic static were not statistically different from the TCPS controls.

Chapter 5

Discussion

Previous research in adipose tissue-engineering has suggested that hypoxic conditions (< 5% O_2) and perfusion culturing have beneficial effects on the long-term survival of tissue constructs incorporating adipose-derived stem cells (ASCs) [35]. Consistent with the literature, the *in vitro* culturing experimental results in the current thesis suggest that there are positive effects of both hypoxic culturing (5% O_2) and medium perfusion on the proliferation of ASCs cultured on decellularized adipose tissue (DAT) scaffolds, relative to normoxic (21% O_2) conditions and static culturing. Further, the differentiation results confirm that the adipogenic potential of the ASCs was maintained with perfusion culturing, as demonstrated by the GPDH results having increased enzyme activity when the constructs were cultured in an adipogenic differentiation medium.

Cell-matrix interactions have been shown to influence ASC proliferation and multilineage differentiation. Previous work by Flynn *et al.* (2010) led to the development of a decellularization process to produce the DAT scaffolds from the adipose extracellular matrix (ECM). This process maintains the 3-dimensional matrix architecture as well as the basement membrane composition (including collagen type IV and laminin), while ensuring a high degree of removal (> 90%) of the cells and cellular components from the tissues [20]. This material was used as the scaffold for cellular attachment within the bioreactor system, as it provides a 3-dimensional growth environment very similar to the native growth environment of the ASCs. It was hypothesized that the DAT may promote normal cell-matrix interactions to initiate a more tissue-like regenerative response, mediating the proliferation of the seeded stem cells.

Adipose tissue is mainly composed of a fibronectin-rich stromal matrix, type I collagen and versican. Adipogenesis leads to the remodeling of the ECM into a laminin-rich basement membrane. Research has shown that the ECM produced during early stage adipogenesis (day 3), inhibits stem cell proliferation, while supporting adipogenesis compared to TCPS [71]. Adipogenesis is inhibited by fibronection (through integrin α5-activated signaling and actin filament) and collagen type I, while enhanced by laminin [71].

5.1 DAT Scaffold Permeability

The permeability coefficient for the 200 mg DAT scaffolds used in the experiments at the flow rate selected (1.5 mL/min) based on the literature [72], was determined to be 149 m^2. At lower flow rates, there was not a large enough pressure drop across the DAT to be read with the pressure transducer used in the experimentation. The scaffold permeability decreased with larger DAT pieces, due to a greater restriction of the medium flow through the thicker, more resistive scaffolding. The permeability also decreased with increasing flow rates, possibly associated with the formation of small microchannels within the DAT due to the higher convective transport. Increased flow rates could potentially raise concerns with cell damage or loss caused by shear forces within the scaffold. The permeability of the DAT was determined without any ASCs, as previous work by Dubois *et al.* (2011) showed that the presence of cells within a gelatin gel did not affect the gel permeability and the apparent diffusion coefficient [19].

There is little literature on the permeability of commonly used scaffolding materials, since this value is dependent on multiple variables including scaffolding manufacturing methods. However, one study investigated the diffusion in fibrin, gelatin, agarose and alginate scaffolds using fluorescence recovery after photobleaching (FRAP) [73]. The alginate scaffolds were composed of 2% (w/v) low-viscosity sodium alginate in 9 mg/mL NaCl. The agarose scaffolds

were composed of 2% (w/v) low-melting-point agarose (Type VII) in 9 mg/mL NaCl. The fibrin scaffolds were composed of 75-115 mg/mL fibrogen solution in a 500 I.U./mL thrombin solution. Gelatins disks of Surgifoam® were used. The size of the dextran molecules used in measuring the FRAP was found to effect the diffusion co-efficient for the scaffolds [73]. The values in Table 5.1 show the mean diffusion coefficients for the scaffold material without cells after one day in DMEM culturing medium. The ranges represent the values calculated from 500 kDa and 3 kDa Dextran sizes.

Table 5.1: Mean diffusion coefficients and standard error for the four different scaffold materials calculated using FRAP [73].

Scaffolding Material	**D ($\mu m^2/s$)**
Agarose	39±5 - 897±139
Alginate	53±9 - 854±109
Fibrin	34±7 - 260±86
Gelatin	91±29 - 538±79

The food colouring perfusion experiment confirmed that there was medium infiltration throughout the DAT scaffold, which is a requirement of perfusion culturing to ensure that the ASCs within the scaffolding have adequate nutrient delivery and waste removal.

5.2 Population Doubling Times

The population doubling times of the cultured ASCs in the normoxic conditions on TCPS in the experiments in this thesis were similar to those found by other investigators [5, 7]. Oedayrajsingh-Varma *et al.* (2006) found that the mean population doubling time of cultured ASCs was 2.6 days when the cells were harvested from resected tissues, and 2.8 days when they

were harvested from tumescent liposuction samples [5]. All of the growth curves in the current study had a 1 to 2 day lag phase, associated with initial cell attachment and spreading, followed by exponential growth for the duration of the experiment.

There was a large donor variability in the growth rate of the ASCs, which was likely related to the differences in the donor body mass index (BMI) and age. These results are consistent with the trends of donor variability reported in the literature, and emphasize the need to consider each specific donor when developing autologous cell-based therapies [30]. In this study, the ASCs extracted from the oldest patient (donor 1) had a greater doubling time under normoxic conditions, consistent with the recognized reduction in the stem cell potential of extracted mesenchymal populations with aging [30]. While the actual doubling times for the ASCs under hypoxic conditions were lower than those in normoxic conditions, the inherent errors in the hemocytometer counting methods used in the current study produced large standard errors. However, the data demonstrated a strong trend towards reduced doubling times under hypoxic conditions regardless of the donor source. Further, larger ASC populations were obtained using the hypoxic culturing environment over the 8-day time frame in the current study. These factors are important for clinical applications, as a shorter culturing period to obtain larger quantities of ASCs would be beneficial and could help to minimize the costs of *ex vivo* culturing.

5.3 Seeding Optimization

When the ASCs were seeded on the DAT, they maintained a spherical morphology, which is more similar to the cellular phenotype found in the *in vivo* environment than what is typically observed in 2-dimensional cultures on TCPS [1, 9]. Cell morphology is known to play an important role in mediating stem cell proliferation and differentiation, and future research could explore whether this change in morphology is consistent with a more tissue-like

regenerative response. When seeded in multicellular aggregates, confocal analysis of the cultured DAT scaffolds showed that the ASCs were generally found in clusters throughout the scaffolding, indicating the importance on cell-cell interactions in maintaining cell viability and supporting proliferation [12, 27].

In order to determine a more optimized initial seeding density, the ASCs were initially seeded in the form of a single-cell suspension at 1, 2.5 and 5 million ASCs per 200 mg DAT scaffold. Interestingly, the samples seeded with 5 million ASCs showed little proliferation, while those seeded with both 1 and 2.5 million ASCs showed similar proliferation levels. The higher seeding densities may not have been beneficial under the static conditions initially studied, due to an inability to support the higher metabolic demands of the larger cell populations by diffusion within the small medium reservoir. Further, the use of high seeding densities raises technical challenges due to the large volumes of tissue that would have to be processed to extract the initial number of cells required for each scaffold. Therefore, an initial seeding density of 1 million ASCs was selected, as this configuration produced high proliferation while minimizing the initial cell requirements.

The experiments were then expanded to compare ASC proliferation within the custom-designed perfusion bioreactor system (Tissue Growth Technologies) under normoxic static, normoxic perfusion, hypoxic static and hypoxic perfusion using the Quant-iTTM PicoGreen® assay to quantify double stranded DNA content, as a measure of the total cell content. While there was some evidence of cell proliferation within the DAT scaffolds using the confocal microscope when 1 million ASCs were seeded in suspension, the level of proliferation achieved with the suspension seeding method proved to be insufficient to produce high amounts of dsDNA indicative of significant cell proliferation, evidenced by the large variability in the dsDNA data

calculated under identical growth conditions. The DAT scaffolding itself produced detectable background fluorescence due to non-specific interactions between the dye and the protein-based scaffold when the digested DAT was incubated with the PicoGreen reagent. These effects were controlled by adaption of the standard assay protocols and the use of non-seeded DAT scaffold controls to normalize the data. With the use of a perfusion bioreactor, the removal of loosely attached and/or dead ASCs was expected, which may have contributed to the low dsDNA, particularly at the first time point (72 hours).

Recent work in the field of stem cells has moved toward the use of multicellular aggregates for culturing cells. In part, multicellular aggregates can help to maintain cell-cell interactions [12]. The initial studies in this thesis with the aggregate culture methods first confirmed the successful attachment and proliferation of the multicellular aggregates seeded on the DAT to assess the potential use of this seeding method as an alternative to single cell suspension seeding. The cells again showed a spherical morphology on the DAT, and were generally observed in clusters throughout the scaffolding. Significant cell attachment and proliferation were observed when the 200 mg DAT was seeded with 50 aggregates, corresponding to a total of 1 million ASCs. However, seeding with a lower initial ASC density did not lead to significant proliferation, potentially due to a lack of sufficient cell-cell interactions within the amorphous DAT scaffolds. dsDNA results from the Quant-iTTM PicoGreen® assay confirmed the qualitative confocal data that a minimum of 50 aggregates, and therefore 1 million ASCs, was required for significant cell attachment and proliferation.

5.4 Application of the Perfusion Bioreactor System

The aggregate seeding method was then expanded to compare ASC proliferation using the perfusion bioreactor system under normoxic static, normoxic perfusion, hypoxic static and

hypoxic perfusion using the Quant-iTTM PicoGreen® assay. Seeding the DAT with aggregates resulted in higher levels of dsDNA within the scaffolds as compared to single cell suspension seeding. This increase was likely due to enhanced cell-cell interactions and paracrine factor secretion in the aggregates, which are essential for cell viability and proliferation.

The normoxic static samples did not show statistically significant proliferation over the course of the study, potentially due to lack of sufficient nutrients within the scaffold, leading to a necrotic center. Similar results have been reported with larger cell aggregates in other studies [42]. These results were not observed in the hypoxic static conditions, which may have been due to greater ASC proliferation on the surface of the DAT due to the stimulating effects of the low oxygen environment [35]. Normoxic perfusion dsDNA levels were low at the 72 hour time point, had reached the same level as the hypoxic perfusion samples after 14 days culturing. Overall, the data suggests that the implementation of a perfusion may be beneficial in increasing the long-term viability of the constructs. Interestingly, when the samples were cultured within the perfusion bioreactor, the DAT showed a decrease in size. One possible explanation for the phenomenon is that the ASCs attached to the collagen fibers in the DAT scaffolding, contracting the matrix as they migrated into the central scaffold regions, and potentially altering the collagen structure of the DAT through the secretion of matrix-degrading enzymes, such as MMPs [25, 73].

The results of the confocal analyses using 50 aggregates (1 million ASCs total) seeded on 200 mg pieces of DAT in both static and perfusion cultures again confirmed that the ASCs maintained their spherical morphology and grew in clusters within the DAT. This cell distribution was expected, particularly at early time points, since the ASCs were seeded as multicellular aggregates. Greater cell proliferation was qualitatively observed in the perfusion samples compared to static samples at each time point, supporting the quantitative dsDNA data and

illustrating the benefit of perfusion on ASC proliferation. Hypoxic culturing conditions led to somewhat increased cell numbers, but this difference was less pronounced than the variations in the cell distribution between the static and perfusion samples. While the confocal work was qualitative, it provided a more complete understanding of the ASC growth and complemented the PicoGreen data. The confocal analyses were limited to the surface and surface pores of the DAT due to the opaque nature of the DAT. Since the entire sample was analyzed using PicoGreen, this gives a more complete picture of ASC proliferation within the DAT. In the confocal images, the ASCs tended to be found along the collagen structures in the DAT, suggesting that this scaffold provided a supportive surface for ASC attachment. Since DAT is derived from adipose tissue, the DAT scaffolding is mainly composed of type I collagen, laminin, fibronectin and versican [71]. Collagens are responsible for the basic structure of the ECM, providing its structural integrity. Many of the fibrillar collagens, including types I, II, III, V, and XI, impart tensile strength [25] in healthy tissues. Laminins are secreted primarily into the basement membrane. Through binding with cell-surface integrins, laminins promote interactions between cells and the basement membrane, leading to cell adhesion, migration and differentiation [25]. Mechanical continuity is achieved through the linking of integrins with the intracellular actin microfilament system of the cytoskeleton through a variety of proteins. Signaling conducted through integrin-integrin interactions influences cell survival, proliferation, the structure and functional activity of the cytoskeleton, and gene transcription

5.5 Adipogenic Differentiation

In order to confirm that the ASC cultured on the DAT scaffolds within the perfusion bioreactor system could be stimulated to undergo adipogenesis after extended culturing, the GPDH activity within the scaffold groups was assessed after the induction of adipogenic

differentiation. Three culturing conditions were used in this experiment: normoxic perfusion, hypoxic perfusion, and hypoxic static. The normoxic static culturing group was not included as it had shown low proliferation in the previous experiments, and a low cell density is not favorable for adipogenesis [22]. The samples were first cultured in the perfusion bioreactor or a 6-well plate in proliferation medium for 14 days. After this growth period, all of the samples were transferred into 6-well plates and cultured statically in adipogenic differentiation medium for 7 days to induce intracellular lipid accumulation. Static culturing was chosen for this portion of the experiment in order to model the *in vivo* environment that would be established if the scaffolds were implanted subcutaneously for soft tissue augmentation. The GPDH assay, which quantitatively measures the levels of a key enzyme involved in triglyceride formation, was run to quantitatively assess the levels of adipogenesis in each of the groups. The non-induced samples had significantly lower GPDH levels than the induced samples for each culture condition, as expected for these negative controls [40]. Low levels of differentiation were also observed in the normoxic perfusion scaffold group. The highest levels of GPDH activity were measured in the hypoxic perfusion scaffold group, indicating that the hypoxic conditions and perfusion bioreactor system enhanced soft tissue formation within the scaffolds. Previous work by Flynn *et al.* (2010) demonstrated that ASCs grown on the DAT scaffolds had greater GPDH activity than ASCs grown on TCPS [20]. In the current study, the GPDH activity from the hypoxic perfusion samples was statistically higher than the induced TCPS ASCs, which could possibly be due to the hypoxic perfusion producing greater ASCs numbers, as evidenced by the previous experiments, or could indicate that the hypoxic perfusion culturing increased the ASC potential to undergo adipogenesis. In previous work by McBeath *et al.* (2004), it was observed that high cell densities, associated with high levels of cell-cell contact and a rounded cell morphology enhanced the

adipogenic differentiation of mesenchymal stem cell populations [74]. As such, the culture conditions that enhanced cell proliferation could have ultimately promoted the ASC differentiation into adipocytes. In addition, the results of this thesis confirmed that the DAT scaffolds provided a supportive environment for ASC adipogenic differentiation, consistent with past results [20].

Overall, in combining the results for all of the experiments, it was evident that both the hypoxic culturing and perfusion culturing had a positive effect on the proliferation of ASCs cultured in aggregates on the DAT scaffolds, and supported their ability to undergo adipogenesis after long-term culturing under these conditions. The data also supports the use of cell aggregate seeding methods for culturing human ASCs on scaffolds, as compared to single cell suspension seeding.

Chapter 6

Conclusion and Recommendations

6.1 Conclusions

The decellularized adipose tissue (DAT) was found to be readily permeable to aqueous medium in the custom-designed perfusion based bioreactor system (Tissue Growth Technologies), with a permeability of 149 m^2 estimated using Darcy's law when 200 mg pieces of the DAT were placed in the perfusion bioreactor with a medium flow rate of 1.5 mL/min. A dye permeation experiment provided further evidence that the medium perfused throughout the entire DAT scaffolding, meeting the requirement for adequate nutrient delivery and waste removal to support cellular growth within the central regions of the DAT, to avoid the creation of a necrotic core within the tissues.

In traditional cell culturing experiments with human adipose-derived stem cells (ASCs), the hypoxic (5% O_2) culturing of ASCs decreased the doubling time and enhanced proliferation relative to culturing under normoxic conditions. Based on these results, the future bioreactor experiments focused on the implementation of hypoxic conditions as a means to drive stem cell proliferation.

In initial cell seeding experiments with the ASCs and DAT, based on both the confocal and PicoGreen dsDNA results, single-cell suspension seeding of the ASCs was insufficient for supporting long-term ASC attachment and proliferation. In these experiments, the ASCs appeared to interact with the collagen fibers in the DAT scaffolding, but maintained a spherical morphology throughout the culturing period.

The seeding of multicellular aggregates of human ASCs was investigated as an alternative approach to try to enhance stem cell survival and proliferation within the DAT by promoting localized cell-cell contacts and paracrine factor secretion, important for maintaining cell viability. When seeded as aggregates, the ASCs attached to the DAT scaffold and underwent measureable proliferation, depending on the specific seeding density. As before, the ASCs maintained their spherical morphology throughout the entire culturing period, compared to the fibroblastic morphology typically observed when the cells are cultured on tissue culture polystyrene (TCPS). The best results were obtained when 50 aggregates of 20,000 cells each, and therefore 1 million total ASCs, were seeded on the 200 mg DAT for proliferation. More limited attachment and proliferation were observed when 12 or 15 aggregates were seeded on the DAT. The seeding of higher numbers of aggregates was not explored as it was technically infeasible to incorporate additional aggregates within the small volume of medium used to promote initial cell attachment to the DAT. Confocal and DNA quantification results illustrated that the perfusion bioreactor improved the culturing environment for the ASCs on the DAT over traditional static culturing. Further, hypoxic (5% O_2) culturing within the bioreactor showed improved proliferation over normoxic (21% O_2) culturing. When combined, the hypoxic perfusion bioreactor culturing for ASCs was beneficial over traditional normoxic static culturing on the cell-adhesive DAT scaffolds.

After 14 days of culturing in proliferation medium within the perfusion bioreactor and under hypoxic conditions, the ASCs seeded on the DAT still possessed the ability to undergo adipogenesis when induced in adipogenic differentiation medium, as determined by the quantitative measurement of GPDH activity, a key enzyme involved in triglyceride synthesis.

This provided evidence that the ASCs retained their stem cell capacity to differentiate over the culture period on the DAT.

6.2 Contributions

The most significant contributions of this thesis to the field were as followed:

- Developed a seeding protocol for the ASC aggregates on the DAT scaffolds
- Demonstrated that hypoxic culturing conditions and the use of a perfusion bioreactor supported greater ASC proliferation and induced a greater adipogenic response, relative to ASCs grown under normoxic and static conditions.

6.3 Recommendations and Further Research

In order to produce enough ASCs for clinical applications, further optimizing of the seeding methods and culturing conditions needs to occur. Many studies have investigated the effects of using bioreactors to seed cells onto 3-dimensional scaffolds [15, 16]. As such, it would be interesting to explore the impact of using the bioreactor to seed the ASCs in aggregate form onto the DAT scaffolding via perfusion, to determine if this could further optimize cell attachment and long-term proliferation.

Hypoxic (5% O_2) culturing of the ASCs was beneficial for their proliferation. Other groups have used hypoxic conditions with as low as 2% O_2 and have found that these lower oxygen concentrations have additional positive effects on cell proliferation [35]. Based on the literature, I would suggest further investigating the influence of low oxygen culturing by expanding the range of oxygen tensions tested between 0 – 5% in order to determine an optimal oxygen concentration for ASC culturing.

Shear stress has been shown to have an important impact on ASC proliferation, differentiation and ECM deposition [72]. The flow rate of the medium through the scaffold is the main source of shear stress within the perfusion bioreactor system, and by modifying this parameter, it is possible to control the shear stress on the ASCs. Further, the flow rate is also responsible for the rate of nutrient delivery and waste removal to and from the ASCs. Previous studies have indicated that there are different optimum shear stresses for each cell type, application, and with different bioreactor configurations, emphasizing the importance of determining the optimum flow rate for each tissue construct [49-51]. Further research should look into different medium perfusion flow rates and assess their effects on the proliferation of the ASCs.

The next step would be to further investigate the multilineage differentiation potential of the ASCs seeded on the DAT and cultured within the bioreactor. This would be achieved through differentiation of the ASCs into osteoblast and chondrocytes, in addition to adipocytes. Commonly used techniques to confirm adipogenesis include Oil Red O staining, which stains the intracellular lipid content, and Glycerol-3-Phosphate Dehydrogenase (GPDH) Enzyme activity, which is a kinetic assay for the conversion of NADH into glycerol-3-phosphate. Osteogenesis results in significantly higher mineralized calcium phosphate matrix levels and ECM mineral deposition, which can be confirmed by alizarin red and von Kossa staining respectively. ALP activity is also increased and can be measured by ALP assay [31]. Chondrogenesis can be confirmed using Toluidine Blue staining for charged proteoglycans in the ECM and immunolabeling for collagen type II [52]. Flow cytometry can be used to assess the expression of key stem cell surface markers over time in culture as well as lineage specific surface markers.

This could include exploring the effects of oxygen tension in the differentiation environments as well as changes over length of time in culture [1].

Appendix A

Growth Environment

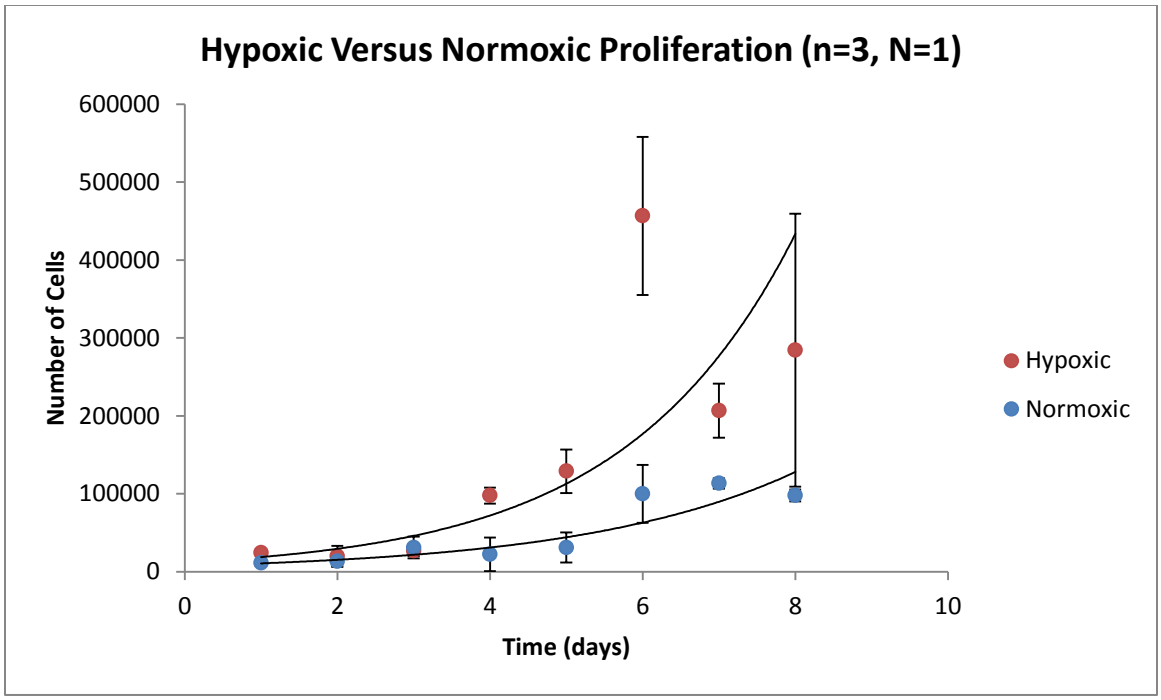

Figure 6.1: Donor 2 cell counts. Donor was a 26 year old female, 83 kg, 167 cm and BMI of 29.5. Data points are given as means ± standard deviations.

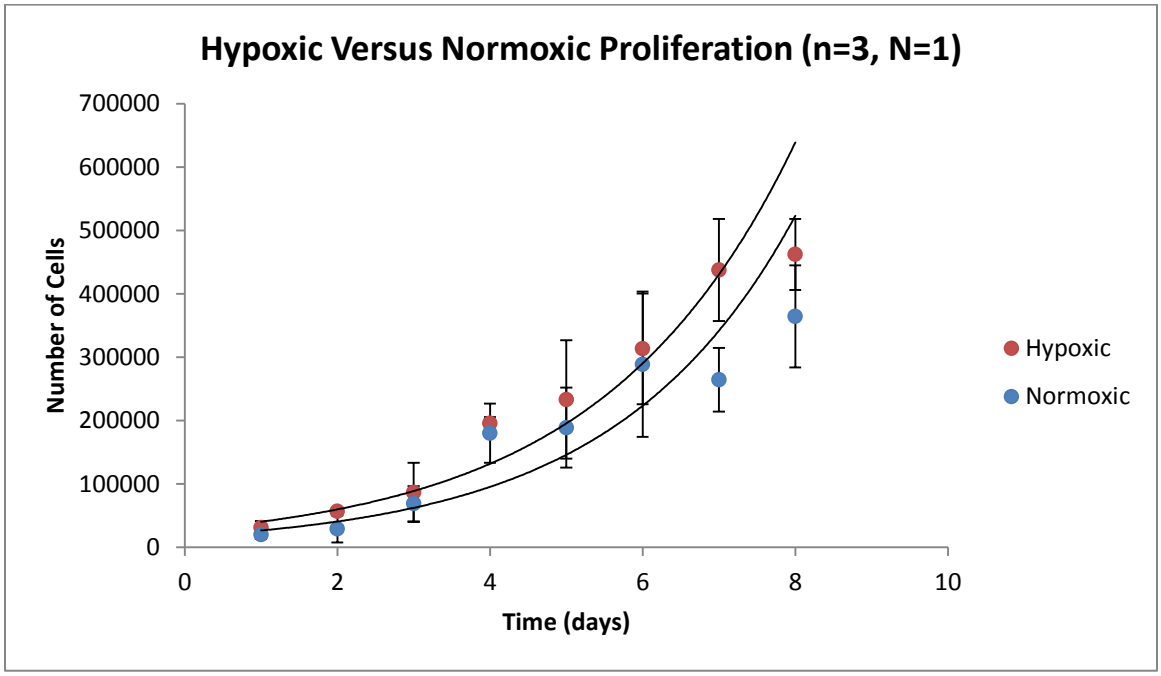

Figure 6.2: Donor 3 cell counts. Donor was a 33 year old female, 109 kg, 170 cm and BMI of 37.7. Data points are given as means ± standard deviations.

Appendix B

Confocal Results

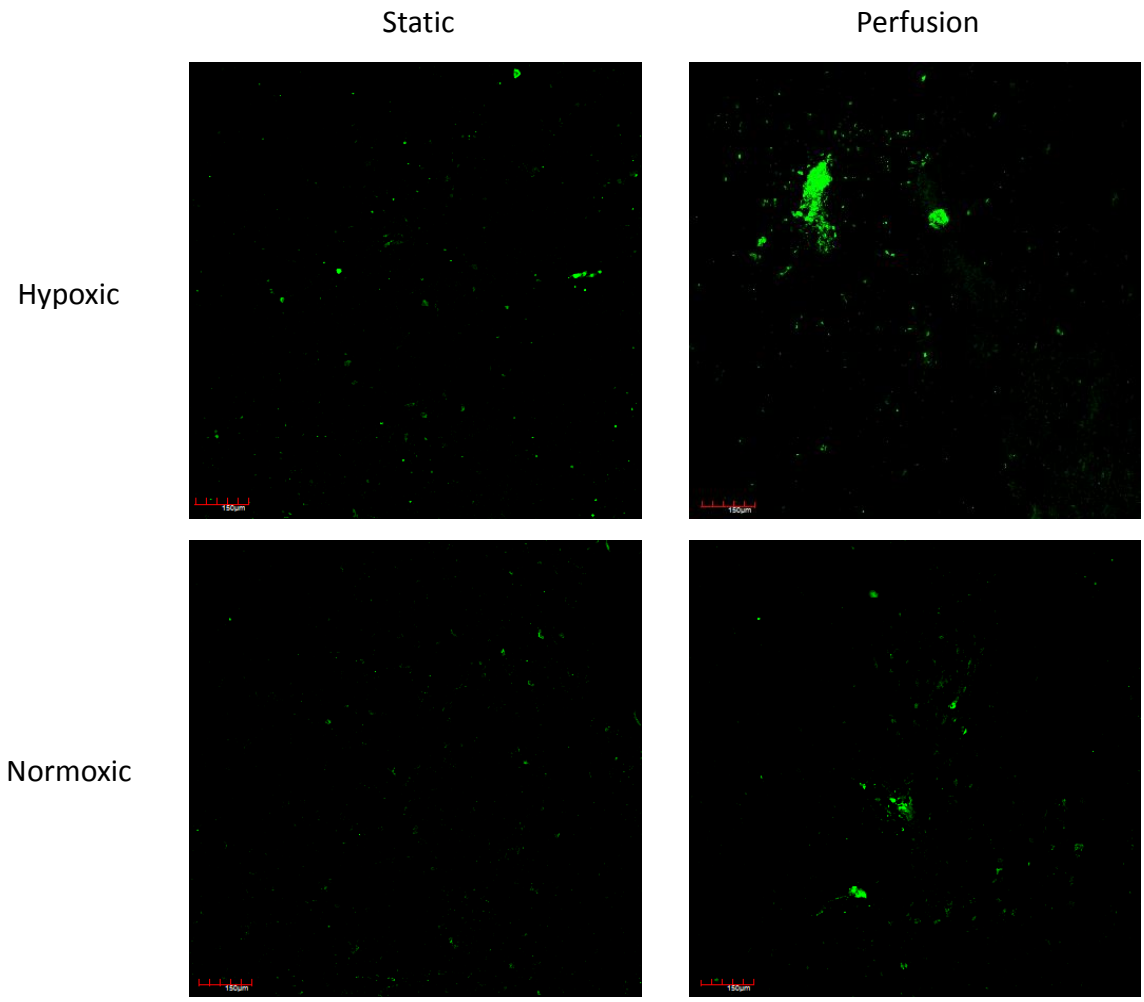

Figure 6.3: 200 mg DAT seeded with ASCs in aggregates of 20,000 (stained with Cell Tracker Green) at 72 hours. Samples were grown either statically or under perfusion and in either normoxic (21% O2) or hypoxic (5% O2) conditions. Donor was a 41 year old female, 98 kg, 173 cm and BMI of 32.8.

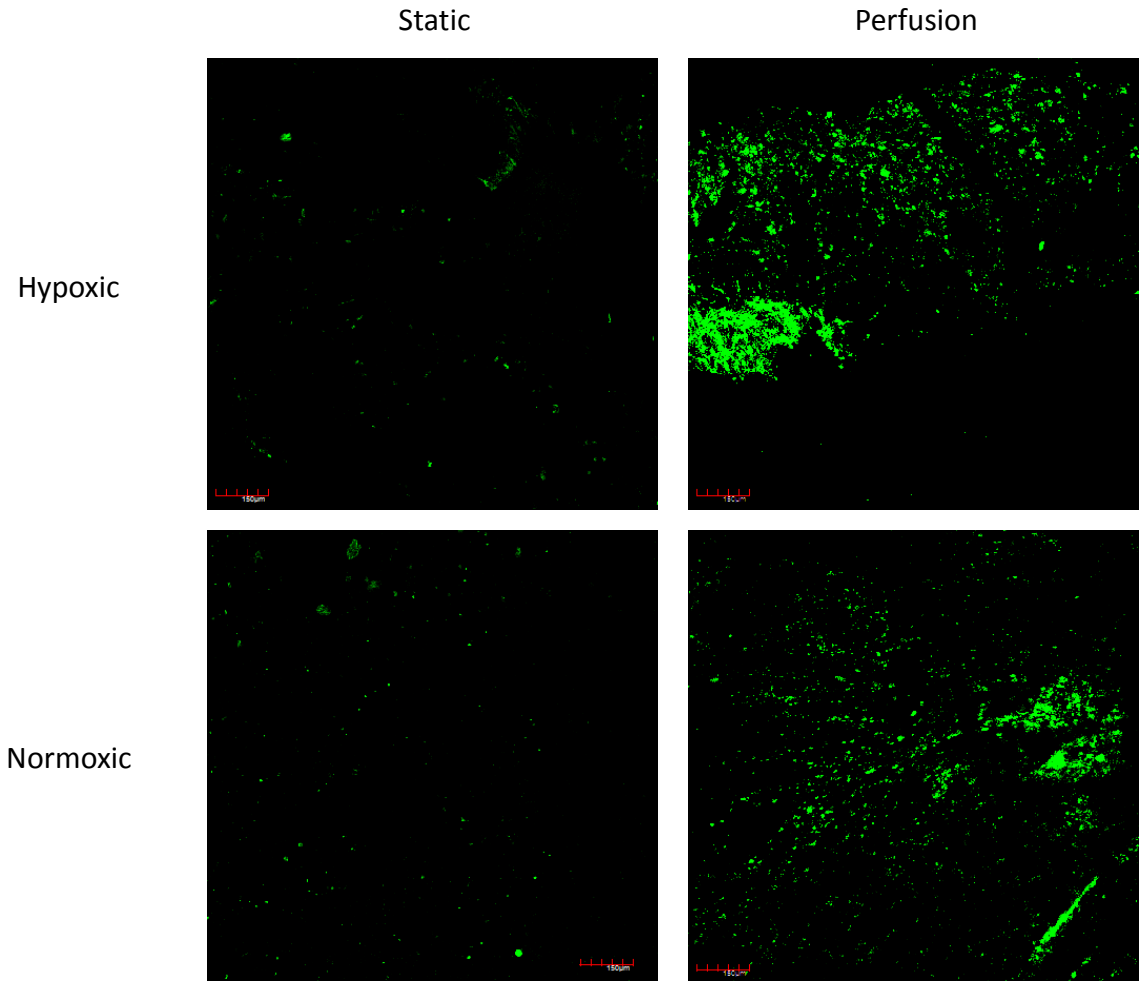

Figure 6.4: 200 mg DAT seeded with ASCs in aggregates of 20,000 (stained with Cell Tracker Green) at 7 days. Samples were grown either statically or under perfusion and in either normoxic (21% O2) or hypoxic (5% O2) conditions. Donor was a 41 year old female, 98 kg, 173 cm and BMI of 32.8.

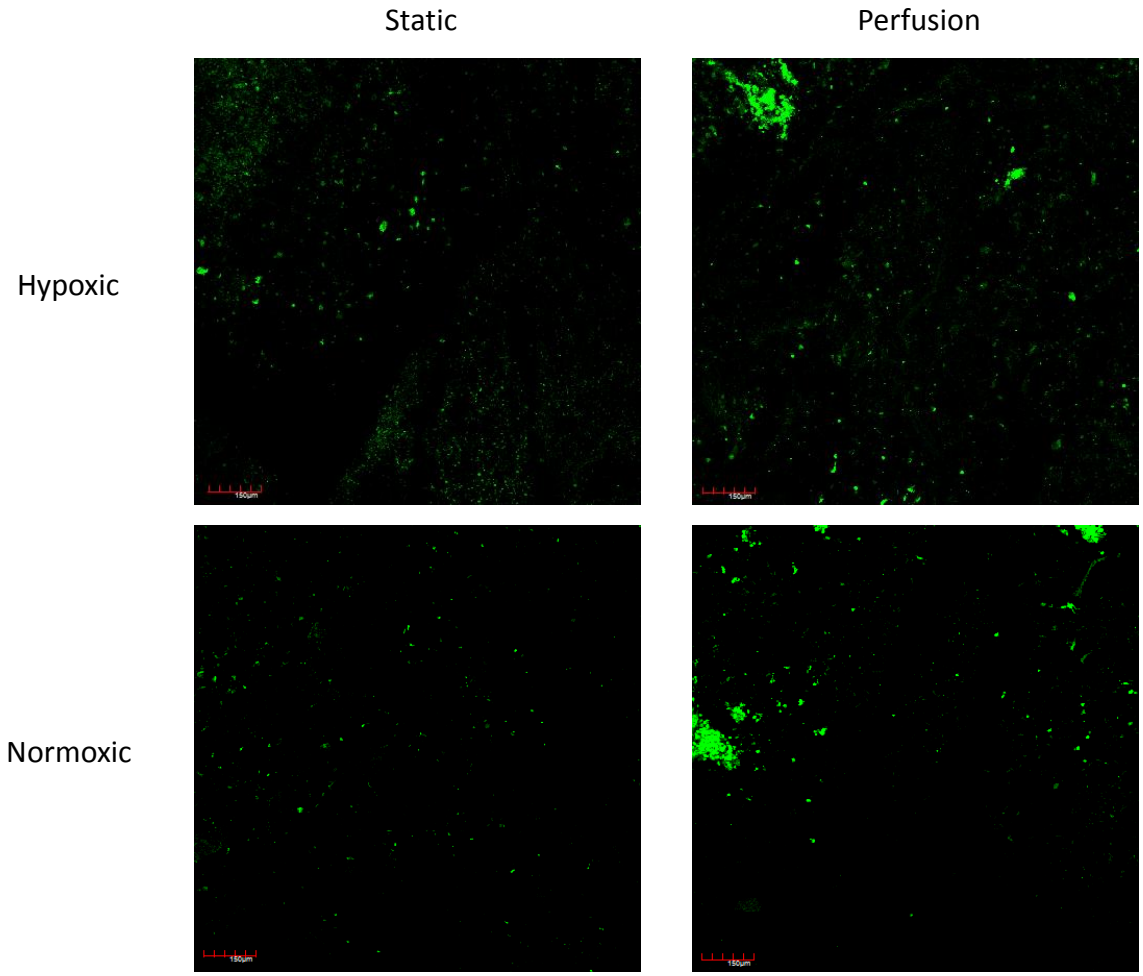

Figure 6.5: 200 mg DAT seeded with ASCs in aggregates of 20,000 (stained with Cell Tracker Green) at 14 days. Samples were grown either statically or under perfusion and in either normoxic (21% O2) or hypoxic (5% O2) conditions. Donor was a 41 year old female, 98 kg, 173 cm and BMI of 32.8.

Bibliography

1. Bailey AM, Kapur S, Katz, AJ. *Characterization of Adipose-Derived Stem Cells: An Update.* Current Stem Cell Research & Therapy, 2010;5:95-102.

2. Liebmann-Vinson A, Presnell SC. *Stem Cells.* Encyclopedia of Biomaterials and Biomediacl Engineering, 2004;1:1385-1390.

3. Lindroos B, Suuronen R, Miettinen S. *The Potential of Adipose Stem Cells in Regenerative Medicine.* Stem Cell Rev, 2011;7:269-291.

4. Katz AJ, Tholpady A, Tholpady SS, Shang H, Ogle RC. *Cell Surface and Transcriptional Characterization of Human Adipose-Derived Adherent Stromal (hADAS) Cells.* Stem Cells, 2005;23:412-423.

5. Oedayrajsingh-Varma MJ, Van Ham SM, Knippenberg M, Helder MN, Klein-Nulend J, Schouten TE, Ritt MJ, Van Milligen FJ. *Adipose Tissue-Derived Mesenchymal Stem Cell Yield and Growth Characteristics are Affected by the Tissue-Harvesting Procedure.* Cytotherapy, 2006;8:166-177.

6. Utsunomiya T, Shimada M., Imura S, Morine Y, Lkemoto T, Mori H, Hanaoka J, Iwahashi S, Saito, Iwaguro H. *Human Adipose-Derived Stem Cells: Potential Clinical Applications in Surgery.* Surg Today, 2011;41:18-23.

7. Zhu M., Kohan E, Bradley J, Hedrick M, Benhaim P, Zuk P. *The Effect of Age on Osteogenic, Adipogenic and Proliferative Potential of Female Adipose-Derived Stem Cells.* J Tissue Eng Regen Med, 2009;3:290-301.

8. Gonzalez-Rey E, Gonzalez MA, Varela N, O'Valle F, Hernandez-Cortes P, Rico L, Buscher D, Delgado M. *Human Adipose-Derived Mesenchymal Stem Cells Reduce Inflammatory and T Cell Responses and Induce Regulatory T cells In Vitro in Rheumatoid Arthritis.* Ann Rheum Dis, 2010;69:241-248.

9. Gimble J, Guilak F. *Adipose-Derived Adult Stem Cells: Isolation, Characterization, and Differentiation Potential.* Cytotherapy, 2003;5:362-369.

10. Wilson A, Butler PE, Seifalian AM. *Adipose-Derived Stem Cells for Clinical Applications: A Review.* Cell Prolif, 2011;44:86-98.

11. Katz AJ. *Compositions and Methods for Modular Soft Tissue Repair*, 2010.

12. Banerjee M, Bhonde RR. *Application of Hanging Drop Technique for Stem Cell Differentiation and Cytotoxicity Studies.* Cytotechnology, 2006;51:1-5.

13. Amos PJ, Kapur SK, Stapor PC, Hulan Shang H, Stefan Bekiranov S, Khurgel M, Rodeheaver GT, Peirce SM, Katz AJ. *Human Adipose-Derived Stromal Cells Accelerate Diabetic Wound Healing: Impact of Cell Formulation and Delivery.* Tissue Egnineering: Part A, 2010;16:1595-1606.

14. Nelson CM, Bissell MJ. *Of extracellular Matrix, Scaffolds, and Signaling, Tissue Architecture Regulates Development, Homeostasis, and Cancer.* Annu Rev Cell Dev Biol, 2006;22:287-309.

15. Martin Y, Vermette P. *Bioreactors for Tissue Mass Culture: Design, Characterization, and Recent Advances.* Biomaterials, 2005;26:7481-7503.

16. Neofytou EA, Chang E, Patlola B, Joubert LM, Rajadas j, Gambhir SS, Cheng Z, Robbins RC, Beygui RE. *Adipose Tissue-Derived Stem Cells Display a Proangiogenic Phenotype on 3D Scaffolds.* J Biomed Mater Res A, 2011;98:383-393.

17. Lee EY, Xia Y, Kim WS, Kim MH, Kim TH, Kim KJ, Park BS, Sung JH. *Hypoxia-Enhanced Wound-Healing Function of Adipose-Derived Stem Cells: Increase in Stem Cell Proliferation and Up-Regulation of VEGF and bFGF.* Wound Repair Regen, 2009;17:540-547.

18. Martin I, Wendt D, Heberer M. *The Role of Bioreactors in Tissue Engineering.* Trends in Biotechnology, 2004;22:80-86.

19. Dubois J, Tremblay L, Lepage M, Vermette P. *Flow Dynamics within a Bioreactor for Tissue Engineering by Residence Time Distribution Analysis Combined with Fluorescence and Magnetic Resonance Imaging to Investigate Forced Permeability and Apparent Diffusion Coefficient in a Perfusion Cell Culture Chamber.* Biotechnol Bioeng, 2011.

20. Flynn LE. *The Use of Decellularized Adipose Tissue to Provide an Inductive Microenvironment for the Adipogenic Differentiation of Human Adipose-Derived Stem Cells.* Biomaterials, 2010;31:4715-4724.

21. Patrick CW. *Adipose Tissue Engineering: The Future of Breast and Soft Tissue Reconstruction Following Tumor Resection.* Seminars in Surgical Oncology, 2000;19:302-311.

22. Zuk PA, Zhu M, Ashjian P, De Ugarte DA, Huang JI, Mizuno H, Alfonso ZC, Fraser JK, Benhaim P, Hedrick MH. *Human Adipose Tissue is a Source of Multipotent Stem Cells.* Mol Biol Cell, 2002;13:4279-4295.

23. Gimble JM, Katz AJ, Bunnell BA. *Adipose-Derived Stem Cells for Regenerative Medicine.* Circ Res, 2007;100:1249-1260.

24. Gomillion CT, Burg KJ. *Stem Cells and Adipose Tissue Engineering.* Biomaterials, 2006;27:6052-6063.

25. Bosman FT, Stamenkovic I. *Functional Structure and Composition of the Extracellular Matrix.* J Pathol, 2003;200:423-428.

26. Patrick CW. *Breast Tissue Engineering.* Annu Rev Biomed Eng, 2004;6:109-130.

27. Lenas P, Luyten F. *An Emerging Paradigm in Tissue Engineering: From Chemical Engineering to Developmental Engineering for Bioartifical Tissue Formation through a Series of Unit Operations that Simulate the In Vivo Successive Developmental Stages.* Ind Eng Chem Res, 2011;50:482-522.

28. Keller G. *In vitro differentiation of embryonic stem cells.* Current Opinion in Cell BIology, 1995;7:862-869.

29. Cherubino M, Rubin JP, Miljkovic N, Kelmendi-Doko A, Marra KG. *Adipose-Derived Stem Cells for Wound Healing Applications.* Ann Plast Surg, 2011;66:210-215.

30. Ng LW, Yip SK, Wong HK, Yam GH, Liu YM, Lui WT, Wang CC, Choy KW. *Adipose-Derived Stem Cells From Pregnant Women Show Higher Proliferation Rate Unrelated to Estrogen.* Hum Reprod, 2009;24:1164-1170.

31. Guilak F, Lott KE, Awad HA, Cao Q, Hicok KC, Fermor B, Gimble JM. *Clonal Analysis of the Differentiation Potential of Human Adipose-Derived Adult Stem Cells.* J Cell Physiol, 2006;206:229-237.

32. Tucker HA, Bunnell BA. *Characterization of Human Adipose-Derived Stem Cells Using Flow Cytometry.* Methods Mol Biol, 2011;702:121-131.

33. Mojallal A, Lequeux C, Shipkov C, Duclos A, Braye F, Rohrich R, Brown S, Damour O. *Influence of Age and Body Mass Index on the Yield and Proliferation Capacity of Adipose-Derived Stem Cells.* Aesthetic Plast Surg, 2011.

34. Rodrigues CAV, Fernandes TG, Diogo MM, Da Silva, CL, Cabral JMS. *Stem Cell Cultivation in Bioreactors.* Biotechnol Adv, 2011;29:815-829.

35. Dos Santos F, Andrade PZ, Boura JS, Abecasis MM, Da Silva CL, Cabral JM. *Ex Vivo Expansion of Human Mesenchymal Stem Cells: A More Effective Cell Proliferation Kinetics and Metabolism Under Hypoxia.* J Cell Physiol, 2010;223:27-35.

36. Carvalho PP, Gimble JM, Dias IR, Gomes ME, Reis RL. *Human Adipose-Derived Stromal/Stem Cells: Use of Animal Free Products and Extended Storage at Room Temperature*, in *Semana de Engenharia* 2010: Guimaraes.1-2.

37. Carvalho PP, Wu X, Yu G, Dietrich M, Dias IR, Gomes ME, Reis RL, Gimble JM. *Use of Animal Protein-Free Products for Passaging Adherent Human Adipose-Derived Stromal/Stem Cells.* Cytotherapy, 2011;13:594-597.

38. Ramirez MA, Pericuesta E, Yanez-Mo M, Palasz A, Gutierrez-Adan A. *Effect of Long-Term Culture of Mouse Embryonic Stem Cells Under Low Oxygen Concentration as well as on Glycosaminoglycan Hyaluronan on Cell Proliferation and Differentiation.* Cell Prolif, 2011;44:75-85.

39. Potier E, Ferreira E, Meunier A, Sedel L, Logeart-Avarmoglou D, Petite H. *Prolonged Hypoxia Concomitant with Serum Deprivation Induces Massive Human Mesenchymal Stem Cell Death.* Tissue Eng, 2007;13:1325-1331.

40. Rodriguez AM, Elabd C, Delteil F, Astier J, Vernochet C, Saint-Marc P, Guesnet J, Guezennec A, Amri EZ, Dani C, Ailhaund G. *Adipocyte Differentiation of Multipotent Cells Established from Human Adipose Tissue.* Biochem Biophys Res Commun, 2004;315:255-263.

41. Rosen ED, MacDougald OA. *Adipocyte Differentiation from the Inside Out.* Nat Rev Mol Cell Biol, 2006;7:885-896.

42. Bartosh TJ, Yiostalo JH, Mohammadipoor A, Bazhanov N, Coble K, Claypool K, Lee RH, Choi H, Prockop DJ. *Aggregation of Human Mesenchymal Stromal Cells (MSCs) into 3D Spheroids Enhances their Antiinflammatory Properties.* PNAS, 2010;107:13724-13729.

43. Aust L, Devlin B, Foster SJ, Halvorsen YD, Hicok K, Du Laney T, Sen A, Willingmyre GD, Gimble JM. *Yield of Human Adipose-Derived Adult Stem Cells From Liposuction Aspirates.* Cytotherapy, 2004;61:7-14.

44. Scherberich A, Muller AM, Schafer DJ, Banfi A, Martin I. *Adipose Tissue-Derived Progenitors for Engineering Osteogenic and Vasculogenic Grafts.* J Cell Physiol, 2010;225:348-353.

45. Carrier RL, Rupnick M, Langer R, Schoen FJ, Freed LE, Vunjak-Novakovic G. *Perfusion Improves Tissue Architecture of Engineered Cardiac Muscle.* Tissue Engineering, 2002;82:175-188.

46. Chen X, Xu H, Wan C, McCaigue M, Li G. *Bioreactor Expansion of Human Adult Bone Marrow-Derived Mesenchymal Stem Cells.* Stem Cells, 2006;24:2052-2059.

47. Kim BS, Putnam AJ, Kulik TJ, Mooney DJ. *Optimizing Seeding and Culture Methods to Engineer Smooth Muscle Tissue on Biodegradable Polymer Matrices.* Biotechnol Bioeng, 1998;57:46-54.

48. Luni C, Zagallo M, Albania L, Piccoli M, Pozzobon M, De Coppi P, Elvassore N. *Design of a Stirred Multiwell Bioreactor for Expansion of CD34(+) Umbilical Cord Blood Cells in Hypoxic Conditions.* Biotechnol Prog, 2011;27:1154-1162.

49. Bancroft GN, Sikavitsas VI, Mikos AG. *Design of a Flow Perfusion Bioreactor System for Bone Tissue-Engineering Applications.* Tissue Engineering, 2003;9:549-554.

50. Grayson WL, Marolt D, Bhumiratana S, Frohlich M, Guo XE, Vunjak-Novakovic, G. *Optimizing the Medium Perfusion Rate in Bone Tissue Engineering Bioreactors.* Biotechnol Bioeng, 2011;108:1159-1170.

51. Davies PF, Andrea R, Gordon EJ, Dewey CF, Gimbrone MA. *Turbulent Fluid Shear Stress Induces Vascular Endothelial Cell Turnover In Vitro.* PNAS, 1986;83:2114-2117.

52. Frohlich M, Grayson WL, Marolt D, Gimble JM, Kregar-Velikonja N, Vunjak-Novakovic G. *Bone Grafts Engineered from Human Adipose-Derived Stem Cells in Perfusion Bioreactor Culture.* Tissue Eng Part A, 2010;16:179-189.

53. Davisson T, Sah R, Ratcliffe A. *Perfusion Increases Cell Content and Matrix Synthesis in Chondrocyte Three-Dimensional Cultures.* Tissue Engineering, 2002;8:807-815.

54. Bauwens C, Yin T, Dang S, Peerani R, Zandstra PW. *Development of a Perfusion Fed Bioreactor for Embryonic Stem Cell-Derived Cardiomyocyte Generation:*

Oxygen-Mediated Enhancement of Cardiomyocyte Output. Biotechnol Bioeng, 2005;90:452-461.

55. Flynn L, Prestwich GD, Semple JL, Woodhouse KA. *Adipose Tissue Engineering with Naturally Derived Scaffolds and Adipose-Derived Stem Cells.* Biomaterials, 2007;28:3834-3842.

56. Schenke-Layland K, Vasilevski O, Optiz F, Konig K, Riemann I, Halbhuber KJ, Wahlers, T, Stock UA. *Impact of Decellularization of Xenogeneic Tissue on Extracellular Matrix Integrity for Tissue Engineering of Heart Valves.* Journal of Structural Biology, 2003;143:201-208.

57. Murphy MB, Blashki D, Buchanan RM, Fan D, De Roas E, Shah RN, Stupp SI, Weiner BK, Simmons PJ, Ferrari M, Tasciotti E. *Multi-Composite Bioactive Osteogenic Sponges Featuring Mesenchymal Stem Cells, Platelet-Rich Plasma, Nanoporous Silicon Enclosures, and Peptide Amphiphiles for Rapid Bone Regeneration.* Journal of Functional Biomaterials, 2011;2:39-66.

58. Rieder E, Kasimir MT, Silberhumer G, Seebacher G, Wolner E, Simon P, Weigel G. *Decellularization Protocols of Porcine Heart Valves Differ Importantly in Efficiency of Cell Removal and Susceptibility of the Matrix to Recellularization with Human Vascular Cells.* J Thorac Cardiovasc Surg, 2004;127:399-405.

59. Girandon L, Kregar-Velikonja N, Bozikov K, Barlic A. *In vitro Models for Adipose Tissue Engineering with Adipose-Derived Stem Cells Using Different Scaffolds of Natural Origin.* Folia Biologica, 2011;57:47-56.

60. Flynn LE, Prestwich GD, Semple JL, Woodhouse KA. *Proliferation and Differentiation of Adipose-Derived Stem Cells on Naturally Derived Scaffolds.* Biomaterials, 2008;29:1862-1871.

61. Holy C, Shoichet M, Davies J. *Engineering Three-Dimensional Bone Tissue In Vitro Using Biodegradable Scaffolds: Investigating Initial Cell-Seeding Density and Culture Period.* J BIomed Mater Res, 2000;51:376-382.

62. Liao J, Joyce EM, Sacks MS. *Effects of Decellularization on the Mechanical and Sproperties of the Porcine Aortic Valve Leaflet.* Biomaterials, 2008;29:1065-1074.

63. Ketchedjian A, Jones AL, Krueger P, Robinson E, Crouch K, Wolfinbarger L, Hopkins R. *Recellularization of Decellularized Allograft Scaffolds in Ovine Great Vessel Reconstructions.* Ann Thorac Surg, 2005;79:888-896.

64. Gilbert TW, Sellaro TL, Badylak SF, *Decellularization of Tissues and Organs.* Biomaterials, 2006;27:3675-3683.

65. Sun F, Zhou K, Mi WJ, Qiu JH. *Repair of Facial Nerve Defects with Decellularized Artery Allografts Containing Autologous Adipose-Derived Stem Cells in a Rat Model.* Neurosci Lett, 2011;499:104-108.

66. Izumi K, Feinberg SE, Iida A, Yoshizawa M. *Intraoral Grafting of an Ex Vivo Produced Oral Mucosa Equivalent: A Preliminary Report.* Int J Oral Maxillofac Surg, 2003;32:188-197.

67. Radisic M, Euloth M, Yang L, Langer R, Freed LE, Vunjak-Novakovic G. *High-Density Seeding of Myocyte Cells for Cardiac Tissue Engineering.* Biotechnol Bioeng, 2003;82:403-414.

68. Ng K, Leong D, Hutmacher D, *The challenge to Measure Cell Proliferation in Two and Three Dimensions.* Tissue Egnineering, 2005;11:182-191.

69. Singer VL, Jones LJ, Yue ST, Haugland RP. *Characterization of PicoGreen Reagent and Development of a Fluorescence-Based Solution Assay for Double-Stranted DNA Quantitation.* Analytical Biochemistry, 1997;249:228-238.

70. Flynn L, Semple JL, Woodhouse KA, *Decellularized placental matrices for adipose tissue engineering.* J Biomed Mater Res A, 2006;79:359-69.

71. Hoshiba T, Kawazoe N, Tateishi T, Chen G. *Development of Extracellular Matrices Mimicking Stepwise Adipogenesis of Mesenchymal Stem Cells.* Adv Mater, 2010;22:3042-3047.

72. Zhao F, Chella R, Ma T. *Effects of Shear Stress on 3-D Human Mesenchymal Stem Cell Construct Development in a Perfusion Bioreactor System: Experiments and Hydrodynamic Modeling.* Biotechnol Bioeng, 2007;96:584-595.

73. Leddy HA, Awad HA, Guilak F. *Molecular Diffusion In Tissue-Engineered Cartilage Constructs: Effects of Scaffold Material, Time, and Culture Conditions.* Journal of Biomedical Materials Research Part B: Applied Biomaterials, 2004; 70B:397-406.

74. McBeath R, Pirone D, Nelson CM, Bhadriraju K, Chen CS. *Cell Shape, Cytoskeletal Tension, and RhoA Regulate Stem Cell Lingeage Commitment.* Developmental Cell, 2004;6:483-495.